Habitat-based density estimates for cetaceans in the California Current Ecosystem based on 1991–2018 survey data

Elizabeth A. Becker, Karin A. Forney, David L. Miller, Paul C. Fiedler, Jay Barlow, and Jeff E. Moore

U.S. DEPARTMENT OF COMMERCE
National Oceanic and Atmospheric Administration
National Marine Fisheries Service
Southwest Fisheries Science Center

NOAA Technical Memorandum NMFS-SWFSC-638

December 2020

NOAA Technical Memorandum NMFS

DECEMBER 2020

HABITAT-BASED DENSITY ESTIMATES FOR CETACEANS IN THE CALIFORNIA CURRENT ECOSYSTEM BASED ON 1991-2018 SURVEY DATA

Elizabeth A. Becker [1], Karin A. Forney [2], David L. Miller [3],
Paul C. Fiedler [4], Jay Barlow [4], and Jeff E. Moore [4]

[1]Ocean Associates, Inc., under contract to the Marine Mammal and Turtle Division, Southwest Fisheries Science Center, National Marine Fisheries Service
8901 La Jolla Shores Dr. La Jolla, CA 92037

[2]Southwest Fisheries Science Center, National Marine Fisheries Service and Moss Landing Marine Laboratories, San Jose State University
7544 Sandholt Rd. Moss Landing, CA 95039

[3]Centre for Research into Ecological & Environmental Modeling and School of Mathematics & Statistics, University of St Andrews, St. Andrews, Fife, Scotland

[4]Marine Mammal and Turtle Division, Southwest Fisheries Science Center, National Marine Fisheries Service, 8901 La Jolla Shores Dr. La Jolla, CA 92037

NOAA-TM-NMFS-SWFSC-638

U.S. DEPARTMENT OF COMMERCE
National Oceanic and Atmospheric Administration
National Marine Fisheries Service
Southwest Fisheries Science Center

About the NOAA Technical Memorandum series

The National Oceanic and Atmospheric Administration (NOAA), organized in 1970, has evolved into an agency which establishes national policies and manages and conserves our oceanic, coastal, and atmospheric resources. An organizational element within NOAA, the Office of Fisheries is responsible for fisheries policy and the direction of the National Marine Fisheries Service (NMFS).

In addition to its formal publications, the NMFS uses the NOAA Technical Memorandum series to issue informal scientific and technical publications when complete formal review and editorial processing are not appropriate or feasible. Documents within this series, however, reflect sound professional work and may be referenced in the formal scientific and technical literature.

SWFSC Technical Memorandums are available online at the following websites:

SWFSC: https://www.fisheries.noaa.gov/about/southwest-fisheries-science-center

NOAA Repository: https://repository.library.noaa.gov/

NTIS National Technical Reports Library: https://ntrl.ntis.gov/NTRL/

Accessibility information

NOAA Fisheries Southwest Fisheries Science Center (SWFSC) is committed to making our publications and supporting electronic documents accessible to individuals of all abilities. The complexity of some of SWFSC's publications, information, data, and products may make access difficult for some. If you encounter material in this document that you cannot access or use, please contact us so that we may assist you.
Phone: 858-546-7000

Recommended citation

Elizabeth A. Becker, Karin A. Forney, David L. Miller, Paul C. Fiedler, Jay Barlow, and Jeff E. Moore. 2020. Habitat-based density estimates for cetaceans in the California Current Ecosystem based on 1991-2018 survey data, U.S. Department of Commerce, NOAA Technical Memorandum NMFS-SWFSC-638.

Table of Contents

List of Tables iv
List of Figures v
Introduction 1
Methods 3
Survey data 3
Environmental predictor data 3
Correction factors 5
Habitat models 5
Results 10
Discussion and Conclusions 13
Acknowledgements 17
Literature Cited 18
Tables 23
Figures 30
Appendix A: SDM functional plots 54

List of Tables

Table 1. Cetacean and ecosystem assessment surveys and effort conducted within the California Current Ecosystem study area during 1991–2018. CA/OR/WA = California/Oregon/Washington, CenCA = central California, SoCA = southern California, Baja = Baja California. DSJ = *David Starr Jordan.* 23

Table 2. Number of sightings and average group size (Avg. GS) of cetacean species observed in the California Current Ecosystem study area during the 1991–2018 shipboard surveys for which habitat-based density models were developed. All sightings were made while on systematic and non-systematic effort in Beaufort sea states ≤5 within the species-specific truncation distances (see text for details). 23

Table 3. Summary of the final models built with the 1991–2018 survey data. Variables are listed in the order of their significance and are as follows: SST = sea surface temperature, SSTsd = standard deviation of SST, MLD = mixed layer depth, SSH = sea surface height, SSHsd = standard deviation of SSH, depth = bathymetric depth, shelf= distance to shelf, d2000=distance to the 2,000m isobath, LON = longitude, and LAT = latitude. Separate encounter rate (ER) and group size (GS) models were built for long- and short-beaked common dolphins due to large and variable group sizes. All single response and encounter rate models were corrected for effort with an offset for the effective area searched (see text for details). Performance metrics included the percentage of explained deviance (Expl. Dev.), the area under the receiver operating characteristic curve (AUC), the true skill statistic (TSS), and the ratio of observed to predicted density for the study area (Obs:Pred). 24

Table 4. Annual model-predicted mean estimates of abundance, density (animals km^{-2}), and corresponding coefficient of variation (CV) within the CCE study area. Annual estimates are predicted from the full model using the habitat characteristics in that year. CV_m (Model) represents the combined uncertainty from three sources: GAM parameters, ESW, and environmental variability. CV_{Tot} is the total CV from CV_m (Model) and CV_{g0} derived using the Delta method (see text for details). Log-normal 95% confidence intervals (Low and High 95% CIs) apply to abundance estimates. Also shown is the 20th percentile for the abundance estimate, corresponding to the "minimum population size (Nmin)" as defined in the Guidelines for Assessing Marine Mammal Stocks, and calculated as the log-normal 20th percentile of the mean abundance estimate using standard formulae..... 25

Table 5. Arithmetic mean of the model-predicted 2014 and 2018 estimates of abundance and density (animals km^{-2}) within the CCE study area. The corresponding coefficient of variation (CV_{Tot}) is the total CV from four sources: environmental variability, GAM parameters, ESW, and *g(0)* (see text for details). Log-normal 95% confidence intervals (Low and High 95% CIs) apply to abundance estimates. Also shown is the 20th percentile for the abundance estimate, corresponding to the "minimum population size (Nmin)" as defined in the Guidelines for Assessing Marine Mammal Stocks, and calculated as the log-normal 20th percentile of the mean abundance estimate using standard formulae. 29

List of Figures

Figure 1. Completed transects for the Southwest Fisheries Science Center systematic ship surveys conducted between 1991 and 2018 in the California Current Ecosystem study area. The lines (green = 1991–2014 surveys, red=2018 survey) show on-effort transect coverage in Beaufort sea states of 0-5. 30

Figure 2a-b. Predicted mean density (animals km^{-2}) and associated coefficients of variation (CV) from the 1991–2018 habitat-based density models for (a) long-beaked common dolphin, and (b) short-beaked common dolphin. Panels show the multi-year average density based on predicted daily cetacean species densities covering the 1996-2018 survey periods (summer/fall). Predictions are shown for the study area (1,141,800 km^2). White dots in the average plots show actual sighting locations from the SWFSC 1996-2018 summer/fall ship surveys for the respective species. 31

Figure 2c-d. Predicted mean density (animals km^{-2}) and associated coefficients of variation (CV) from the 1991–2018 habitat-based density models for (c) Risso's dolphin, and (d) Pacific white-sided dolphin. Panels show the multi-year average density based on predicted daily cetacean species densities covering the 1996-2018 survey periods (summer/fall). Predictions are shown for the study area (1,141,800 km^2). White dots in the average plots show actual sighting locations from the SWFSC 1996-2018 summer/fall ship surveys for the respective species. 32

Figure 2e-f. Predicted mean density (animals km^{-2}) and associated coefficients of variation (CV) from the 1991–2018 habitat-based density models for (e) northern right whale dolphin, and (f) striped dolphin. Panels show the multi-year average density based on predicted daily cetacean species densities covering the 1996-2018 survey periods (summer/fall). Predictions are shown for the study area (1,141,800 km^2). White dots in the average plots show actual sighting locations from the SWFSC 1996-2018 summer/fall ship surveys for the respective species. 33

Figure 2g-h. Predicted mean density (animals km^{-2}) and associated coefficients of variation (CV) from the 1991–2018 habitat-based density models for (g) common bottlenose dolphin, and (h) Dall's porpoise. Panels show the multi-year average density based on predicted daily cetacean species densities covering the 1996-2018 survey periods (summer/fall). Predictions are shown for the study area (1,141,800 km^2). White dots in the average plots show actual sighting locations from the SWFSC 1996-2018 summer/fall ship surveys for the respective species. 34

Figure 2i-j. Predicted mean density (animals km^{-2}) and associated coefficients of variation (CV) from the 1991–2018 habitat-based density models for (i) sperm whale, and (j) minke whale. Panels show the multi-year average density based on predicted daily cetacean species densities covering the 1996-2018 survey periods (summer/fall). Predictions are shown for the study area (1,141,800 km^2). White dots in the average plots show actual sighting locations from the SWFSC 1996-2018 summer/fall ship surveys for the respective species. 35

Figure 2k-l. Predicted mean density (animals km^{-2}) and associated coefficients of variation (CV) from the 1991–2018 habitat-based density models for (k) blue whale, and (l) fin whale. Panels show the multi-year average density based on predicted daily cetacean species densities covering the 1996-2018 survey periods (summer/fall). Predictions are shown for the study area (1,141,800 km^2). White dots in the average plots show actual sighting

locations from the SWFSC 1996-2018 summer/fall ship surveys for the respective species. 36
Figure 2m-n. Predicted mean density (animals km^{-2}) and associated coefficients of variation (CV) from the 1991–2018 habitat-based density models for (m) humpback whale, and (n) Baird's beaked whale. Panels show the multi-year average density based on predicted daily cetacean species densities covering the 1996-2018 survey periods (summer/fall). Predictions are shown for the study area (1,141,800 km^2). White dots in the average plots show actual sighting locations from the SWFSC 1996-2018 summer/fall ship surveys for the respective species. 37
Figure 2o. Predicted mean density (animals km^{-2}) and associated coefficients of variation (CV) from the 1991–2018 habitat-based density models for (o) small beaked whale guild. Panels show the multi-year average density based on predicted daily cetacean species densities covering the 1996-2018 survey periods (summer/fall). Predictions are shown for the study area (1,141,800 km^2). White dots in the average plots show actual sighting locations from the SWFSC 1996-2018 summer/fall ship surveys for the respective species. 38
Figure 3a. Predicted annual (1996-2018) mean density (animals km^{-2}) and associated coefficients of variation (CV) from the 1991–2018 habitat-based density models for long-beaked common dolphin. Panels show the yearly average density based on predicted daily long-beaked common dolphin densities covering the 1996-2018 survey periods (summer/fall). Predictions are shown for the study area (1,141,800 km^2). White dots in the average plots show actual sighting locations from the respective SWFSC summer/fall ship surveys… 39
Figure 3b. Predicted annual (1996-2018) mean density (animals km^{-2}) and associated coefficients of variation (CV) from the 1991–2018 habitat-based density models for short-beaked common dolphin. Panels show the yearly average density based on predicted daily short-beaked common dolphin densities covering the 1996-2018 survey periods (summer/fall). Predictions are shown for the study area (1,141,800 km^2). White dots in the average plots show actual sighting locations from the respective SWFSC summer/fall ship surveys… 40
Figure 3c. Predicted annual (1996-2018) mean density (animals km^{-2}) and associated coefficients of variation (CV) from the 1991–2018 habitat-based density models for Risso's dolphin. Panels show the yearly average density based on predicted daily Risso's dolphin densities covering the 1996-2018 survey periods (summer/fall). Predictions are shown for the study area (1,141,800 km^2). White dots in the average plots show actual sighting locations from the respective SWFSC summer/fall ship surveys. 41
Figure 3d. Predicted annual (1996-2018) mean density (animals km^{-2}) and associated coefficients of variation (CV) from the 1991–2018 habitat-based density models for Pacific white-sided dolphin. Panels show the yearly average density based on predicted daily Pacific white-sided dolphin densities covering the 1996-2018 survey periods (summer/fall). Predictions are shown for the study area (1,141,800 km^2). White dots in the average plots show actual sighting locations from the respective SWFSC summer/fall ship surveys… 42
Figure 3e. Predicted annual (1996-2018) mean density (animals km^{-2}) and associated coefficients of variation (CV) from the 1991–2018 habitat-based density models for northern right whale dolphin. Panels show the yearly average density based on predicted daily northern right whale dolphin densities covering the 1996-2018 survey periods (summer/fall). Predictions are shown for the study area (1,141,800 km^2). White dots in the average plots show actual sighting locations from the respective SWFSC summer/fall ship surveys… 43

Figure 3f. Predicted annual (1996-2018) mean density (animals km^{-2}) and associated coefficients of variation (CV) from the 1991–2018 habitat-based density models for striped dolphin. Panels show the yearly average density based on predicted daily striped dolphin densities covering the 1996-2018 survey periods (summer/fall). Predictions are shown for the study area (1,141,800 km^2). White dots in the average plots show actual sighting locations from the respective SWFSC summer/fall ship surveys. 44
Figure 3g. Predicted annual (1996-2018) mean density (animals km^{-2}) and associated coefficients of variation (CV) from the 1991–2018 habitat-based density models for common bottlenose dolphin. Panels show the yearly average density based on predicted daily common bottlenose dolphin densities covering the 1996-2018 survey periods (summer/fall). Predictions are shown for the study area (1,141,800 km^2). White dots in the average plots show actual sighting locations from the respective SWFSC summer/fall ship surveys. 45
Figure 3h. Predicted annual (1996-2018) mean density (animals km^{-2}) and associated coefficients of variation (CV) from the 1991–2018 habitat-based density models for Dall's porpoise. Panels show the yearly average density based on predicted daily Dall's porpoise densities covering the 1996-2018 survey periods (summer/fall). Predictions are shown for the study area (1,141,800 km^2). White dots in the average plots show actual sighting locations from the respective SWFSC summer/fall ship surveys. 46
Figure 3i. Predicted annual (1996-2018) mean density (animals km^{-2}) and associated coefficients of variation (CV) from the 1991–2018 habitat-based density models for sperm whale. Panels show the yearly average density based on predicted daily sperm whale densities covering the 1996-2018 survey periods (summer/fall). Predictions are shown for the study area (1,141,800 km^2). White dots in the average plots show actual sighting locations from the respective SWFSC summer/fall ship surveys. 47
Figure 3j. Predicted annual (1996-2018) mean density (animals km^{-2}) and associated coefficients of variation (CV) from the 1991–2018 habitat-based density models for minke whale. Panels show the yearly average density based on predicted daily minke whale densities covering the 1996-2018 survey periods (summer/fall). Predictions are shown for the study area (1,141,800 km^2). White dots in the average plots show actual sighting locations from the respective SWFSC summer/fall ship surveys. 48
Figure 3k. Predicted annual (1996-2018) mean density (animals km^{-2}) and associated coefficients of variation (CV) from the 1991–2018 habitat-based density models for blue whale. Panels show the yearly average density based on predicted blue whale densities covering the 1996-2018 survey periods (summer/fall). Predictions are shown for the study area (1,141,800 km^2). White dots in the average plots show actual sighting locations from the respective SWFSC summer/fall ship surveys. 49
Figure 3l. Predicted annual (1996-2018) mean density (animals km^{-2}) and associated coefficients of variation (CV) from the 1991–2018 habitat-based density models for fin whale. Panels show the yearly average density based on predicted fin whale densities covering the 1996-2018 survey periods (summer/fall). Predictions are shown for the study area (1,141,800 km^2). White dots in the average plots show actual sighting locations from the respective SWFSC summer/fall ship surveys. 50
Figure 3m. Predicted annual (1996-2018) mean density (animals km^{-2}) and associated coefficients of variation (CV) from the 1991–2018 habitat-based density models for humpback whale. Panels show the yearly average density based on predicted humpback

whale densities covering the 1996-2018 survey periods (summer/fall). Predictions are shown for the study area (1,141,800 km^2). White dots in the average plots show actual sighting locations from the respective SWFSC summer/fall ship surveys. 51
Figure 3n. Predicted annual (1996-2018) mean density (animals km^{-2}) and associated coefficients of variation (CV) from the 1991–2018 habitat-based density models for Baird's beaked whale. Panels show the yearly average density based on predicted Baird's beaked whale densities covering the 1996-2018 survey periods (summer/fall). Predictions are shown for the study area (1,141,800 km^2). White dots in the average plots show actual sighting locations from the respective SWFSC summer/fall ship surveys. 52
Figure 3o. Predicted annual (1996-2018) mean density (animals km^{-2}) and associated coefficients of variation (CV) from the 1991–2018 habitat-based density models for the small beaked whale guild (Mesoplodonts and Cuvier's beaked whale). Panels show the yearly average density based on predicted small beaked whale guild densities covering the 1996-2018 survey periods (summer/fall). Predictions are shown for the study area (1,141,800 km^2). White dots in the average plots show actual sighting locations from the respective SWFSC summer/fall ship surveys. 53

Introduction

The 2018 California Current Ecosystem Survey (CCES) was conducted between 26 June and 4 December 2018 as a joint project of the Marine Mammal and Turtle Division (MMTD) and the Fisheries Resources Division (FRD) of NOAA's Southwest Fisheries Science Center (SWFSC). One of the primary objectives of this line-transect survey was to collect marine mammal sighting data to support the derivation of cetacean density estimates for the California Current Ecosystem (CCE) study area. Given the heterogeneity of the 2018 survey coverage in the CCE study area (Henry et al. 2020), density estimation required model-based (rather than design-based) analytical approaches for updating population size estimates for US West Coast marine mammal stocks. This report summarizes the results of the cetacean habitat modeling effort.

Habitat models, or species distribution models (SDMs), have been recognized as valuable tools for estimating the density and distribution of cetaceans and assessing potential impacts from a wide range of anthropogenic activities (e.g., Abrahms et al. 2019; Gilles et al. 2011; Goetz et al. 2012; Hammond et al. 2013; Redfern et al. 2013). SDMs for cetaceans have been developed for US West Coast waters from systematic ship survey data collected by SWFSC since 1991 (Barlow et al. 2009; Becker et al. 2010, 2014, 2016, 2018, 2020; Forney 2000; Forney et al. 2012). The most recent models provide spatially-explicit density predictions at a 0.1˚ (approximately 10km x 10km) grid resolution (Becker et al. 2020), and multi-year average density surfaces have been used by the US Navy to assess potential impacts on cetaceans as required by US regulations such as the Marine Mammal Protection Act and Endangered Species Act (U.S. Department of the Navy 2013, 2015, 2017).

The overall goal of this study was to include the 2018 survey data in the previous 1991–2014 modeling dataset in order to improve SMDs for the CCE study area. Specific objectives included:

- Generating multi-year average density surfaces for the Navy and others to use in their long-term (2–7 year) environmental planning efforts; and
- Providing updated abundance and "minimum population size (Nmin)" estimates as defined in the Guidelines for Assessing Marine Mammal Stocks (National Oceanic and Atmospheric Administration 2016).

To develop improved SDMs and to update US West Coast cetacean stock abundance estimates, sighting data from CCES 2018 were combined with previous line-transect survey data collected within the CCE to create a robust modeling database spanning more than 25 years (1991–2018). Habitat models were developed based on previously established methods that allow for the incorporation of segment-specific estimates of detection probability and included dynamic covariates from an ocean model calibrated to the CCE study area (Becker et al. 2016). In addition, recently-developed techniques for deriving more comprehensive estimates of uncertainty in SDM predictions (Miller et al. *In Prep.*) were used to provide variance estimates for the model-based abundance estimates. SDMs were developed for long-beaked common dolphin (*Delphinus delphis bairdii*), short-beaked common dolphin (*Delphinus delphis delphis*), Risso's dolphin (*Grampus griseus*), Pacific white-sided dolphin (*Lagenorhynchus obliquidens*), northern right whale dolphin (*Lissodelphis borealis*), striped dolphin (*Stenella coeruleoalba*), common bottlenose dolphin (*Tursiops truncatus*), Dall's porpoise (*Phocoenoides dalli*), sperm

whale (*Physeter macrocephalus*), blue whale (*Balaenoptera musculus*), fin whale (*B. physalus*), humpback whale (*Megaptera novaeangliae*), Baird's beaked whale (*Berardius bairdii*), and a "small beaked whale guild" that included Mesoplodonts (*Mesoplodon* spp.) and Cuvier's beaked whale (*Ziphius cavirostris*). Sample sizes were also sufficient to develop the first model-based density estimates for minke whale (*B. acutorostrata*) in this study area.

The habitat-based models of cetacean density developed in this study represent an improvement over the previous models described by Becker et al. (2020) because they included additional sighting data over the continental shelf and slope that were surveyed more sparsely in previous years, providing better representation of these important habitat regions. In addition, the model-based abundance estimates more accurately account for uncertainty than prior iterations owing to methodological improvements.

Methods

Survey data

Cetacean sighting data used to build the SDMs were collected within waters of the CCE from 1991–2018 (Table 1) using line-transect methods (Buckland et al. 2001). The 1991–1993 surveys covered waters off the state of California while the 1996–2008 and 2014 surveys covered waters off the entire west coast of the United States, with all surveys extending approximately 300 nautical miles offshore (Barlow and Forney 2007). The 2009 survey was a finer-scale survey that focused on waters off central and southern California, as well as the west coast of Baja California (Carretta et al. 2011). The 2018 survey covered waters along the west coasts of southern Canada (Vancouver Island), the west coast of the United States, and Baja California out to a distance of approximately 200 nautical miles offshore (Henry et al. 2020). When combined across years, the surveys provided comprehensive coverage of waters throughout the CCE study area, although the spatial heterogeneity of the 2018 survey is clearly apparent (Figure 1). Only on-effort data collected in Beaufort sea state conditions ≤5 within the study area were used in model development.

The survey protocols were the same for all years (see Barlow 2006; Kinzey et al. 2000) and are briefly summarized here. Each survey used a NOAA research vessel and a team of six experienced visual observers. For each rotation, three observers stationed on the flying bridge of the ship visually searched for and recorded cetacean sightings between 0 and 90 degree to port and starboard using standard line-transect protocols. Port and starboard observers searched with pedestal-mounted 25 × 150 binoculars and a center-stationed third observer searched by eye or with handheld 7 × 50 binoculars. When cetaceans were detected within 3 nautical miles (5.6 km) of the trackline, the sighting was recorded (along with distance and direction from the vessel, from which perpendicular sighting distance was calculated), and the ship would then typically divert from the transect line and go “off-effort” to approach the animals and enable more accurate estimation of group size and species identification. All observers independently provided best, high, and low group size estimates. If the sighting included more than one species, the observers also estimated the percentage of each species in the group. The best estimate from each observer or the best estimate multiplied by the percentage of each species was averaged (i.e., arithmetic mean) to obtain a single group size estimate for each sighting.

Systematic survey effort was conducted along predetermined tracklines at a target survey speed of 18.5 km/hr. During transit between tracklines, transits to or from port, or deviations from pre-determined tracklines for other purposes, the visual observers generally maintained standard data collection protocols. Although such non-systematic effort is generally not used to derive encounter rate for design-based density estimates, it is incorporated into the SDMs as the uneven distribution of effort can be accounted for within the statistical framework (Hedley and Buckland 2004).

Environmental predictor data

To create samples for modeling, continuous portions of on-effort survey tracklines were divided into approximate 5-km segments using methods described by Becker et al. (2010). The total number of species-specific sightings and associated average group size estimates were assigned to each segment and habitat covariates were derived based on the segment’s geographical

midpoint. To maintain consistency with the species-specific effective-strip-width estimates derived for this study based on methods described in Barlow et al. (2011a) and used to estimate cetacean densities, sighting data were truncated at a distance of 5.5 km perpendicular to the trackline for the delphinids and large whales, 4.0 km for small whales (Mesoplodonts, minke whale, and Cuvier's beaked whale), and at 3.0 km for Dall's porpoise (Buckland et al. 2001).

Environmental variables from a data-assimilative CCE implementation of the Regional Ocean Modeling System (ROMS), produced by the University of California Santa Cruz Ocean Modeling and Data Assimilation group (Moore et al. 2011), were used as dynamic predictors as they have proven effective in similar SDMs for this study area (Becker et al. 2016, 2018, 2020). Daily averages for each variable at the 0.1 degree (~10 km) horizontal resolution of the ROMS output were used in the models. The suite of potential dynamic predictors included sea surface temperature (SST) and its standard deviation (sd(SST)), calculated for a 3 × 3-pixel box around the modeling segment midpoint, mixed layer depth (MLD, defined by a 0.5˚C deviation from the SST), sea surface height (SSH), and sd(SSH). Water depth (m) was also included as a potential predictor, derived from the ETOPO1 1-arc-min global relief model (Amante and Eakins 2009) and obtained for the midpoint of each transect segment. In addition, distance to the 200-m isobath derived from the geomorphic feature map of the global ocean (Harris et al. 2014) was included in model selection as it represents the edge of the shelf break for much of the U.S. west coast and can be a distinguishing habitat feature for many cetacean species (Becker et al. 2010; Fiedler et al. 1998, 2018). In addition, for those species known to primarily inhabit offshore waters (beaked whales, sperm whale, striped dolphin), distance to the 2,000-m isobath was also included in the list of potential predictor variables, as this depth roughly represents the transition from the continental slope to the continental rise. To differentiate continental shelf, slope, and rise waters, negative values of the distance to isobath terms were used for waters shallower than the 200m or 2,000m isobath. Although the modeling framework applied in our analysis (*mgcv*; see 'Habitat Models' section below) is robust to correlated variables (Wood 2008), distance to the two isobath terms and depth (absolute correlation = 0.75–0.85) were considered separately in the models to avoid any confounding effects.

A spatial term (bivariate spline of longitude and latitude) was also included in the suite of potential predictors because SDMs that explicitly account for geographic effects have exhibited improved explanatory performance as they often account for unmeasured static variables that might be important for driving species distributions (Becker et al. 2018; Cañadas and Hammond 2008; Forney et al. 2015; Hedley and Buckland 2004; Tynan et al. 2005; Williams et al. 2006). The inclusion of a spatial term can result in more robust models but invalidates predictions outside the study area.

A continuous year term was also included as a potential predictor in the models to capture population trends both for species whose abundance has changed substantially during the time period considered in our analyses, and for species for which distribution shifts have resulted in abundance changes over time. For example, increases in population have been documented for both fin whale (Moore and Barlow 2011) and humpback whale (Barlow et al. 2011b), while notable shifts in distribution over the last few decades have resulted in a decline in the number of blue whales (Monnahan et al. 2015), and an increase in the number of short-beaked common dolphins (Barlow 2016; Becker et al. 2018) in the CCE study area. The degrees of freedom for the year term were constrained (i.e., < the maximum of 8 available) in order to capture linear or

thresholds in the response curves rather than simply tracking the variable encounter rates over the survey periods. In addition, since environmental covariates are often correlated with time, and year can serve as a proxy for unmeasured habitat variables, the functional forms of all the other dynamic variables were inspected during the modeling process to ensure they remained stable with the addition of the year term.

Correction factors

During CCES 2018, operational requirements necessitated that some of the effort be conducted in passing mode (i.e., when a cetacean/cetacean group is sighted the ship continues on course and is not diverted to the vicinity of the sighting for species identification or group size enumeration). This led to a high proportion of recorded "unidentified large whale" and "*Delphinus* spp." sightings, when observers could not confirm which species of large whale or common dolphin subspecies was present, respectively. Omitting these sightings from the modeling dataset would have resulted in an underestimation of animal density for blue, fin, and humpback whales, as well as both long-and short-beaked common dolphins. To reduce this potential downward bias, species-specific correction factors were applied to account for unidentified animals, using the methods described in Becker et al. (2017) and summarized below.

For both the large whale and common dolphin groups, the correction factor c was estimated from the 2018 sighting data according to the simplified formula:

$$c = 1 + \frac{t_{unid}}{t_{tgt} + t_{oth}} \tag{1}$$

where t_{tgt} is the number of individuals identified as the target species, t_{oth} is the number of individuals identified as other species within the broader species group, and t_{unid} is the number of unidentified individuals in that species group. Due to the potential effect of Beaufort sea state on detectability (Barlow et al. 2001, 2011a; Barlow 2015), the correction factors were evaluated to determine if they varied by sea state. If so, separate correction factors were developed by sea state; otherwise a single correction factor was applied. The correction factors were applied to the numbers of animals estimated per segment in the SDMs for the common dolphin and large whale species (see equation 2 below).

The protocol for estimating sperm whale group size changed over the course of the 1991–2018 survey period, with less effort spent estimating group size during the three surveys conducted in the 1990's. Group size estimates for larger sperm whale groups (> 2 animals) are now known to have been underestimated in the earlier surveys, and a correction factor has been estimated to account for this bias (Moore and Barlow 2014). Prior to modeling, this correction factor (2.3x) was applied to the average group size estimates for observed sperm whale group sizes > 2 for the 1991–1996 surveys. No group size corrections were applied to the other species.

Habitat models

Generalized Additive Models (GAM; Wood 2017) were developed in R (v. 3.4.1; R Core Team, 2017) using the package "*mgcv*" (v. 1.8-31; Wood 2011). Methods largely followed those described in Becker et al. (2016) and are summarized here. One of two modeling frameworks was used for each species, depending on its group size characteristics. For the two *Delphinus*

species that have very large and variable group sizes (e.g., 1 to 2,000 animals per sighting), separate encounter rate and group size models were developed. Encounter rate models were built using all transect segments, regardless of whether they included sightings, using the number of sightings per segment as the response variable and a Tweedie distribution to account for overdispersion (Miller et al. 2013). Group size models were built using only those segments that included sightings, using the natural log of group size as the response variable, and a Gaussian link function. For the rest of the species, GAMs were fit using the number of individuals of the given species per transect segment as the response variable using all transect segments, and a Tweedie distribution to account for overdispersion. The full suite of potential habitat predictors was offered to both the encounter rate and single response GAMs. A tensor product smooth of latitude and longitude (Wood 2003) was the only predictor variable included in the *Delphinus* group size models.

In all models, restricted maximum likelihood (REML) was used to obtain parameter estimates (Marra and Wood 2011). The shrinkage approach of Marra and Wood (2011) was used to potentially remove terms from each model by modifying the smoothing penalty, allowing the smooth effect to be shrunk to zero. Additionally, to avoid overfitting, an iterative forwards/backwards selection process was used to remove variables that had P-values > 0.05 (Redfern et al. 2017; Roberts et al. 2016). The natural log of the effective area searched (described below) was included as an offset in both the single response and encounter rate models.

Predictions from the final model were incorporated into the standard line-transect equation (Buckland et al. 2001) to estimate density (*D*; number of animals per km^2):

$$D_i = \frac{n_i \cdot s_i \cdot c_i}{A_i} \tag{2}$$

where *i* is the segment, *n* is the number of sightings on segment *i*, *s* is the average group size (i.e., number of a given species present in a group) on segment *i*, *c* is the species-specific correction factor for unidentified common dolphins or large whales (derived in equation 1 and assumed to be 1 for all other species) based on sea state conditions on segment *i*, and *A* is the effective area searched for segment *i*:

$$A_i = 2 \cdot L_i \cdot ESW_i \cdot g(0)_i \tag{3}$$

where L_i is the length of the effort segment *i*, ESW_i is the effective strip half-width, and $g(0)_i$ is the probability of detection on the transect line. Following the methods of Becker et al. (2016), species-specific and segment-specific estimates of both *ESW* and *g(0)* were incorporated into the models based on the recorded detection conditions on that segment and using coefficients estimated specifically for the CCE dataset based on methods of Barlow et al. (2011a) for *ESW* and Barlow (2015) for *g(0)*. For those segments where the average Beaufort sea state was 0 (< 1% of the segments), *g(0)* was assumed to be 1, i.e., that all animals directly on the transect line were detected, for all species except Cuvier's beaked whale (*g(0)* = 0.584) and Mesoplodon *spp*. (*g(0)* = 0.813), which were <1 based on dive behavior (Barlow 2015).

In equation (3) above, the effective area searched is multiplied by two to account for observers searching on both sides of the transect line. During the 2018 survey, coastal fog and other conditions occasionally prohibited visual observations on one side of the ship, so that cetacean sighting data were collected on only one side of the transect line. These portions of reduced effort were systematically recorded in the dataset and the effective area searched was reduced accordingly along these segments, i.e., the constant was changed to a "1" in equation (3) above.

Model performance was evaluated using established metrics, including the percentage of explained deviance, the area under the receiver operating characteristic curve (AUC; Fawcett 2006), the true skill statistic (TSS; Allouche et al. 2006), and visual inspection of predicted and observed distributions during the 1991–2018 cetacean surveys (Barlow et al. 2009; Becker et al. 2010, 2016; Forney et al. 2012). AUC measures the accuracy of predicting observed presences and absences; values range from 0 to 1, where a score > 0.5 indicates better than random skill. TSS accounts for both false negative and false positive errors and ranges from -1 to +1, where +1 indicates perfect agreement and values of zero or less indicate a performance no better than random. To calculate TSS, the sensitivity-specificity sum maximization approach (Liu et al. 2005) was used to obtain thresholds for species presence. In addition, the model-based abundance estimates for the CCE study area based on the sum of individual modeling segment predictions were compared to standard line-transect estimates derived from the same dataset used for modeling in order to assess potential bias in the habitat-based model predictions. The standard line-transect estimates were derived from the 1991–2018 survey data using equations (2) and (3) above, but without the inclusion of habitat predictors (i.e., observed rather than predicted densities).

Spatially-explicit density values for the CCE study area were derived from model predictions on the environmental conditions specific to the 1991–2018 CCE effort periods at a 0.1˚ (approximately 10km x 10km) grid resolution. Model predictions were made on separate environmental conditions for each day encompassing the survey periods, thus taking into account the varying oceanographic conditions during the 1991–2018 cetacean surveys. The separate daily predictions thus provide a dataset from which averages can be derived for any temporal period of interest. In past years, the Navy has used a "multi-year average" of predicted daily cetacean species densities to assess potential impacts on cetaceans as required by U.S. regulations such as the MMPA and ESA (U.S. Department of the Navy 2015, 2017). To ensure that the multi-year average reflects more recent conditions and is based on those survey years that more comprehensively covered the study area, predictions for 1991, 1993, and 2009 were not included in the multi-year average. Further, for the two species with documented population increases in the study area (i.e., fin and humpback whales), the year covariate was set to 2018 to decrease the potential for biased-low density estimates derived from the multi-year average surfaces. The daily predictions were also used to create individual yearly averages for 1996–2018. The prediction grid was clipped to the boundaries of the approximate 1,141,800-km^2 study area to ensure that predictions were not extrapolated outside the region used for model development.

The model-based abundance estimates were calculated as the sum of the individual grid cell abundance estimates, which were derived by multiplying the cell area (in km^2) by the predicted grid cell density, exclusive of any portions of the cells located outside the CCE study area or on land. Area calculations were completed using the R packages *geosphere* and *gpclib* in R (version 2.15.0).

In highly dynamic ecosystems such as the California Current, variation in environmental conditions has been shown to be one of the greatest sources of uncertainty when predicting density as a function of habitat variables, and this source has been used to provide spatially-explicit variance measures for past CCE SDM model predictions (Barlow et al. 2009; Becker et al. 2016, 2018, 2020; Forney et al. 2012). Recently, Miller et al. (*In Prep.*) developed techniques for deriving more comprehensive measures of uncertainty in GAM predictions that, in addition to environmental variability, also account for the uncertainty from the GAM parameters, *ESW*, and *g(0)*. These techniques include generating multiple daily density surfaces taking into account model parameter uncertainty and providing a range of density estimates from which variance can be calculated.

Preliminary analyses in our study, however, revealed that the simulated model parameter draws can – for some species – result in a subset of unrealistic simulated surfaces (i.e., surfaces that infer high densities of a species in habitats where the species is not generally found), so this method was not yet deemed suitable for estimating spatially explicit uncertainty estimates for the pixel-based densities. The method did, however, confirm that environmental variability contributes the most substantial source of uncertainty in the CCE model predictions. Therefore, the methods of Becker et al. (2016, 2018) were applied to estimate spatially-explicit measures of uncertainty based on environmental variability, calculated as pixel-specific standard errors using the set of daily predictions that went into the multi-year average density estimates. The pixel-based variance estimates are thus under-estimated to some degree, but the dominant source of uncertainty (environmental variability) was accounted for.

The methods described in Miller et al. (*In Prep.*) were found to be suitable for estimating uncertainty in the overall model-based abundances for the entire CCE study area, and thus were used to derive variance estimates that included the combined uncertainty from environmental variability, the GAM parameters, and *ESW*. Study area variance was estimated based on the average values of each of the 200 simulations within each year, thereby providing an overall measure of uncertainty associated with the individual yearly average density surfaces for 1996–2018. One additional source of uncertainty in abundance estimates is introduced by *g(0)*, the probability of detecting animals directly on the trackline. The estimates of *g(0)* developed by Barlow (2015) are based on segment-specific Beaufort sea state conditions, but they were not compatible with the Miller et al. (*In Prep*.) methods of incorporating *g(0)*; therefore, this source of uncertainty was handled separately. An overall estimate of uncertainty in *g(0)* was derived using the variance estimates for this parameter weighted by the proportion of survey effort conducted within each of the Beaufort sea state categories and estimated based on 10,000 bootstrap values. Barlow (2015) did not provide *g(0)* estimates for northern right whale dolphin, and the result for Pacific white-sided dolphin was considered an outlier (Barlow 2015), so for both species the *g(0)* estimates for *Delphinus* spp. were used. *Delphinus* spp. was considered a suitable surrogate for Pacific white-sided dolphin since they have similar sighting characteristics. In addition, the *Delphinus* spp. *g(0)* values were similar to the average of all the delphinids and were thus selected as a surrogate for northern right whale dolphin as well. The weighted *g(0)* uncertainty was combined into the study area variance estimates using the delta method (Seber 1982).

For purposes of calculating Potential Biological Removal (PBR) of US West Coast cetacean stocks, the pooled average of the 2014 and 2018 model-predicted study area abundance estimates

and associated variance estimates, as well as minimum abundance estimates, were also calculated (National Oceanic and Atmospheric Administration 2016). Abundance estimates were based on the arithmetic mean of the model-predicted estimates for 2014 and 2018. Study area variance was estimated based on the methods described above for individual years but including data specific to 2014 and 2018.

Results

Habitat-based density models were developed for 14 species and one guild (Mesoplodonts and Cuvier's beaked whale) using 92,214 km of on-effort survey data collected between 1991 and 2018 within the CCE study area. The number of sightings within the species-specific truncation distances and available for modeling ranged from 39 to 1,034 (Table 2).

Correction factors for unidentified large whales were applied separately by Beaufort sea state for the 2018 blue, fin, and humpback whale sightings, because the proportion of unidentified whales increased with increasing sea state. For blue and humpback whales, these correction factors were 1.03, 1.04, 1.05, 1.20, and 1.26 for Beaufort sea states 0-1, 2, 3, 4, and 5, respectively, and 1.04, 1.08, 1.10, 1.30, and 1.46 for fin whales. For the common dolphin group, higher multipliers were not associated with higher sea states, so a uniform correction factor of 1.71 was applied across all sea states for the 2018 sightings of both long- and short-beaked common dolphins.

Consistent with past modeling studies in the CCE study area (Becker et al. 2016, 2018, 2020), the most commonly selected predictor variables for the encounter rate models of groups (long- and short-beaked common dolphins) or individuals (all other species) included SST, MLD, and the smooth of latitude and longitude (Table 3). SSH and depth were also selected in many of the models. The group size model for both subspecies of common dolphin included a bivariate spline of longitude and latitude, consistent with other studies that have demonstrated significant spatial variation in group size, particularly for Delphinids (Barlow 2015; Ferguson et al. 2006). The functional forms of the key predictor variables were also consistent with those of SDMs built with subsets of the modeling dataset used for this study (Becker et al. 2016, 2018, 2020; Appendix A).

A year covariate was included in the final fin and humpback whale models, and both captured the documented increasing population trends for these species in the CCE study area (Moore and Barlow 2011; Barlow et al. 2011a; Calambokidis et al. 2017). A year term was also included in the models for short-beaked common dolphin and blue whale, consistent with observed northern shifts in the relative distribution of these two species that have resulted in increasing numbers of short-beaked common dolphins and decreasing numbers of blue whales in the CCE study area (Barlow 2016; Becker et al. 2018; Monnahan et al. 2015). A year term was also included in the SDMs for Risso's, striped, and common bottlenose dolphins, as well as Dall's porpoise (Table 3). The functional forms for the year term in all but the striped dolphin model suggest a decreasing trend in the numbers of these species in the CCE study area during the course of the survey period (Appendix A). For all three species, year represents a significant but very small effect as indicated by the range of values on the y-axis (i.e., relative to the other covariates the y-axis value for year is <1; Figures A3,A7, A8). The functional form of the year term in the striped dolphin model fluctuates throughout the 1991–2018 survey period (Figure A6), consistent with the highly variable abundance estimates for this species for each of the individual survey years (Barlow 2016; Becker et al. 2018).

Deviance explained by the models was variable, ranging from approximately 7% to 57% (Table 3). With the exception of sperm whale, AUC values for all models were greater than 0.7 and the majority were greater than 0.8, indicating that the models did a good job predicting true positives and negatives. The TSS values, which account for both omission and commission errors, were

more variable, ranging from 0.18 (sperm whale) to 0.90 (long-beaked common dolphin). All models had observed: predicted density ratios higher than 0.7, with the majority higher than 0.9, indicating that the sum of the segment-based density predictions captured overall abundance in the study area as derived from design-based line-transect methods.

The 1996–2018 multi-year average density surface maps generally captured observed distribution patterns as illustrated by actual sightings during the surveys (Figure 2). For the two species with documented population increases in the study area (i.e., fin and humpback whales), the density estimates were scaled to the 2018 abundance to decrease the potential for biased-low density estimates derived from the multi-year average surfaces (Figures 2l and 2m). The CVs, which were based on the environmental variability of the daily predictions, showed substantial variation among the species, with a few individual pixel values as high as 6.0 (e.g., common bottlenose dolphin and fin whale, Figures 2g and 2l).

The yearly average density surface maps show high annual variability for some species (e.g., short-beaked common dolphin, striped dolphin, Dall's porpoise, blue whale, fin whale) and less so for other species (e.g., minke whale, Baird's beaked whale) (Figure 3). There is almost no variability in the yearly density plots for sperm whale (Figure 3i), due to the overwhelming contribution of the distance to 2,000m isobath term. The pixel-based CVs were generally highest in 2005, suggesting that there was substantial variability in the habitat covariates within this year. For the majority of the species, the yearly sightings match well with the density predictions. However, given the heterogeneity of survey coverage in 2018, sighting data from this survey are not as useful for cross validation since survey coverage needs to be taken into account when assessing the accuracy of the density predictions. For example, the models for both short-beaked common and striped dolphins predict high density in the southwestern portion of the CCE study area in 2018 (Figures 3b and 3f), where there was no survey effort (Figure 1).

The model-based yearly abundance estimates were highly variable for the majority of the species considered here, particularly for those with documented trends due to either changes in abundance or shifts in distribution (i.e., fin, humpback, and blue whales, and short-beaked common dolphin; Table 4). Even for those species for which a year term did not enter the model, substantial variability in the annual model-predicted abundance values were apparent, particularly for the most recent survey years (e.g., long-beaked common dolphin, northern right whale dolphin, Baird's beaked whale). Interestingly, the most stable mean abundance estimates over the 1991–2018 survey period were for sperm whale and the small beaked whale guild (Table 4), the two SMDs that generally had the worst performance metrics among all the species models (Table 3).

Four sources of uncertainty (i.e., environmental variability, GAM parameters, *ESW*, and *g(0))* were combined to provide an overall measure of variance for the model-based study area abundance estimates (Table 4). Uncertainty estimates from the combination of environmental variability, GAM parameters, and ESW estimates ("CV_m (Model)" in Table 4) were variable, ranging from 0.017 for sperm whale to 0.782 for northern right whale dolphin. The final model for sperm whale included only two predictors, of which one was dynamic (Table 3), so the low "Model" CVs are likely due to low parameter variability. Conversely, the final model for northern right whale dolphin included five predictors with large standard error bands around four (Table 3 and Figure A-5), resulting in high variability in the parameter simulations used to derive

the variance estimates. Uncertainty due to the Beaufort-weighted g(0) values was quite high for many of the species, particularly Dall's porpoise (CV = 0.518) and minke whale (CV = 0.787). When combined, overall measures of CV for the study area abundance estimates were highly variable among the species, ranging from 0.127 (Risso's dolphin) to 0.799 (minke whale). Similar to the yearly estimates, CVs for the pooled 2014 and 2018 abundance estimates were also variable among species (Table 5).

Discussion and Conclusions

During the last 20 years, subsets of the 1991–2018 SWFSC survey data have been used to model the relationship between habitat predictors and species density, both to improve abundance estimates and to gain valuable insight on spatial and temporal changes in species distributions (Barlow et al. 2009; Becker et al. 2010, 2014, 2016, 2018, 2020; Forney 2000; Forney et al. 2012). With each added year of survey data, the models for most species have become more robust, as increased numbers of sightings collected over a broader range of oceanic conditions have been able to better inform the models. The key functional forms for many of the species have become stable over time, suggesting that at this decadal temporal scale relationships with certain habitat predictors have not changed, despite changing oceanic conditions (e.g., Becker et al. 2018). For example, the functional form of SST in the Dall's porpoise GAM consistently shows a threshold effect at approximately 16°C (Figure A8), apparent in previous GAMs built with only the 1991 and 1996 survey data (Forney 2000). The relationship between SST and fin whale density has also remained constant throughout the 1991 to 2018 period, with the highest densities of whales in waters between about 14°C and 18°C (Figure A12), consistent with GAMs developed with only four years of survey data (1991–2001; Becker et al. 2010). Although high seasonal and interannual variability in cetacean abundance and distribution patterns have been observed and predicted from habitat models developed for the CCE study area (Barlow and Forney 2007; Becker et al. 2014, 2017, 2018; Forney and Barlow 1998; Forney et al. 2012), the multi-year average density plots for the majority of species are broadly similar over the 1991–2018 time period, demonstrating consistency in "average" distribution patterns. These density estimates represent a composite view for the summer/fall survey months (typically July through November) and should not be extrapolated outside of these seasons, given the seasonality of the California Current Ecosystem.

Since a main objective of this study was to produce robust average multi-year density surfaces, a bivariate spline of longitude and latitude was included in the SDMs to increase their explanatory performance (Cañadas and Hammond 2008; Forney et al. 2015; Hedley and Buckland 2004; Tynan et al. 2005; Williams et al. 2006). As Becker et al. (2018) demonstrated, however, for many species the inclusion of a spatial term does not improve a model's novel predictive power, suggesting that these models may not provide the best nowcasts or forecasts.

For Risso's dolphin, sperm whale, and the small beaked whale guild, previous SDMs have not performed well, and there has generally been poor correlation between predicted density patterns and the sighting data used to build the models (Becker et al. 2010, 2020; Forney et al. 2012). Sightings of Risso's dolphins within the CCE study area are concentrated either along the continental shelf (mainly south of 38°N) or in offshore deep waters, with a distinct longitudinal absence between these two areas (Barlow 2016; Barlow and Forney 2007). In the present study, this observed spatial pattern was captured quite well (Figure 2c), likely due to the addition of the CCES 2018 survey data, which contributed an additional 39 sightings to the modeling dataset and provided improved sampling of the continental shelf habitat.

Conversely, models for both sperm whale and the small beaked whale guild showed little to no improvement, with some of the worst model metrics among all species and predicted distribution patterns that match poorly to actual sightings during the surveys (Table 3, Figures 2h, 2n). The addition of the CCES 2018 survey data did not improve either of these models, likely due to the

very sparse sampling of offshore waters where both sperm and small beaked whales are typically found. These results also suggest that the current suite of environmental variables offered to the models are not effective proxies for their habitat and prey. Model improvements for these deep-diving species may only be realized by identifying an available proxy that better captures the ecological processes driving their distribution or by using alternative data (e.g., acoustics) for model input.

Unlike previous modeling efforts where a year term was considered only for those species with documented population increases or decreases in the CCE study area, a year term was included in the list of potential predictors for all the SDMs in this study. To ensure that year did not simply track the variable encounter rates over the 1991–2018 survey period, this term was constrained (i.e., the degrees of freedom were reduced) in the GAMs in order to identify a trend or threshold effect. Consistent with past modeling efforts, the year term entered the SDMs for those species with documented increases in population in the study area (fin and humpback whales; Moore and Barlow 2011; Barlow et al. 2011a; Calambokidis et al. 2017) and for those species with documented distribution shifts that have resulted in substantial changes in the number of animals present in the study area (blue whale and short-beaked common dolphin; Barlow 2016; Becker et al. 2018; Monnahan et al. 2015). A year term was also included in the striped dolphin GAM, indicating flucutating numbers of this species in the study area over the survey period (Figure A6). This result is consistent with past studies that suggest that available striped dolphin habitat fluctuates substantially with changing ocean conditions (Barlow 2016; Becker et al. 2018, 2020), and since the range of this species extends continuously from the study area south to waters offshore Mexico (Perrin et al. 1985; Mangels and Gerrodette 1994), there can be a large increase or decrease of animals in the study area in any single year.

A year term was also included in the models for Risso's dolphin, common bottlenose dolphin, and Dall's porpoise, suggesting a decreasing trend in the numbers of these species in the CCE study area during the course of the survey period (Figures A3, A7, A8). A negative year trend indicates that the numbers of these species in the study area has decreased either due to a true change in population or to a distribution shift out of the study area. Boyd et al. (2018) demonstrated that the amount of suitable Dall's porpoise habitat within the CCE study area changed substantially during the 1991–2008 survey period, so perhaps this could be driving the apparent decrease in numbers of this species over time. The yearly density predictions for Dall's porpoise do not appear consistent with a shift in distribution to the north, however, but rather imply a contraction of suitable habitat centered off Oregon and northern California (Figure 3h). Bayesian hierarchical approaches have been used to improve population trend analyses for fin, sperm, and beaked whales in the CCE (Moore and Barlow 2011, 2014, 2017). Similar trend analyses that incorporate the additional 2018 survey data are needed to resolve what is driving the apparent decrease in abundance indicated by the GAMs for Risso's dolphin, common bottlenose dolphin, and Dall's porpoise.

The modeling framework used in the present analysis was largely the same as that used in Becker et al. (2016), but incorporated updated measures of uncertainty in the study area abundance estimates based on a modification of the methods described in Miller et al. (*In Prep.*). This is an improvement from past studies that only accounted for uncertainty due to environmental variability. Uncertainty estimates for the overall study-area abundance estimates based on the combined sources of environmental variability, GAM parameters, and *ESW* were

generally lower for species with high sighting numbers and lower variability in encounter rates such as short-beaked common dolphin, Dall's porpoise, and blue, fin, and humpback whales (Table 4). Uncertainty due to the Beaufort-weighted *g(0)* values was quite high for many of the species, and served to increase uncertainty in the overall study area abundance estimates. This is not surprising given the nontrivial uncertainty estimates associated with the Beaufort-specific *g(0)* values calculated by Barlow (2015) and used in this study. Similar to past studies, the pixel-based variance estimates presented here account for uncertainty due to environmental variability and are thus under-estimated to some degree. Methods to derive spatially-explicit variance measures that also account for uncertainty in the GAM parameters, *ESW*, and *g(0)* are currently in development (Miller et al. *In Prep*.).

For all species, abundance estimates derived from the habitat-based models are more stable than previous design-based estimates for each of the 1996–2014 survey years (Barlow 2016). Design-based estimates are based on the realized encounter rates within each year, and are thus subject to high variation due to sampling error and patchiness in both the environment and animal distribution. This generally results in highly variable single year abundance estimates that often appear inconsistent with long-term trends in animal abundance (Moore and Barlow 2014). Conversely, habitat models establish relationships between environmental predictors and species density based on the full, multi-year dataset, and yearly abundance estimates derived from the models are based on the temporally-specific environmental conditions throughout the study area, thus serving to smooth across the annual variation in observed encounter rates along transect lines. This results in less variability in model-based abundance estimates between years, as much of the remaining variance is largely attributed to environmental variability rather than to low single year sample size (Barlow et al. 2009; Forney et al. 2012). The most variable yearly design-based estimates are thus typically for those species with the highest variation in encounter rates (Barlow 2016), and these tend to differ most from the more stable model-based estimates (e.g., common bottlenose dolphin, Table 4).

GAMs are able to effectively deal with spatial heterogeneity of survey coverage within the statistical framework (Hedley and Buckland 2004), and thus the CCES 2018 survey contributed valuable data to the CCE modeling dataset and allowed for population size updates for many of the US West Coast cetacean stocks. Offshore waters were undersampled, however, and SDMs for species that primarily inhabit these regions did not improve with the addition of the CCES 2018 data (i.e., sperm whale, beaked whales). One of the greatest strengths of the SWFSC dataset is the broad, consistent survey coverage of the CCE study area over multiple years, which has supported novel analyses and methodological improvements in SDM development. For example, the SWFSC CCE dataset has supported the evaluation of different modeling approaches, different sampling scales, different interpolation methods, and different sources of habitat data (Barlow et al. 2009; Becker et al. 2010, 2016, 2020; Forney et al. 2012; Redfern et al. 2008). This extensive dataset has also supported studies evaluating the predictive ability of SDMs to provide nowcasts, forecasts, and across-season predictions (Becker et al. 2012, 2014, 2018), as well as allow for robust trend analyses (Moore and Barlow 2011, 2014, 2017). While systematic regional surveys or those that cover only portions of the CCE study area provide valuable data, routine survey coverage of the full study area is required to maintain and increase the utility of this unique dataset.

As additional data are collected on future surveys, model improvements are expected to continue, both from increased sample sizes and ideally from surveys conducted in more anomalous conditions that will allow for an even broader range of habitat conditions to be represented. Model improvements are also expected from the availability of additional habitat variables that are more relevant to the cetaceans than the proxy variables used here. Improvements to ocean model products may in turn produce more robust cetacean SDMs, particularly if the ocean model outputs can be produced at finer spatial resolutions. Continued methodological improvements are also expected, with active research aimed at developing robust methods for combining data from different sources, e.g., visual line-transect, passive acoustics, tagging data, etc. For those species that exhibit substantial distribution shifts in and out of the CCE study area, e.g., striped dolphin, long-beaked common dolphin, and Dall's porpoise (Becker et al 2018; Boyd et al. 2018; Carretta et al. 2011), SDMs that incorporate survey data that better sample the broader distribution range of these species should provide greater insight into observed abundance changes within the study area. SDMs that incorporate data from portions of the CCES 2018 survey that covered waters along the west coasts of southern Canada and Baja California will help in this regard, and SDMs for waters off Baja California are currently in development.

Acknowledgements

The California Current Ecosystem survey data used in this analysis were collected by a large dedicated team from NOAA's Southwest Fisheries Science Center. We gratefully acknowledge the survey coordinators, cruise leaders, marine mammal observers, ships' officers and crew who all contributed to collecting these data. Chief Scientists for the ship surveys included Tim Gerrodette, Susan Chivers, and three of the co-authors (JB, JEM, and KAF). We thank the UCSC Ocean Modeling group for providing ROMS output. The ROMS near real-time system is supported by NOAA through a grant to the CeNCOOS Regional Association. The methods used to derive uncertainty estimates were developed as part of "DenMod: Working Group for the Advancement of Marine Species Density Surface Modeling" funded by OPNAV N45 and the SURTASS LFA Settlement Agreement, and managed by the U.S. Navy's Living Marine Resources (LMR) program under Contract No. N39430-17-C-1982. This modeling project was funded by the Navy, Commander, U.S. Pacific Fleet (U.S. Navy), the Bureau of Ocean Energy Management (BOEM), and by the National Oceanic and Atmospheric Administration (NOAA), National Marine Fisheries Service (NMFS), Southwest Fisheries Science Center (SWFSC). The 2018 survey was conducted as part of the Pacific Marine Assessment Program for Protected Species (PacMAPPS), a collaborative effort between NOAA Fisheries, the U.S. Navy, and BOEM to collect data necessary to produce updated abundance estimates for cetaceans in the CCE study area. BOEM funding was provided via Interagency Agreement (IAA) M17PG00025, and Navy funding via IAA N0007018MP4C560. This report was improved by the helpful reviews of Chip Johnson, Desray Reeb, and Jim Carretta.

Literature Cited

Abrahms B, Welch H, Brodie S, Jacox MG, Becker EA, Bograd S, Irvin LM, Palacios DM, Mate BR, Hazen EL. 2019. Dynamic ensemble models to predict distributions and anthropogenic risk exposure for highly mobile species. Diversity and Distributions, 25(8): 1182–1193. doi: 10.1111/ddi.12940

Allouche O, Tsoar A, Kadmon R. 2006. Assessing the accuracy of species distribution models: Prevalence, kappa and the true skill statistic (tss). Journal of Applied Ecology. 43(6):1223-1232.

Amante C, Eakins BW. 2009. Etopo1 1 arc-minute global relief model: Procedures, data sources and analysis. U.S. Dep. Commer., NOAA Tech. Memo., NESDIS NGDC-24.

Barlow J. 2006. Cetacean abundance in Hawaiian waters estimated from a summer–fall survey in 2002. Marine Mammal Science. 22(2):446–464.

Barlow J. 2015. Inferring trackline detection probabilities, g(0), for cetaceans from apparent densities in different survey conditions. Marine Mammal Science. 31(3):923-943.

Barlow J. 2016. Cetacean abundance in the California Current estimated from ship-based line-transect surveys in 1991-2014. NOAA Administrative Report LJ-16-01. La Jolla, CA, USA. National Marine Fisheries Service.

Barlow J, Balance LT, Forney KA. 2011a. Effective strip widths for ship-based line-transect surveys of cetaceans. NOAA Technical Memorandum. (NOAA-TM-NMFS-SWFSC-484).

Barlow J, Calambokidis J, Falcone EA, Baker CS, Burdin AM, Clapham PJ, Ford JKB, … Yamaguchi M. 2011b. Humpback whale abundance in the North Pacific estimated by photographic capture-recapture with bias correction from simulation studies. Marine Mammal Science, 27, 793–818.

Barlow J, Ferguson MC, Becker EA, Redfern JV, Forney KA, Vilchis IL, Fiedler PC, Gerrodette T, Ballance LT. 2009. Predictive modeling of cetacean densities in the eastern Pacific Ocean. NOAA Technical Memorandum NMFS-SWFSC-444: La Jolla, CA, USA.

Barlow J, Forney KA. 2007. Abundance and population density of cetaceans in the California Current Ecosystem. Fishery Bulletin. 105:509–526.

Barlow J, Gerrodette T, Forcada J. 2001. Factors affecting perpendicular sighting distances on shipboard line-transect surveys for cetaceans. Journal of Cetacean Research and Management 3:201–212

Becker EA, Carretta JV, Forney KA, Barlow J, Brodie S, Hoopes R, Jacox MG, Maxwell SM, Redfern JV, Sisson NB, Welch H, Hazen EL. 2020. Performance evaluation of cetacean species distribution models developed using generalized additive models and boosted regression trees. Ecology and Evolution, 10, 5759-578.

Becker EA, Foley DG, Forney KA, Barlow J, Redfern JV, Gentemann CL. 2012. Forecasting cetacean abundance patterns to enhance management decisions. Endangered Species Research. 16, 97–112.

Becker EA, Forney KA, Ferguson MC, Foley DG, Smith RC, Barlow J, Redfern JV. 2010. Comparing California Current cetacean–habitat models developed using in situ and remotely sensed sea surface temperature data. Marine Ecology Progress Series. 413:163–183.

Becker EA, Forney KA, Fiedler PC, Barlow J, Chivers SJ, Edwards CA, Moore AM, Redfern JV. 2016. Moving towards dynamic ocean management: How well do modeled ocean products predict species distributions? Remote Sens-Basel. 8(2):149.

Becker EA, Forney KA, Foley DG, Smith RC, Moore TJ, Barlow J. 2014. Predicting seasonal density patterns of California cetaceans based on habitat models. Endangered Species Research, 23, 1–22.

Becker EA, Forney KA, Redfern JV, Barlow J, Jacox MG, Roberts JJ, Palacios DM. 2018. Predicting cetacean abundance and distribution in a changing climate. Diversity and Distributions. 25(4):626-643.

Becker EA, Forney KA, Thayre BJ, Debich AJ, Campbell GS, Whitaker K, Douglas AB, Gilles A, Hoopes R, Hildebrand JA. 2017. Habitat-based density models for three cetacean species off southern California illustrate pronounced seasonal differences. Frontiers in Marine Science. 4(121):1–14.

Boyd C, Barlow J, Becker EA, Forney KA, Gerrodette T, Moore JE, Punt, AE. 2018. Estimation of population size and trends for highly mobile species with dynamic spatial distributions. Diversity and Distributions, 24, 1–12

Buckland ST, Anderson DR, Burnham KP, Laake JL, Borchers DL, Thomas L. 2001. Introduction to distance sampling: Estimating abundance of biological populations. Oxford, United Kingdom: Oxford University Press.

Calambokidis J, Barlow J, Flynn K, Dobson E, Steiger GH. 2017. Update on abundance, trends, and migrations of humpback whales along the US West Coast. International Whaling Commission Paper, SC/A17/NP/13. 17 p.

Cañadas A, Hammond PS. 2008. Abundance and habitat preferences of the short-beaked common dolphin *Delphinus delphis* in the southwestern Mediterranean: Implications for conservation. Endangered Species Research. 4(3):309-331.

Carretta JV, Chivers SJ, Perryman WL. 2011. Abundance of the long-beaked common dolphin (*Delphinus capensis*) in California and western Baja California waters estimated from a 2009 ship-based line-transect survey. Bulletin of the Southern California Academy of Sciences, 110, 152–164.

Fawcett T. 2006. An introduction to roc analysis. Pattern Recognition Letters. 27(8):861-874.

Ferguson MC, Barlow J, Fiedler P, Reilly SB, Gerrodette T. 2006. Spatial models of delphinid (family delphinidae) encounter rate and group size in the eastern tropical Pacific Ocean. Ecological Modelling. 193:645–662.

Fiedler PC, Reilly B., Hewitt RP, Demer D, Philbrick VA, Smith S., … Mate BR. 1998. Blue whale habitat and prey in the California Channel Islands. Deep Sea Research Part II: Topical Studies in Oceanography, 45, 1781–1801.

Fiedler PC, Redfern JV, Forney KA, Palacios DM, Sheredy C, Rasmussen K, García-Godos I, Santillán L, Tetley MJ, Félix F, Ballance LT. 2018. Prediction of large whale distributions: A comparison of presence–absence and presence-only modeling techniques. Frontiers in Marine Science, 5, 1527.

Forney KA. 2000. Environmental models of cetacean abundance: Reducing uncertainty in population trends. Conservation Biology, 14, 1271–1286.

Forney KA, Barlow J. 1998. Seasonal patterns in the abundance and distribution of California cetaceans, 1991–1992. Marine Mammal Science. 14(3):460–489.

Forney KA, Becker EA, Foley DG, Barlow J, Oleson EM. 2015. Habitat-based models of cetacean density and distribution in the central North Pacific. Endangered Species Research. 27:1–20.

Forney KA, Ferguson MC, Becker EA, Fiedler PC, Redfern JV, Barlow J, Vilchis IL, Ballance LT. 2012. Habitat-based spatial models of cetacean density in the eastern Pacific Ocean. Endangered Species Research. 16(2):113-133.

Gilles A, Adler E, Kaschner K, Scheidat M, Siebert U. 2011. Modelling harbor porpoise seasonal density as a function of German bight environment: Implications for management. Endangered Species Research. 14:157-169.

Goetz KT, Montgomery RA, Ver Hoef JM, Hobbs RC, Johnson DS. 2012. Identifying essential summer habitat of the endangered belluga whale *Delphinapterus leucas* in Cook Inlet, Alaska. Endangered Species Research. 16:135-147.

Hammond PS, McLeod KL, Berggren P, Borchers DL, Burt L, Canadas A, Desportes G, Donovan GP, Gilles A, Gillespie D et al. 2013. Cetacean abundance and distribution in european atlantic shelf waters to inform conservation and management. Biological Conservation. 164:107-122.

Harris PT, Macmillan-Lawler M, Rupp J, Baker EK. 2014. Geomorphology of the oceans. Marine Geology 352: 4-24.

Hastie TJ, Tibshirani RJ. 1990. Generalized additive models. Boca Raton, USA: Chapman and Hall/CRC.

Hedley SL, Buckland ST. 2004. Spatial models for line transect sampling. J Agr Biol Envir St. 9(2):181-199.

Henry AE, Moore JE, Barlow J, Calambokidis J, Ballance LT. 2020. Report on the California Current Ecosystem Survey (CCES): Cetacean and Seabird Data Collection Efforts, June 26 – December 4, 2018. U.S. Department of Commerce, NOAA Technical Memorandum NMFS-SWFSC.

Kinzey D, Olson P, Gerrodette T. 2000. Marine mammal data collection procedures on research ship line-transect surveys by the Southwest Fisheries Science Center. Southwest Fisheries Science Center, Administrative Report LJ-00-08.

Liu C, Berry PM, Dawson TP, Pearson RG. 2005. Selecting thresholds of occurrence in the prediction of species distributions. Ecography. 28(3):385-393.

Mangels KF, Gerrodette T. 1994. Report of cetacean sightings during a marine mammal survey in the eastern Pacific Ocean and Gulf of California aboard the NOAA ships McARTHUR and DAVID STARR JORDAN July 28–November 6, 1993. NOAA Technical Memorandum NMFS-SWFSC-211. La Jolla, CA, USA. National Marine Fisheries Service.

Marra G, Wood SN. 2011. Practical variable selection for generalized additive models. Comput Stat Data An. 55(7):2372-2387.

Miller DL, Becker EA, Forney KA, Roberts JR, Cañadas A. Schick R. *In Preparation*. Estimating uncertainty in density surface models.

Miller DL, Burt ML, Rexstad EA, Thomas L. 2013. Spatial models for distance sampling data: Recent developments and future directions. Methods in Ecology and Evolution. 4(11):1001-1010.

Monnahan CC, Branch TA, Punt AE. 2015. Do ship strikes threaten the recovery of endangered eastern North Pacific blue whales? Marine Mammal Science, 31(1), 279–297.

Moore AM, Arango HG, Broquet G, Edwards CA, Veneziani M, Powell B, … Robinson P. 2011. The regional ocean modeling system (ROMS) 4-dimensional variational data assimilation systems. II: Performance and application to the California Current system. Progress in Oceanography, 91, 50–73.

Moore JE, Barlow J. 2011. Bayesian state-space model of fin whale abundance trends from a 1991-2008 time series of line-transect surveys in the California Current. Journal of Applied Ecology, 48, 1195–1205

Moore JE, Barlow JP. 2014. Improved abundance and trend estimates for sperm whales in the eastern north pacific from bayesian hierarchical modeling. Endangered Species Research. 25(2):141-150.

Moore JE, Barlow J. 2017. Population abundance and trend estimates for beaked whales and sperm whales in the California Current from ship-based visual line-transect data, 1991-2014. NOAA Technical Memorandum NMFS-SWFSC-585. La Jolla, CA, USA. National Marine Fisheries Service.

National Oceanic and Atmospheric Administration (NOAA). 2016. Guidelines for preparing Stock Assessment Reports pursuant to the 1994 Amendments to the Marine Mammal Protection Act. https://www.fisheries.noaa.gov/national/marine-mammal-protection/guidelines-assessing-marine-mammal-stocks

Perrin WF, Scott MD, Walker GJ, Cass VL. 1985. Review of geographical stocks of tropical dolphins (*Stenella* spp. and I) in the eastern Pacific. NOAA Technical Memorandum NMFS-SWFSC-28. La Jolla, CA, USA. National Marine Fisheries Service.

R Core Team (2017). R: A language and environment for statistical computing. R Foundation for Statistical Computing, Vienna, Austria. Available at: http://www.R-project.org/

Redfern JV, Barlow J, Balance LT, Gerrodette T, Becker EA. 2008. Absence of scale dependence in cetacean-habitat models for the eastern tropical Pacific Ocean. Marine Ecology Progress Series, 363, 1–14.

Redfern JV, McKenna MF, Moore TJ, Calambokidis J, Deangelis ML, Becker EA, Barlow J, Forney KA, Fiedler PC, Chivers SJ. 2013. Assessing the risk of ships striking large whales in marine spatial planning. Conservation Biology. 27(2):292–302.

Redfern JV, Moore TJ, Fiedler PC, de Vos A, Brownell RL, Jr., Forney KA, Becker EA, Ballance LT. 2017. Predicting cetacean distributions in data-poor marine ecosystems. Diversity and Distributions.1–15.

Roberts JJ, Best BD, Mannocci L, Fujioka E, Halpin PN, Palka DL, Garrison LP, Mullin KD, Cole TVN, Khan CB et al. 2016. Habitat-based cetacean density models for the U.S. Atlantic and Gulf of Mexico. Scientific Reports. 6:22615.

Seber GAF. 1982. The estimation of animal abundance and related parameters. New York, USA: Macmillan.

Tynan CT, Ainley DG, Barth JA, Cowles TJ, Pierce SD, Spear LB. 2005. Cetacean distributions relative to ocean processes in the northern California Current system. Deep-Sea Research Part Ii-Topical Studies in Oceanography. 52(1-2):145-167.

U.S. Department of the Navy. 2013. Hawaii-Southern California Training and Testing, Final Environmental Impact Statement/Overseas Environmental Impact Statement (EIS/OEIS). Prepared by Naval Facilities Engineering Command Pacific, Pearl Harbor, HI.

U.S. Department of the Navy. 2015. U.S. Navy Marine Species Density Database for the Pacific Ocean. NAVFAC Pacific Technical Report. Naval Facilities Engineering Command Pacific, Pearl Harbor, HI. 492 pp.

U.S. Department of the Navy. 2017. U.S. Navy Marine Species Density Database Phase III for the Hawaii-Southern California Training and Testing Study Area. NAVFAC Pacific Technical Report. Naval Facilities Engineering Command Pacific, Pearl Harbor, HI. 272 pp.

Williams R, Lusseau D, Hammond PS. 2006. Estimating relative energetic costs of human disturbance to killer whales (*orcinus orca*). Biological Conservation. 133:301–311.

Wood SN. 2003. Thin plate regression splines. J R Stat Soc B. 65:95-114.

Wood SN. 2008. Fast stable direct fitting and smoothness selection for generalized additive models. J R Stat Soc B. 70:495-518.

Wood SN. 2011. Fast stable restricted maximum likelihood and marginal likelihood estimation of semiparametric generalized linear models. J R Stat Soc B. 73:3-36.

Wood SN. 2017. Generalized Additive Models: An Introduction with R, Second Edition.Texts in Statistical Science. CRC Press. 476 pp.

Tables

Table 1. Cetacean and ecosystem assessment surveys and effort conducted within the California Current Ecosystem study area during 1991–2018. CA/OR/WA = California/Oregon/Washington, CenCA = central California, SoCA = southern California, Baja = Baja California. DSJ = *David Starr Jordan.*

Cruise numbers	Period	Research vessel	Region
1426	Jul-Nov 1991	*McArthur*	California
1508/1509	Jul-Nov 1993	*McArthur/DSJ*	California
1604/1605	Jul-Nov 1996	*McArthur/DSJ*	CA/OR/WA
1617/1619	Jul-Dec 2001	*McArthur/DSJ*	CA/OR/WA
1627/1628	June-Dec 2005	*McArthur II/DSJ*	CA/OR/WA
1642	Jul-Nov 2008	*McArthur II*	CA/OR/WA
1635	Sept-Dec 2009	*McArthur II*	CenCA/SoCAL/Baja
1647	Aug-Dec 2014	*Ocean Starr**	CA/OR/WA
2017	June-Dec 2018	*Reuben Lasker*	Canada/CA/OR/WA/Baja

*Previously the *David Starr Jordan*

Table 2. Number of sightings and average group size (Avg. GS) of cetacean species observed in the California Current Ecosystem study area during the 1991–2018 shipboard surveys for which habitat-based density models were developed. All sightings were made while on systematic and non-systematic effort in Beaufort sea states ≤5 within the species-specific truncation distances (see text for details).

Common name	Taxonomic name	No. of sightings	Avg. GS
Long-beaked common dolphin	*Delphinus delphis bairdii*	160	291.82
Short-beaked common dolphin	*Delphinus delphis delphis*	1,034	155.73
Risso's dolphin	*Grampus griseus*	249	18.57
Pacific white-sided dolphin	*Lagenorhynchus obliquidens*	296	54.70
Northern right whale dolphin	*Lissodelphis borealis*	147	45.31
Striped dolphin	*Stenella coeruleoalba*	153	39.38
Common bottlenose dolphin	*Tursiops truncatus*	66	14.48
Dall's porpoise	*Phocoenoides dalli*	678	3.72
Sperm whale	*Physeter macrocephalus*	105	6.67
Minke whale	*Balaenoptera acutostrata*	49	1.13
Blue whale	*Balaenoptera musculus*	316	1.66
Fin whale	*Balaenoptera physalus*	558	2.06
Humpback whale	*Megaptera novaeangliae*	967	1.70
Baird's beaked whale	*Berardius bairdii*	39	7.46
Small beaked whale guild	*Mesoplodon spp. & Ziphius cavirostris*	92	2.12

Table 3. Summary of the final models built with the 1991–2018 survey data. Variables are listed in the order of their significance and are as follows: SST = sea surface temperature, SSTsd = standard deviation of SST, MLD = mixed layer depth, SSH = sea surface height, SSHsd = standard deviation of SSH, depth = bathymetric depth, shelf= distance to shelf, d2000=distance to the 2,000m isobath, LON = longitude, and LAT = latitude. Separate encounter rate (ER) and group size (GS) models were built for long- and short-beaked common dolphins due to large and variable group sizes. All single response and encounter rate models were corrected for effort with an offset for the effective area searched (see text for details). Performance metrics included the percentage of explained deviance (Expl. Dev.), the area under the receiver operating characteristic curve (AUC), the true skill statistic (TSS), and the ratio of observed to predicted density for the study area (Obs:Pred).

Species	Predictor variables	Expl.Dev.	AUC	TSS	Obs:Pred
Long-beaked common dolphin					
	ER: LON:LAT + SST + SSHsd + SSH	52.50	0.98	0.90	0.95
	GS: LON:LAT	6.55			
Short-beaked common dolphin					
	ER: LON:LAT + year + SST + SSH + MLD	17.00	0.77	0.40	0.95
	GS: LON:LAT	11.10			
Risso's dolphin					
	LON:LAT + SST + MLD + year + SSTsd	22.40	0.76	0.41	0.87
Pacific white-sided dophin					
	LON:LAT + shelf + SST + SSH + MLD	51.70	0.87	0.62	0.86
Northern right whale dolphin					
	LON:LAT + SST + depth + MLD + SSTsd	44.40	0.83	0.51	0.92
Striped dolphin					
	depth + LON:LAT + SST + year + MLD	33.20	0.76	0.41	0.72
Common bottlenose dolphin					
	LON:LAT + MLD + SSTsd + SST + year	51.20	0.92	0.74	0.94
Dall's porpoise					
	LON:LAT + SSH + year + SST + SSHsd + SSTsd	32.20	0.89	0.63	0.95
Sperm whale					
	d2000 + MLD	13.30	0.61	0.17	0.91
Minke whale					
	shelf + SST + LON:LAT	7.73	0.85	0.59	1.00
Blue whale					
	LON:LAT + year + SSH + depth + SST + MLD	23.90	0.78	0.42	0.94
Fin whale					
	LON:LAT + SST + SSH + year + MLD + depth	22.40	0.75	0.39	0.88
Humpback whale					
	LON:LAT + year + depth + SST + MLD	57.40	0.94	0.75	0.98
Baird's beaked whale					
	LON:LAT + depth + MLD + SSH	46.00	0.90	0.65	0.96
Small beaked whale guild					
	shelf + MLD + SST + LON:LAT	8.19	0.73	0.39	0.97

Table 4. Annual model-predicted mean estimates of abundance, density (animals km^{-2}), and corresponding coefficient of variation (CV) within the CCE study area. Annual estimates are predicted from the full model using the habitat characteristics in that year. CV_m (Model) represents the combined uncertainty from three sources: GAM parameters, ESW, and environmental variability. CV_{Tot} is the total CV from CV_m (Model) and CV_{g0} derived using the Delta method (see text for details). Log-normal 95% confidence intervals (Low and High 95% CIs) apply to abundance estimates. Also shown is the 20th percentile for the abundance estimate, corresponding to the "minimum population size (Nmin)" as defined in the Guidelines for Assessing Marine Mammal Stocks, and calculated as the log-normal 20th percentile of the mean abundance estimate using standard formulae.

	Year					
	1996	**2001**	**2005**	**2008**	**2014**	**2018**
Long-beaked common dolphin						
Abundance	57,623	53,044	52,356	58,624	58,794	83,379
Density	0.0506	0.0465	0.0459	0.0514	0.0516	0.0732
CV_m (Model)	0.151	0.128	0.146	0.087	0.101	0.161
CV_{g0}	0.165	0.165	0.165	0.165	0.165	0.165
CV_{Tot}	0.224	0.209	0.220	0.187	0.193	0.231
Low 95% CI	37,370	35,381	34,170	40,799	40,380	53,377
High 95% CI	88,851	79,524	80,221	84,236	85,605	130,244
Nmin	47,841	44,574	43,587	50,170	50,031	68,841
Short-beaked common dolphin						
Abundance	328,134	391,356	394,610	433,628	880,425	1,056,308
Density	0.2879	0.3434	0.3462	0.3804	0.7724	0.9267
CV_m (Model)	0.145	0.196	0.139	0.163	0.090	0.126
CV_{g0}	0.165	0.165	0.165	0.165	0.165	0.165
CV_{Tot}	0.220	0.256	0.216	0.232	0.188	0.208
Low 95% CI	214,423	238,750	259,781	276,866	611,073	706,207
High 95% CI	502,146	641,507	599,417	679,148	1,268,504	1,579,970
Nmin	273,320	316,497	329,739	357,612	752,592	888,532
Risso's dolphin						
Abundance	15,761	15,462	12,044	11,657	8,153	8,977
Density	0.0138	0.0136	0.0106	0.0102	0.0072	0.0079
CV_m (Model)	0.116	0.087	0.123	0.128	0.189	0.190
CV_{g0}	0.093	0.093	0.093	0.093	0.093	0.093
CV_{Tot}	0.149	0.127	0.154	0.158	0.211	0.212
Low 95% CI	11,796	12,059	8,918	8,565	5,419	5,957
High 95% CI	21,060	19,826	16,265	15,865	12,265	13,528
Nmin	13,916	13,896	10,586	10,211	6,841	7,527
Pacific white-sided dolphin						
Abundance	37,147	38,533	39,008	37,369	28,901	34,999
Density	0.0326	0.0338	0.0342	0.0328	0.0254	0.0307
CV_m (Model)	0.230	0.235	0.506	0.323	0.292	0.149
CV_{g0}	0.165	0.165	0.165	0.165	0.165	0.165

CV_{Tot}	0.283	0.287	0.532	0.363	0.335	0.222
Low 95% CI	21,558	22,194	14,657	18,761	15,240	22,756
High 95% CI	64,010	66,900	103,814	74,432	54,807	53,829
Nmin	29,404	30,402	25,617	27,794	21,954	29,090
Northern right whale dolphin						
Abundance	33,893	39,697	27,370	42,767	18,031	29,285
Density	0.0297	0.0348	0.0240	0.0375	0.0158	0.0257
CV_m (Model)	0.706	0.782	0.445	0.661	0.534	0.698
CV_{g0}	0.165	0.165	0.165	0.165	0.165	0.165
CV_{Tot}	0.725	0.798	0.475	0.681	0.559	0.717
Low 95% CI	9,481	10,012	11,314	12,750	6,489	8,284
High 95% CI	121,158	157,397	66,211	143,454	50,099	103,521
Nmin	19,608	21,966	18,727	25,428	11,624	17,024
Striped dolphin						
Abundance	17,758	26,215	47,974	46,563	70,107	29,988
Density	0.0156	0.0230	0.0421	0.0409	0.0615	0.0263
CV_m (Model)	0.293	0.193	0.357	0.317	0.324	0.282
CV_{g0}	0.098	0.098	0.098	0.098	0.098	0.098
CV_{Tot}	0.309	0.216	0.370	0.332	0.338	0.299
Low 95% CI	9,826	17,235	23,765	24,714	36,762	16,913
High 95% CI	32,093	39,875	96,843	87,727	133,696	53,170
Nmin	13,772	21,893	35,478	35,470	53,128	23,448
Common bottlenose dolphin						
Abundance	6,198	5,408	3,855	3,493	5,908	3,477
Density	0.0054	0.0047	0.0034	0.0031	0.0052	0.0031
CV_m (Model)	0.504	0.357	0.503	0.508	0.510	0.647
CV_{g0}	0.256	0.256	0.256	0.256	0.256	0.256
CV_{Tot}	0.565	0.439	0.564	0.569	0.571	0.696
Low 95% CI	2,208	2,374	1,375	1,237	2,087	1,015
High 95% CI	17,398	12,320	10,806	9,861	16,726	11,915
Nmin	3,978	3,797	2,476	2,237	3,778	2,048
Dall's porpoise						
Abundance	49,811	44,418	36,373	34,654	21,219	16,498
Density	0.0437	0.0390	0.0319	0.0304	0.0186	0.0145
CV_m (Model)	0.244	0.166	0.178	0.152	0.199	0.319
CV_{g0}	0.518	0.518	0.518	0.518	0.518	0.518
CV_{Tot}	0.573	0.544	0.548	0.540	0.555	0.608
Low 95% CI	17,541	16,376	13,328	12,861	7,686	5,493
High 95% CI	141,452	120,481	99,264	93,374	58,580	49,554
Nmin	31,813	28,933	23,630	22,637	13,717	10,286
Sperm whale						
Abundance	2,783	2,896	2,691	2,869	2,656	2,606
Density	0.0024	0.0025	0.0024	0.0025	0.0023	0.0023
CV_m (Model)	0.078	0.109	0.111	0.090	0.186	0.017

CV_{g0}	0.285	0.285	0.285	0.285	0.285	0.285
CV_{Tot}	0.295	0.305	0.306	0.299	0.340	0.286
Low 95% CI	1,578	1,614	1,497	1,617	1,388	1,506
High 95% CI	4,907	5,197	4,836	5,090	5,082	4,511
Nmin	2,181	2,253	2,092	2,243	2,010	2,059
Minke whale						
Abundance	847	812	819	804	1,062	915
Density	0.0007	0.0007	0.0007	0.0007	0.0009	0.0008
CV_m (Model)	0.139	0.11	0.11	0.113	0.109	0.071
CV_{g0}	0.787	0.787	0.787	0.787	0.787	0.787
CV_{Tot}	0.799	0.795	0.795	0.795	0.795	0.790
Low 95% CI	214	206	208	204	270	234
High 95% CI	3,358	3,200	3,227	3,170	4,184	3,584
Nmin	469	451	454	446	589	509
Blue whale						
Abundance	1,946	1,657	1,042	919	1,077	670
Density	0.0017	0.0015	0.0009	0.0008	0.0009	0.0006
CV_m (Model)	0.224	0.139	0.149	0.227	0.273	0.299
CV_{g0}	0.309	0.309	0.309	0.309	0.309	0.309
CV_{Tot}	0.382	0.339	0.343	0.383	0.412	0.430
Low 95% CI	945	868	542	445	495	299
High 95% CI	4,009	3,162	2,004	1,899	2,342	1,502
Nmin	1,427	1,255	787	673	771	474
Fin whale						
Abundance	3,804	5,733	7,319	7,606	10,139	11,065
Density	0.0033	0.0050	0.0064	0.0067	0.0089	0.0097
CV_m (Model)	0.200	0.212	0.250	0.303	0.175	0.202
CV_{g0}	0.230	0.230	0.230	0.230	0.230	0.230
CV_{Tot}	0.305	0.313	0.340	0.381	0.289	0.306
Low 95% CI	2,120	3,149	3,828	3,699	5,817	6,152
High 95% CI	6,826	10,439	13,994	15,640	17,672	19,902
Nmin	2,959	4,432	5,540	5,580	7,986	8,599
Humpback whale						
Abundance	1,181	1,364	1,575	1,727	2,178	4,784
Density	0.0010	0.0012	0.0014	0.0015	0.0019	0.0042
CV_m (Model)	0.147	0.081	0.113	0.175	0.271	0.118
CV_{g0}	0.283	0.283	0.283	0.283	0.283	0.283
CV_{Tot}	0.319	0.294	0.305	0.333	0.392	0.307
Low 95% CI	642	775	878	915	1,038	2,658
High 95% CI	2,173	2,400	2,824	3,259	4,568	8,609
Nmin	909	1,070	1,226	1,315	1,584	3,717
Baird's beaked whale						
Abundance	739	730	590	681	977	1,363
Density	0.0006	0.0006	0.0005	0.0006	0.0009	0.0012

CV_m (Model)	0.458	0.434	0.628	0.521	0.423	0.284
CV_{g0}	0.326	0.326	0.326	0.326	0.326	0.326
CV_{Tot}	0.562	0.543	0.708	0.615	0.534	0.432
Low 95% CI	265	270	169	225	366	606
High 95% CI	2,064	1,976	2,057	2,065	2,608	3,068
Nmin	475	476	345	423	641	962
Small beaked whale guild						
Abundance	4,979	5,701	4,399	5,088	4,670	4,989
Density	0.0044	0.0050	0.0039	0.0045	0.0041	0.0044
CV_m (Model)	0.153	0.113	0.213	0.201	0.188	0.032
CV_{g0}	0.438	0.438	0.438	0.438	0.438	0.438
CV_{Tot}	0.464	0.452	0.487	0.482	0.477	0.439
Low 95% CI	2,096	2,447	1,781	2,078	1,924	2,190
High 95% CI	11,830	13,281	10,866	12,461	11,336	11,363
Nmin	3,433	3,964	2,983	3,463	3,191	3,503

Table 5. Arithmetic mean of the model-predicted 2014 and 2018 estimates of abundance and density (animals km^{-2}) within the CCE study area. The corresponding coefficient of variation (CV_{Tot}) is the total CV from four sources: environmental variability, GAM parameters, ESW, and *g(0)* (see text for details). Log-normal 95% confidence intervals (Low and High 95% CIs) apply to abundance estimates. Also shown is the 20th percentile for the abundance estimate, corresponding to the "minimum population size (Nmin)" as defined in the Guidelines for Assessing Marine Mammal Stocks, and calculated as the log-normal 20th percentile of the mean abundance estimate using standard formulae.

Species	Abundance	Density	CV_{Tot}	Low 95% CI	High 95% CI	Nmin
Long-beaked common dolphin						
	71,087	0.0624	0.206	47,635	106,085	59,855
Short-beaked common dolphin						
	968,367	0.8496	0.198	659,662	1,421,537	821,143
Risso's dolphin						
	8,565	0.0075	0.216	5,635	13,018	7,155
Pacific white-sided dolphin						
	31,950	0.0280	0.284	18,514	55,137	25,274
Northern right whale dolphin						
	23,658	0.0208	0.733	6,545	85,518	13,622
Striped dolphin						
	50,048	0.0439	0.506	19,646	127,499	33,490
Common bottlenose dolphin						
	4,693	0.0041	0.647	1,473	14,951	2,853
Dall's porpoise						
	18,859	0.0165	0.591	6,453	55,112	11,897
Sperm whale						
	2,631	0.0023	0.329	1,403	4,935	2,008
Minke whale						
	986	0.0009	0.800	249	3,911	546
Blue whale						
	874	0.0008	0.471	363	2,103	599
Fin whale						
	10,602	0.0093	0.300	59	18,865	8,277
Humpback whale						
	3,481	0.0031	0.474	1,441	8,410	2,383
Baird's beaked whale						
	1,170	0.0010	0.548	429	3,192	760
Small beaked whale guild						
	4,830	0.0042	0.474	1,999	11,671	3,306

Figures

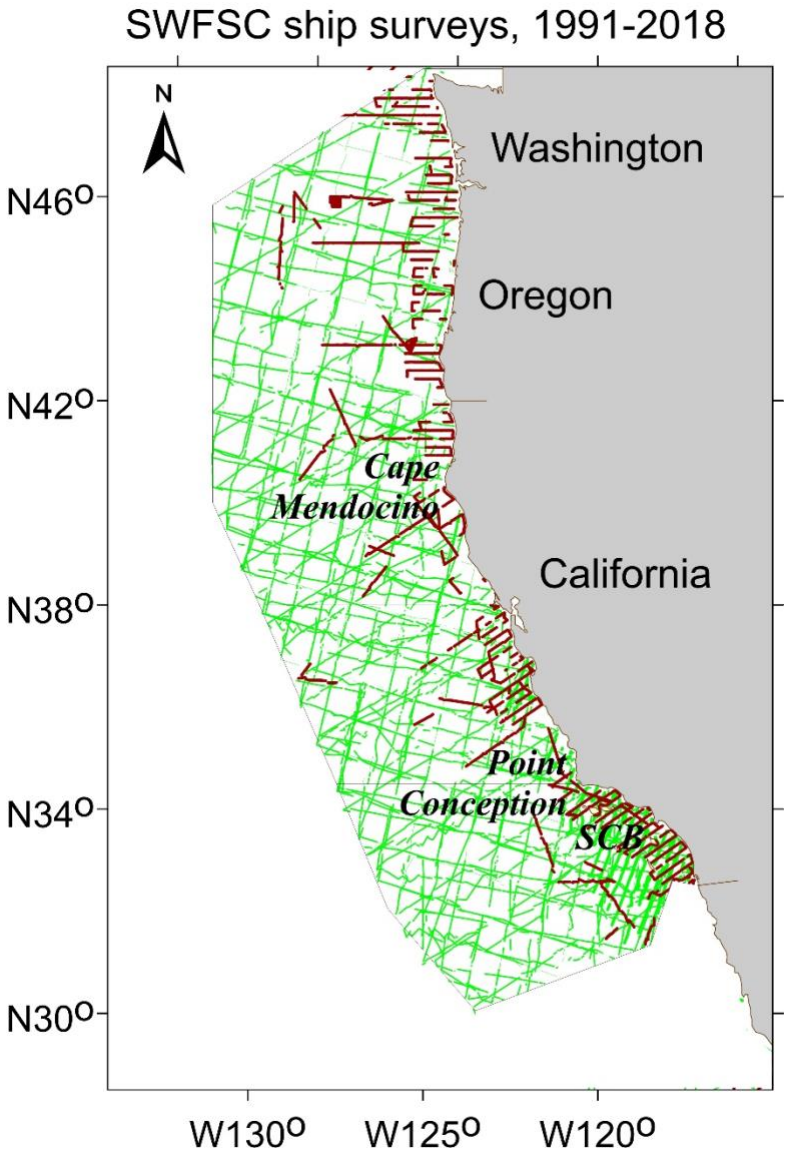

Figure 1. Completed transects for the Southwest Fisheries Science Center systematic ship surveys conducted between 1991 and 2018 in the California Current Ecosystem study area. The lines (green = 1991–2014 surveys, red=2018 survey) show on-effort transect coverage in Beaufort sea states of 0-5.

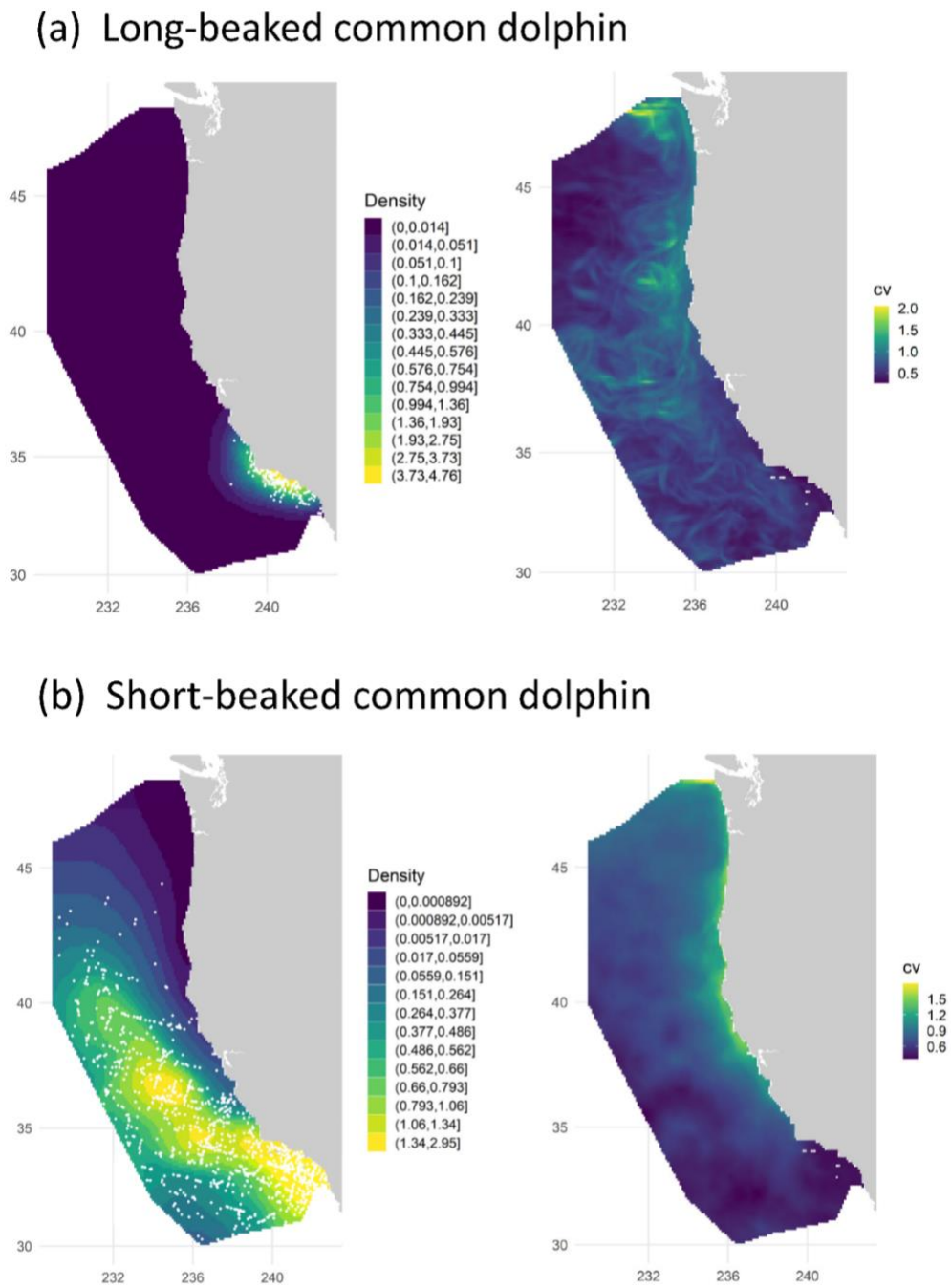

Figure 2a-b. Predicted mean density (animals km^{-2}) and associated coefficients of variation (CV) from the 1991–2018 habitat-based density models for (a) long-beaked common dolphin, and (b) short-beaked common dolphin. Panels show the multi-year average density based on predicted daily cetacean species densities covering the 1996-2018 survey periods (summer/fall). Predictions are shown for the study area (1,141,800 km^2). White dots in the average plots show actual sighting locations from the SWFSC 1996-2018 summer/fall ship surveys for the respective species.

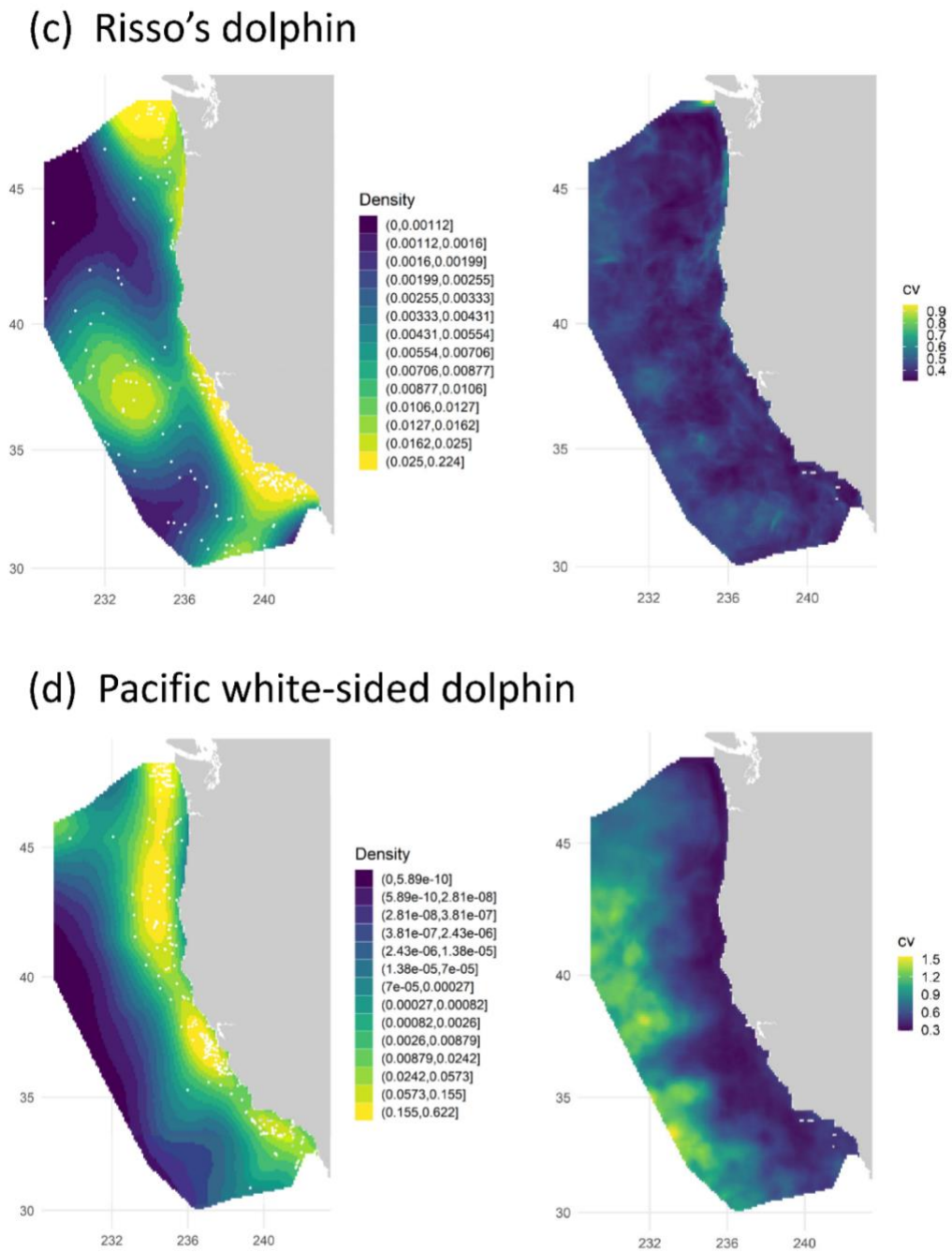

Figure 2c-d. Predicted mean density (animals km^{-2}) and associated coefficients of variation (CV) from the 1991–2018 habitat-based density models for (c) Risso's dolphin, and (d) Pacific white-sided dolphin. Panels show the multi-year average density based on predicted daily cetacean species densities covering the 1996-2018 survey periods (summer/fall). Predictions are shown for the study area (1,141,800 km^2). White dots in the average plots show actual sighting locations from the SWFSC 1996-2018 summer/fall ship surveys for the respective species.

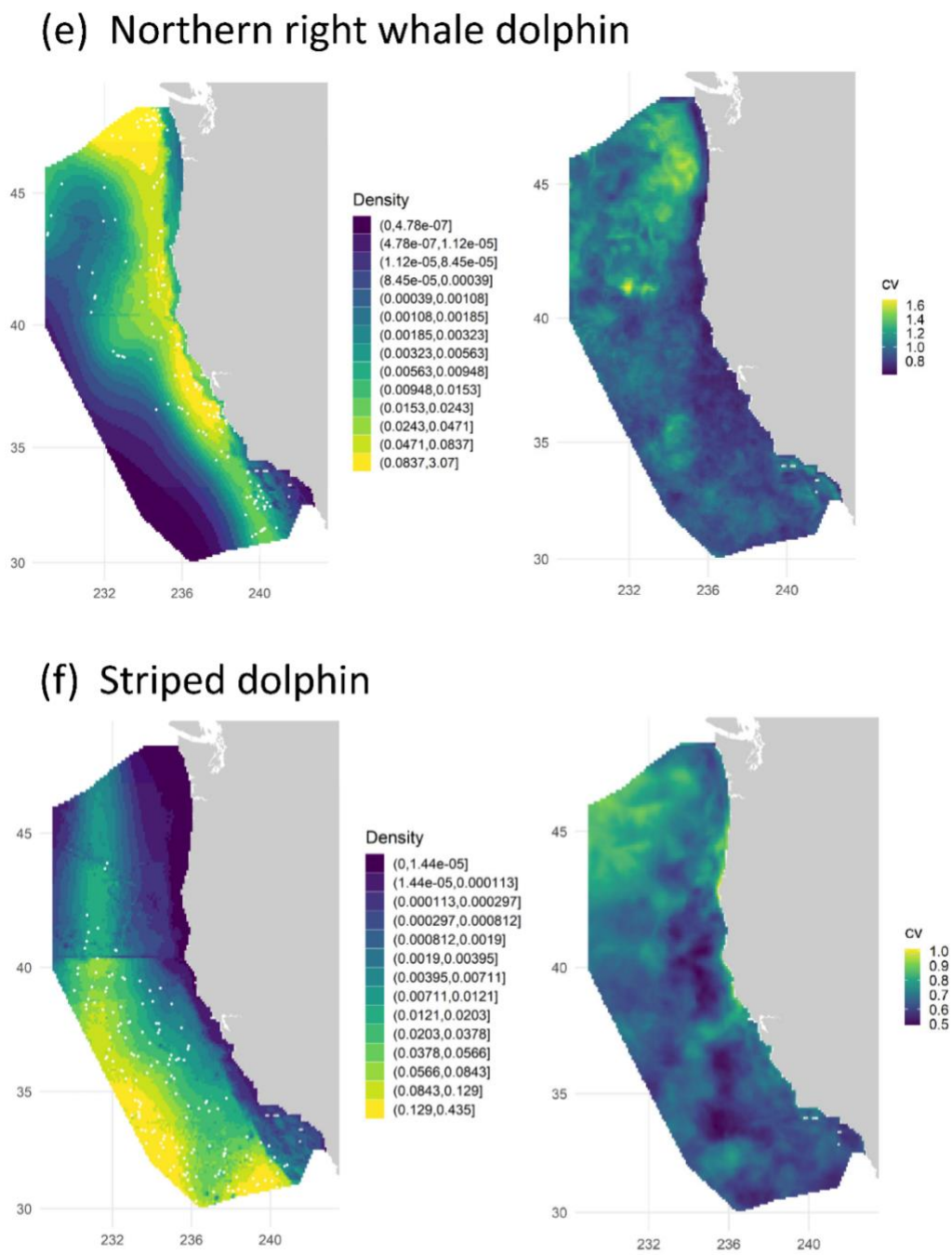

Figure 2e-f. Predicted mean density (animals km^{-2}) and associated coefficients of variation (CV) from the 1991–2018 habitat-based density models for (e) northern right whale dolphin, and (f) striped dolphin. Panels show the multi-year average density based on predicted daily cetacean species densities covering the 1996-2018 survey periods (summer/fall). Predictions are shown for the study area (1,141,800 km^2). White dots in the average plots show actual sighting locations from the SWFSC 1996-2018 summer/fall ship surveys for the respective species.

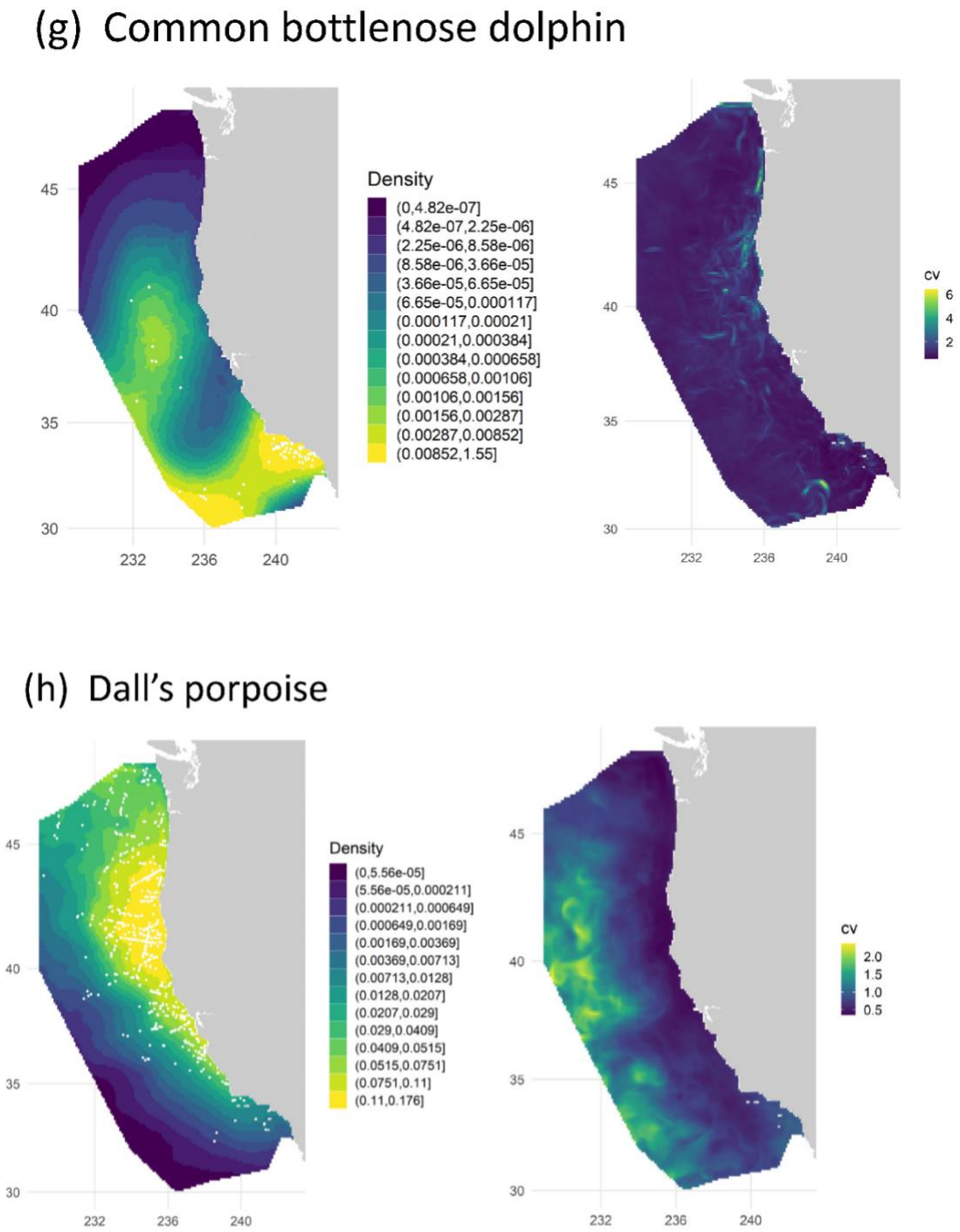

Figure 2g-h. Predicted mean density (animals km^{-2}) and associated coefficients of variation (CV) from the 1991–2018 habitat-based density models for (g) common bottlenose dolphin, and (h) Dall's porpoise. Panels show the multi-year average density based on predicted daily cetacean species densities covering the 1996-2018 survey periods (summer/fall). Predictions are shown for the study area (1,141,800 km^2). White dots in the average plots show actual sighting locations from the SWFSC 1996-2018 summer/fall ship surveys for the respective species.

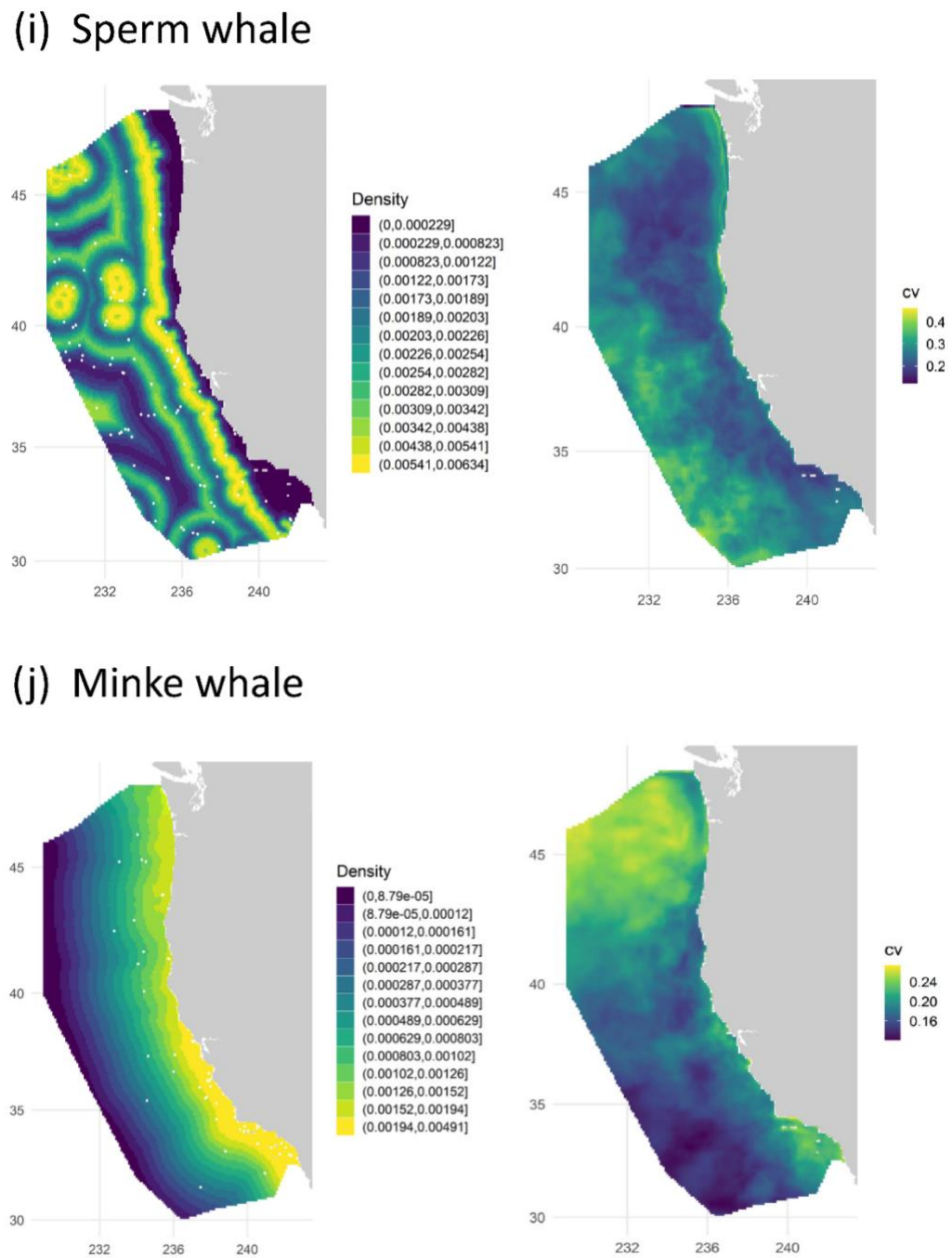

Figure 2i-j. Predicted mean density (animals km^{-2}) and associated coefficients of variation (CV) from the 1991–2018 habitat-based density models for (i) sperm whale, and (j) minke whale. Panels show the multi-year average density based on predicted daily cetacean species densities covering the 1996-2018 survey periods (summer/fall). Predictions are shown for the study area (1,141,800 km^2). White dots in the average plots show actual sighting locations from the SWFSC 1996-2018 summer/fall ship surveys for the respective species.

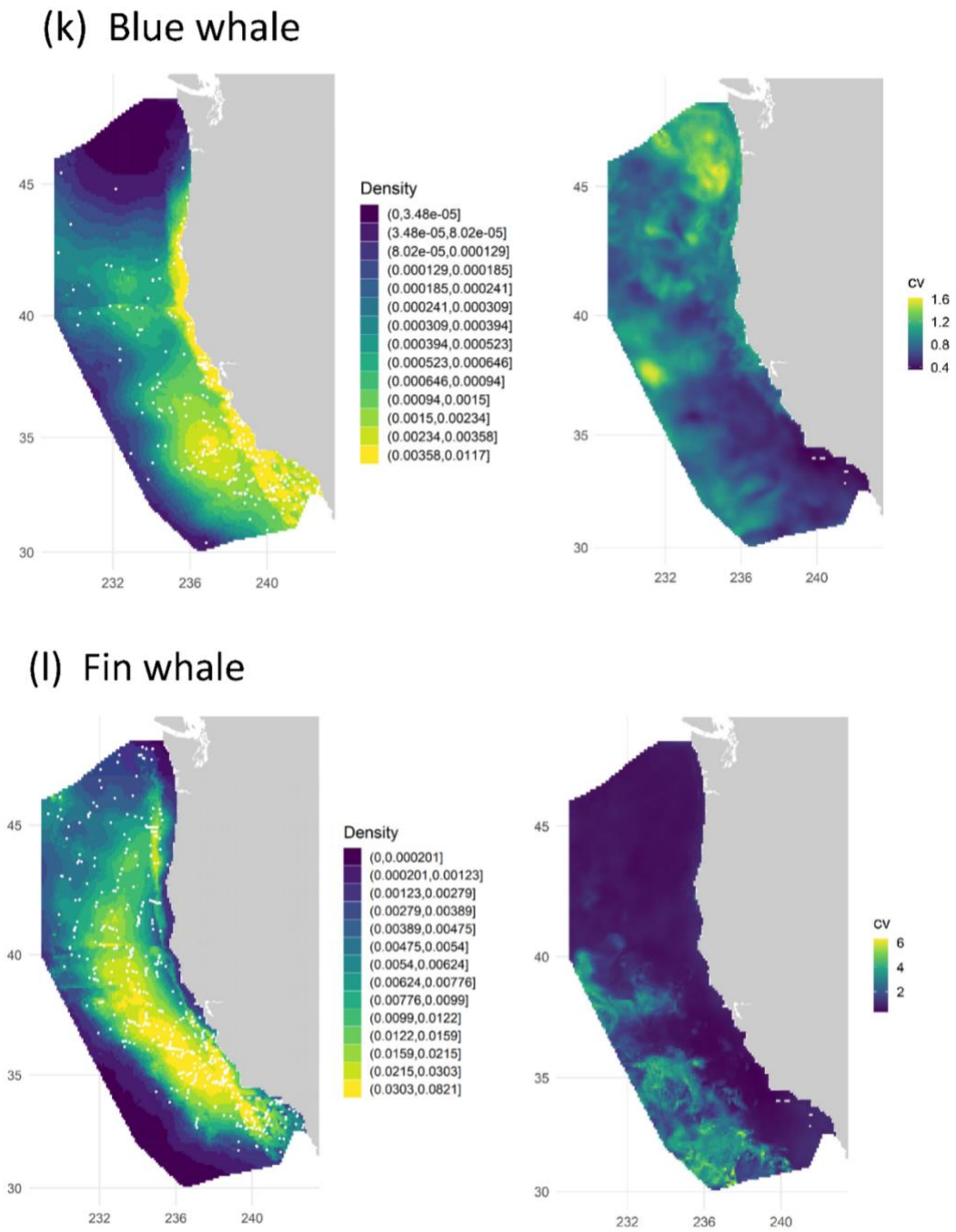

Figure 2k-l. Predicted mean density (animals km^{-2}) and associated coefficients of variation (CV) from the 1991–2018 habitat-based density models for (k) blue whale, and (l) fin whale. Panels show the multi-year average density based on predicted daily cetacean species densities covering the 1996-2018 survey periods (summer/fall). Predictions are shown for the study area (1,141,800 km^2). White dots in the average plots show actual sighting locations from the SWFSC 1996-2018 summer/fall ship surveys for the respective species.

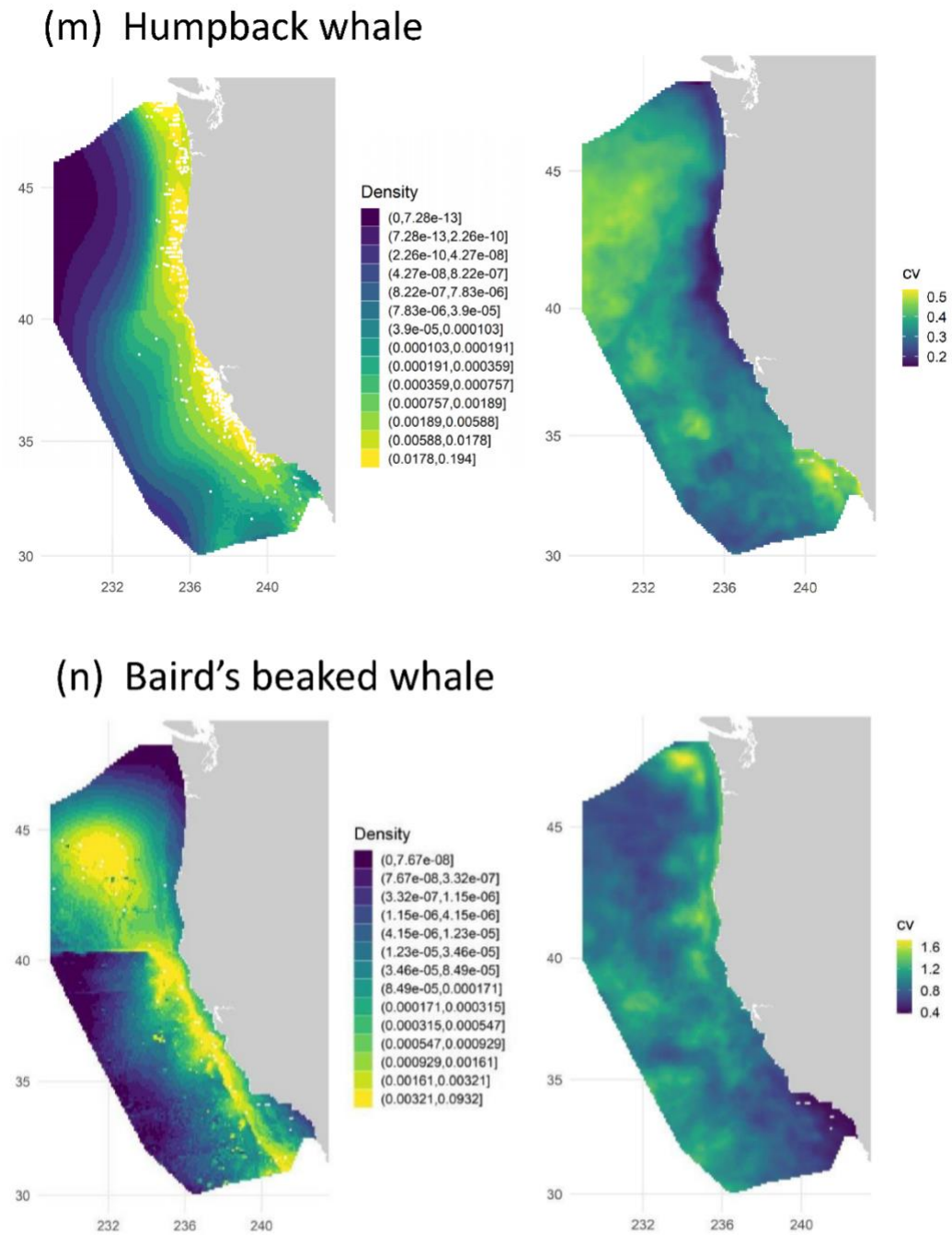

Figure 2m-n. Predicted mean density (animals km^{-2}) and associated coefficients of variation (CV) from the 1991–2018 habitat-based density models for (m) humpback whale, and (n) Baird's beaked whale. Panels show the multi-year average density based on predicted daily cetacean species densities covering the 1996-2018 survey periods (summer/fall). Predictions are shown for the study area (1,141,800 km^2). White dots in the average plots show actual sighting locations from the SWFSC 1996-2018 summer/fall ship surveys for the respective species.

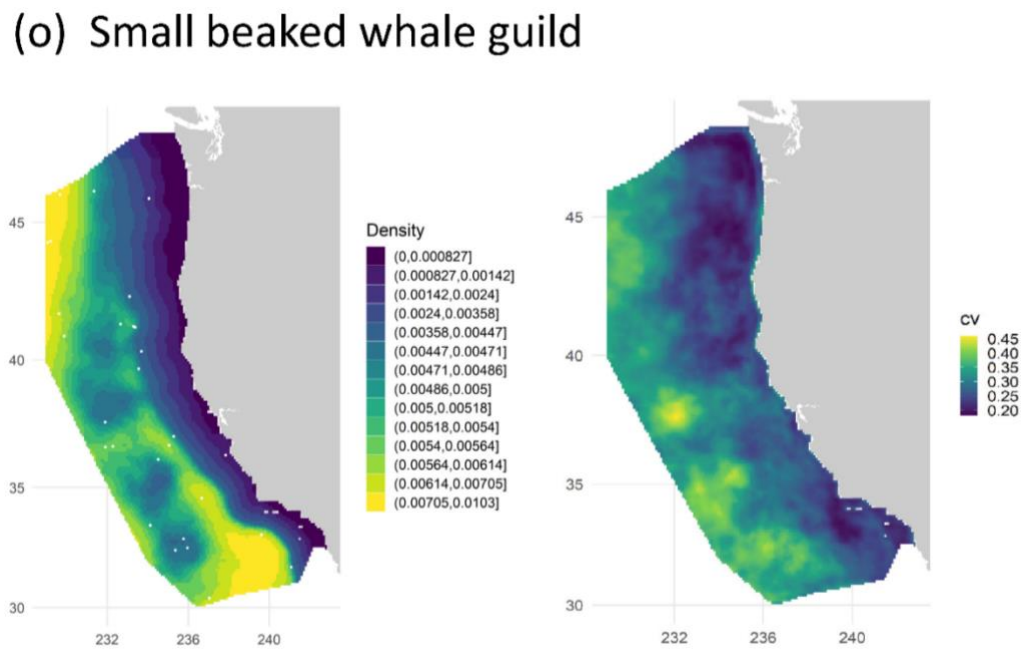

Figure 2o. Predicted mean density (animals km^{-2}) and associated coefficients of variation (CV) from the 1991–2018 habitat-based density models for (o) small beaked whale guild. Panels show the multi-year average density based on predicted daily cetacean species densities covering the 1996-2018 survey periods (summer/fall). Predictions are shown for the study area (1,141,800 km^2). White dots in the average plots show actual sighting locations from the SWFSC 1996-2018 summer/fall ship surveys for the respective species.

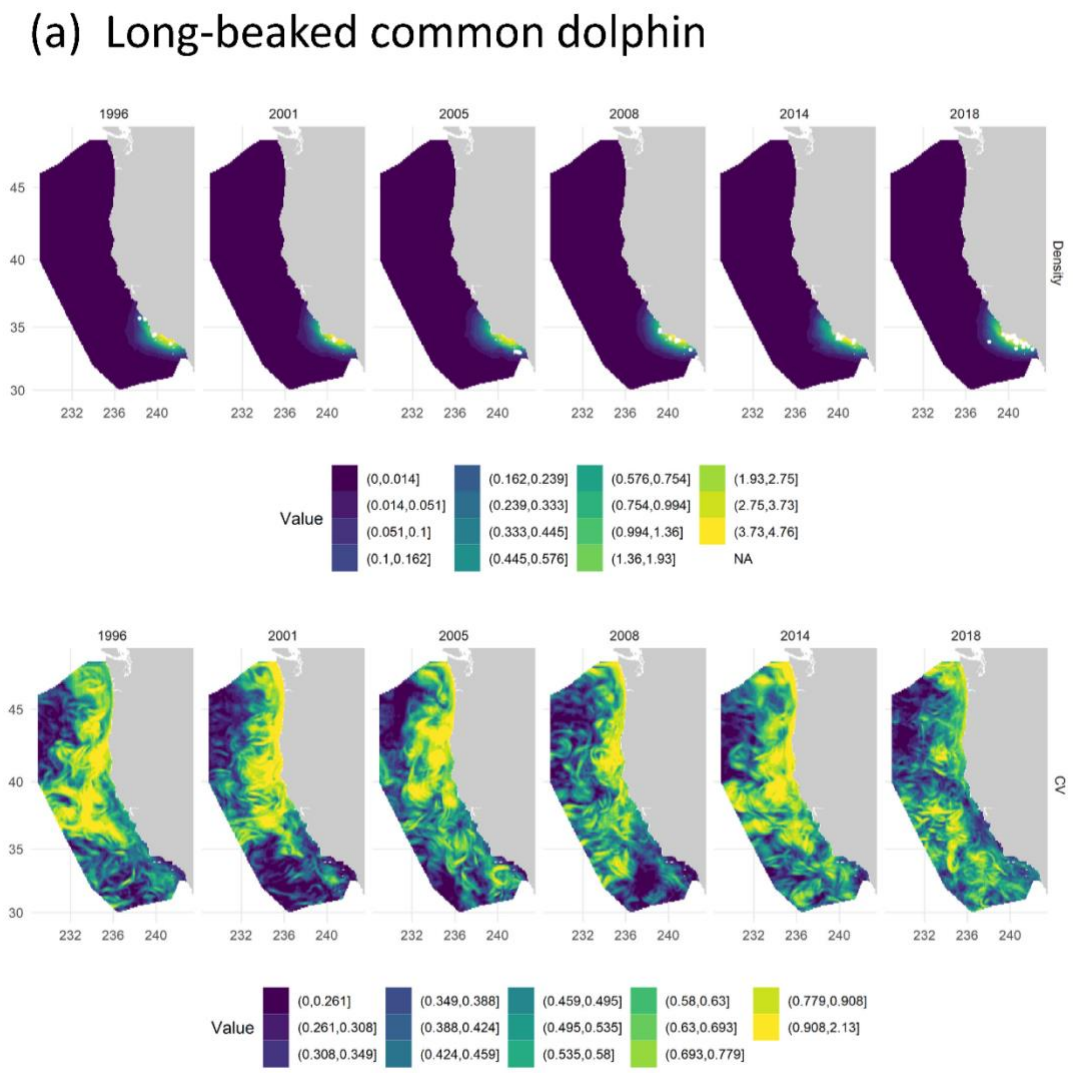

Figure 3a. Predicted annual (1996-2018) mean density (animals km^{-2}) and associated coefficients of variation (CV) from the 1991–2018 habitat-based density models for long-beaked common dolphin. Panels show the yearly average density based on predicted daily long-beaked common dolphin densities covering the 1996-2018 survey periods (summer/fall). Predictions are shown for the study area (1,141,800 km^2). White dots in the average plots show actual sighting locations from the respective SWFSC summer/fall ship surveys.

(b) Short-beaked common dolphin

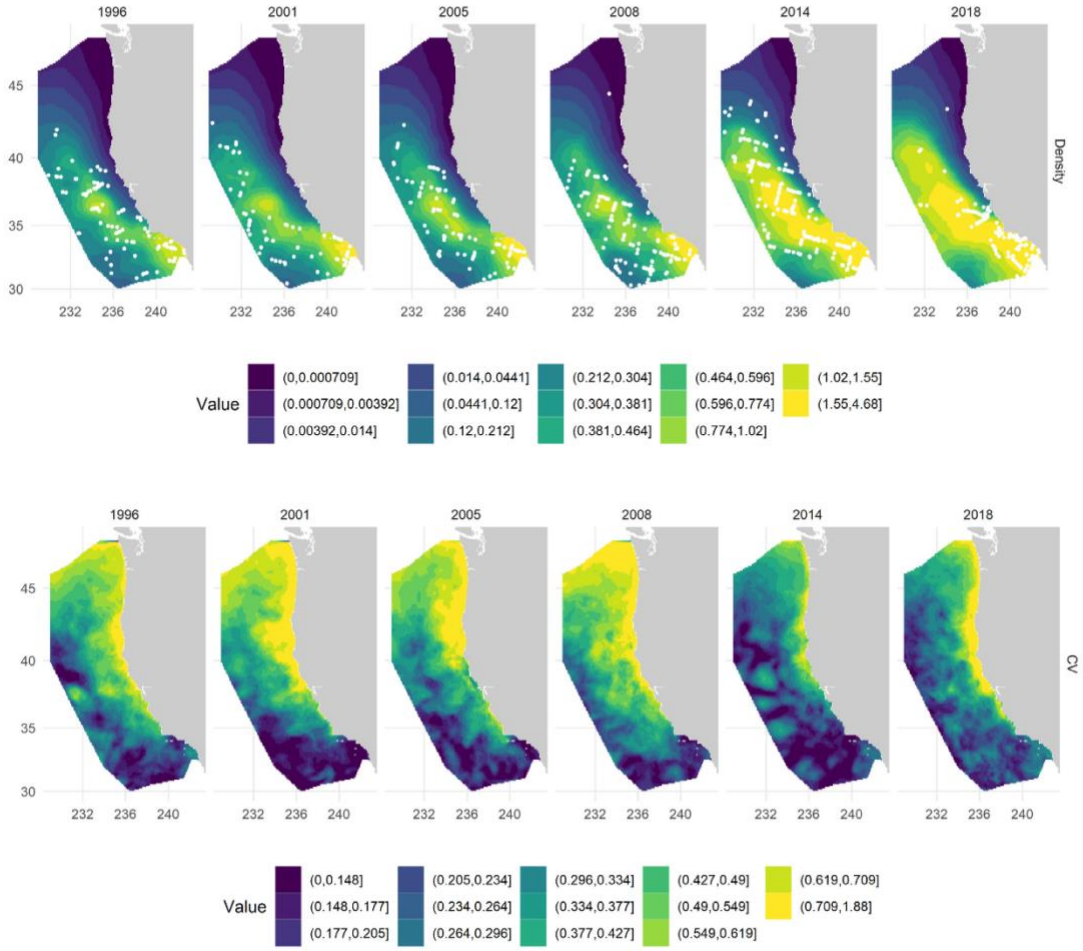

Figure 3b. Predicted annual (1996-2018) mean density (animals km^{-2}) and associated coefficients of variation (CV) from the 1991–2018 habitat-based density models for short-beaked common dolphin. Panels show the yearly average density based on predicted daily short-beaked common dolphin densities covering the 1996-2018 survey periods (summer/fall). Predictions are shown for the study area (1,141,800 km^2). White dots in the average plots show actual sighting locations from the respective SWFSC summer/fall ship surveys.

(c) Risso's dolphin

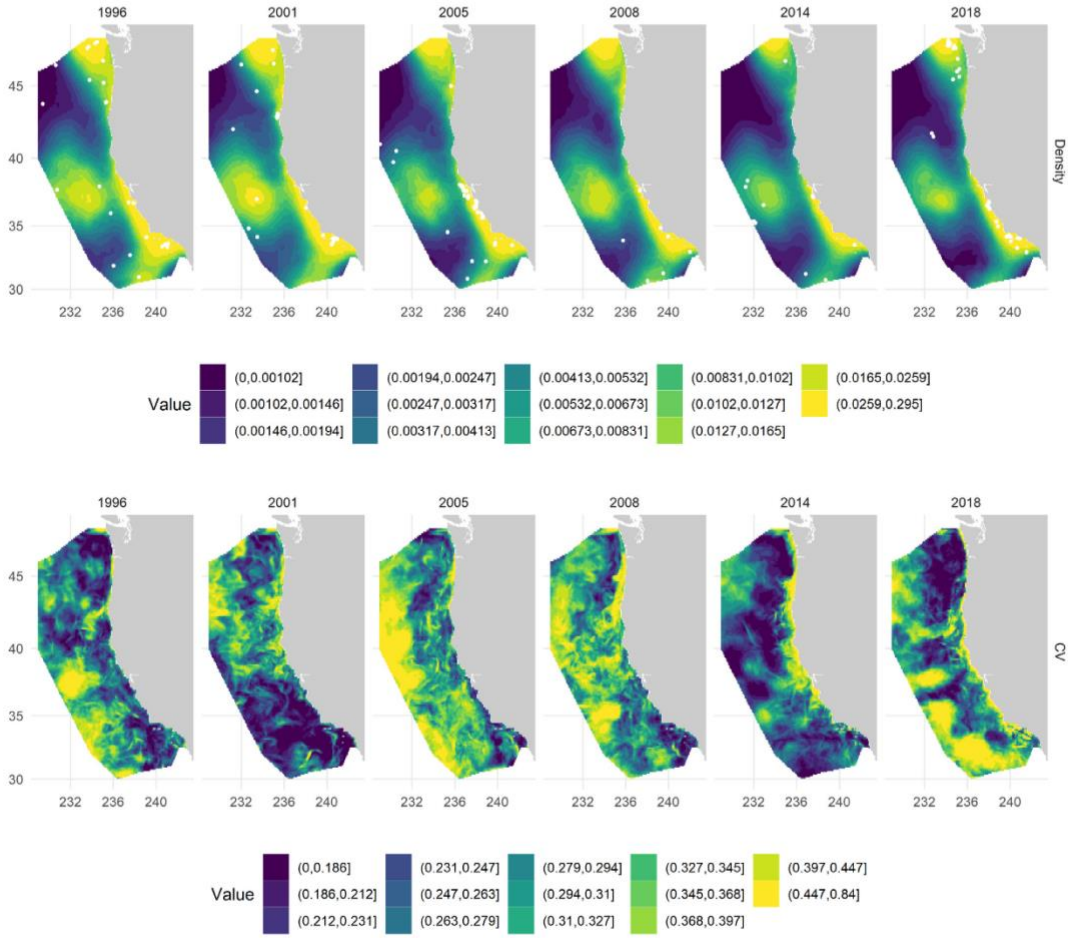

Figure 3c. Predicted annual (1996-2018) mean density (animals km^{-2}) and associated coefficients of variation (CV) from the 1991–2018 habitat-based density models for Risso's dolphin. Panels show the yearly average density based on predicted daily Risso's dolphin densities covering the 1996-2018 survey periods (summer/fall). Predictions are shown for the study area (1,141,800 km^2). White dots in the average plots show actual sighting locations from the respective SWFSC summer/fall ship surveys.

(d) Pacific white-sided dolphin

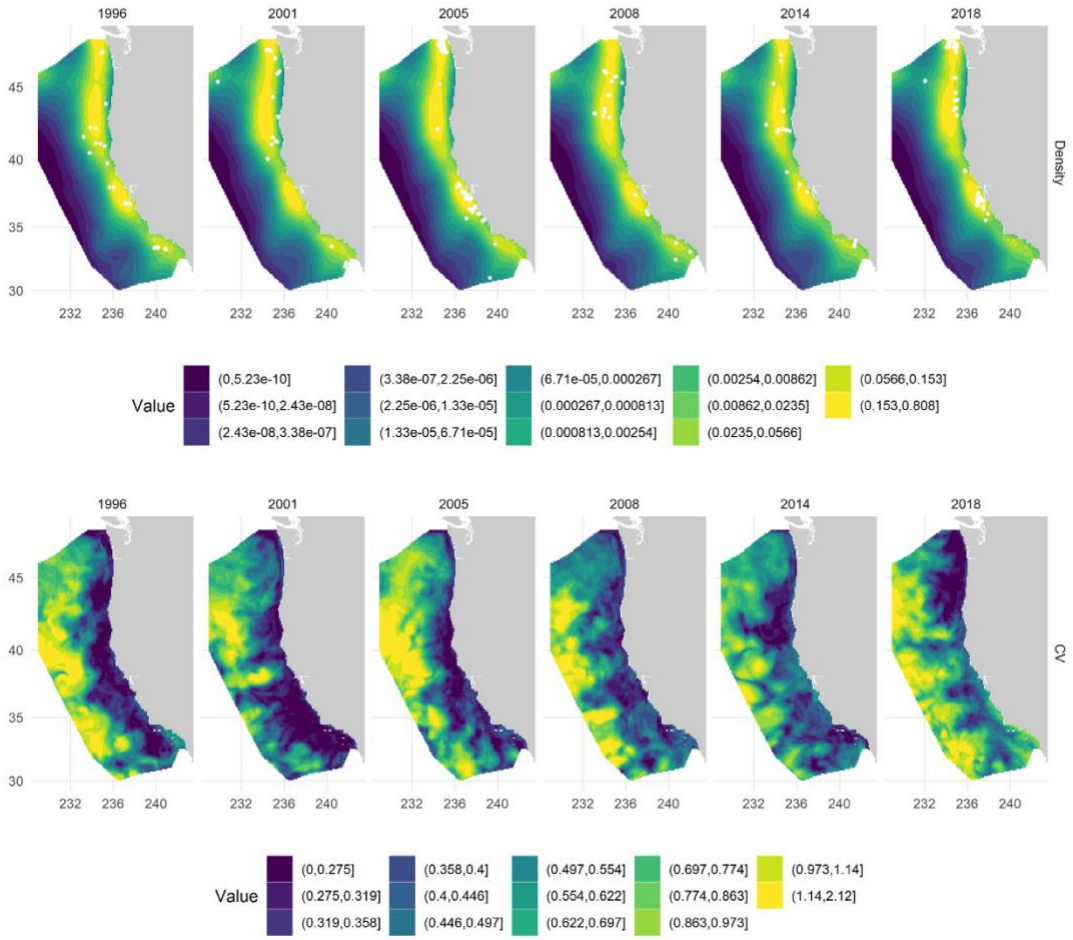

Figure 3d. Predicted annual (1996-2018) mean density (animals km^{-2}) and associated coefficients of variation (CV) from the 1991–2018 habitat-based density models for Pacific white-sided dolphin. Panels show the yearly average density based on predicted daily Pacific white-sided dolphin densities covering the 1996-2018 survey periods (summer/fall). Predictions are shown for the study area (1,141,800 km^2). White dots in the average plots show actual sighting locations from the respective SWFSC summer/fall ship surveys.

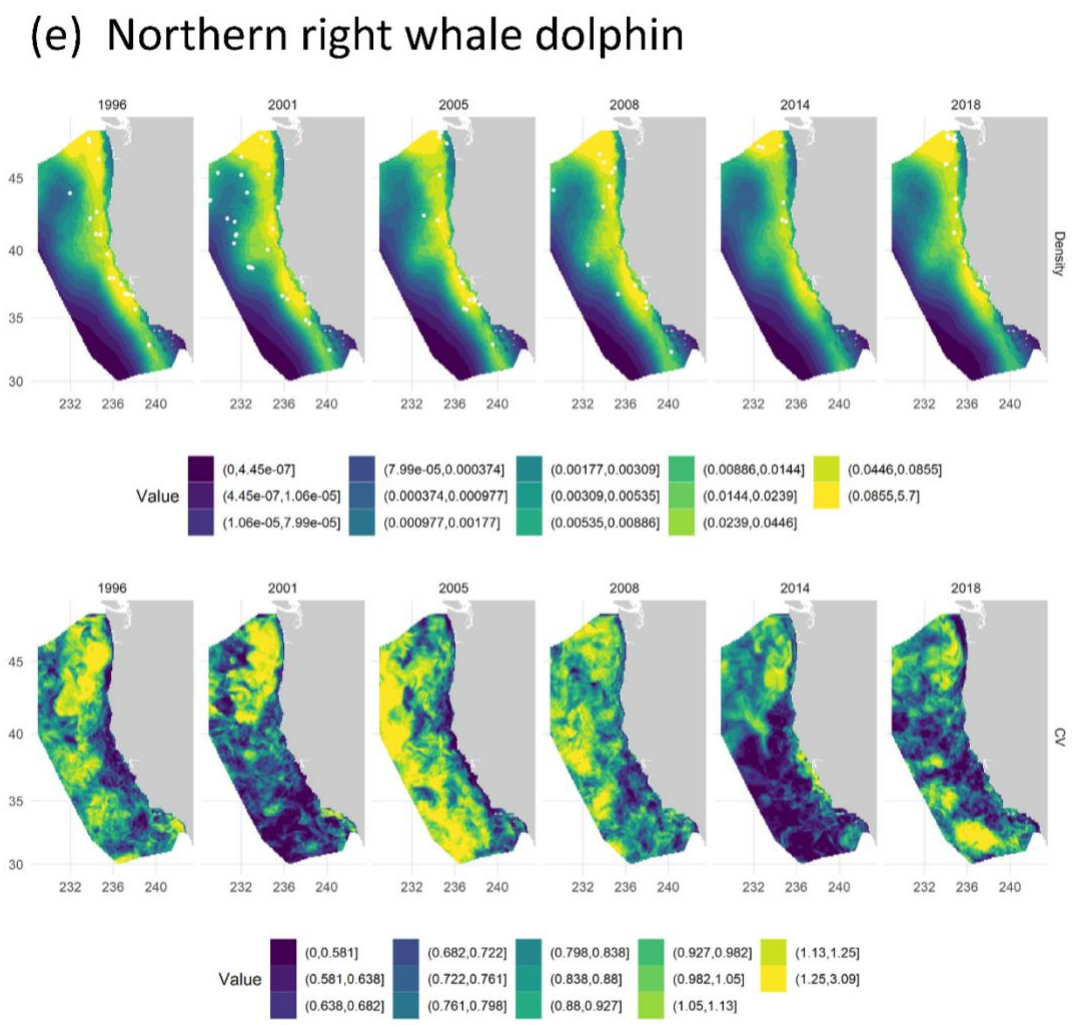

Figure 3e. Predicted annual (1996-2018) mean density (animals km^{-2}) and associated coefficients of variation (CV) from the 1991–2018 habitat-based density models for northern right whale dolphin. Panels show the yearly average density based on predicted daily northern right whale dolphin densities covering the 1996-2018 survey periods (summer/fall). Predictions are shown for the study area (1,141,800 km^2). White dots in the average plots show actual sighting locations from the respective SWFSC summer/fall ship surveys.

(f) Striped dolphin

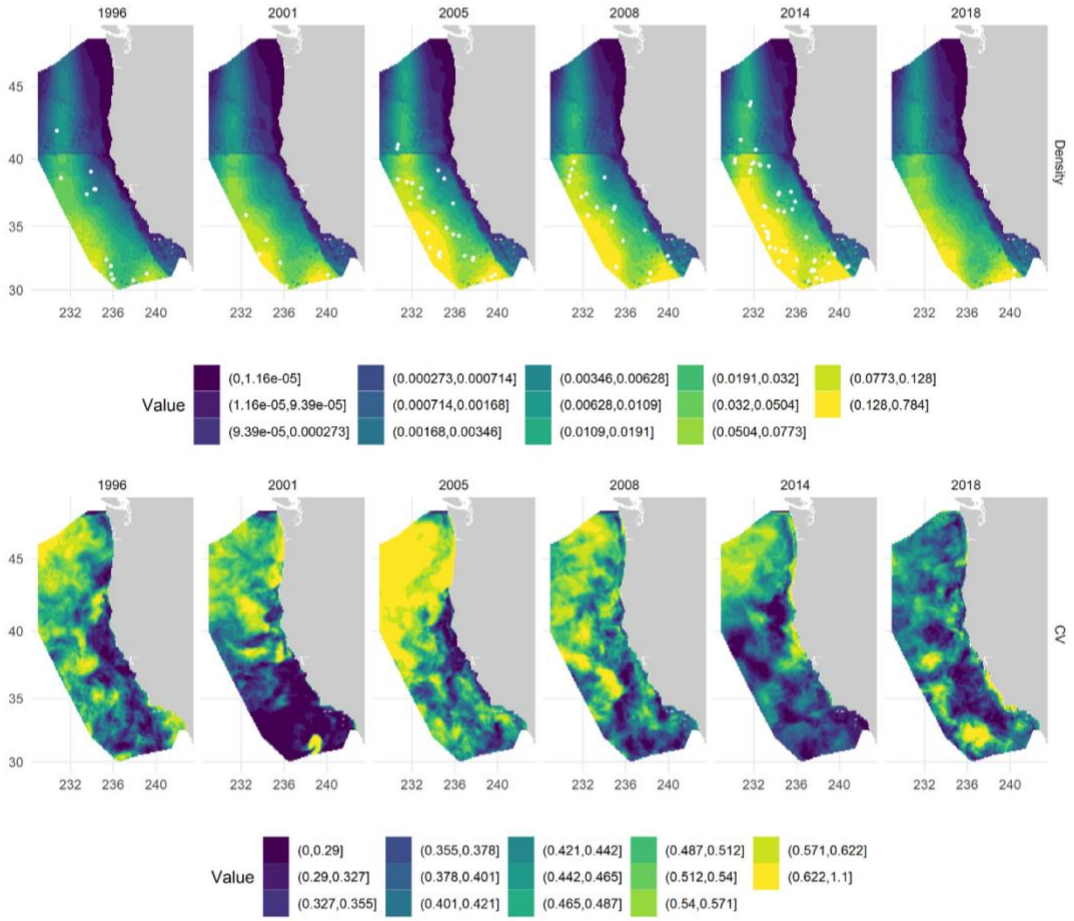

Figure 3f. Predicted annual (1996-2018) mean density (animals km^{-2}) and associated coefficients of variation (CV) from the 1991–2018 habitat-based density models for striped dolphin. Panels show the yearly average density based on predicted daily striped dolphin densities covering the 1996-2018 survey periods (summer/fall). Predictions are shown for the study area (1,141,800 km^2). White dots in the average plots show actual sighting locations from the respective SWFSC summer/fall ship surveys.

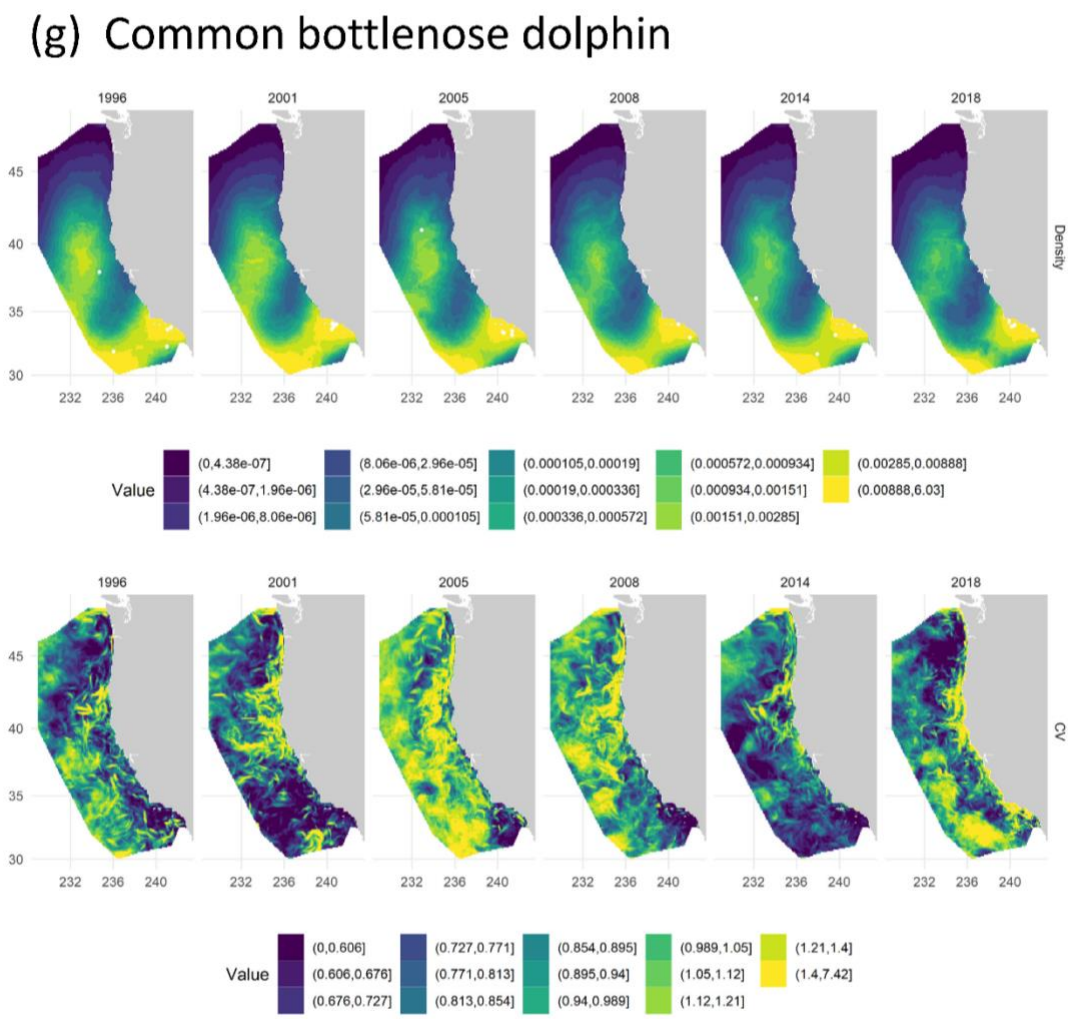

Figure 3g. Predicted annual (1996-2018) mean density (animals km^{-2}) and associated coefficients of variation (CV) from the 1991–2018 habitat-based density models for common bottlenose dolphin. Panels show the yearly average density based on predicted daily common bottlenose dolphin densities covering the 1996-2018 survey periods (summer/fall). Predictions are shown for the study area (1,141,800 km^2). White dots in the average plots show actual sighting locations from the respective SWFSC summer/fall ship surveys.

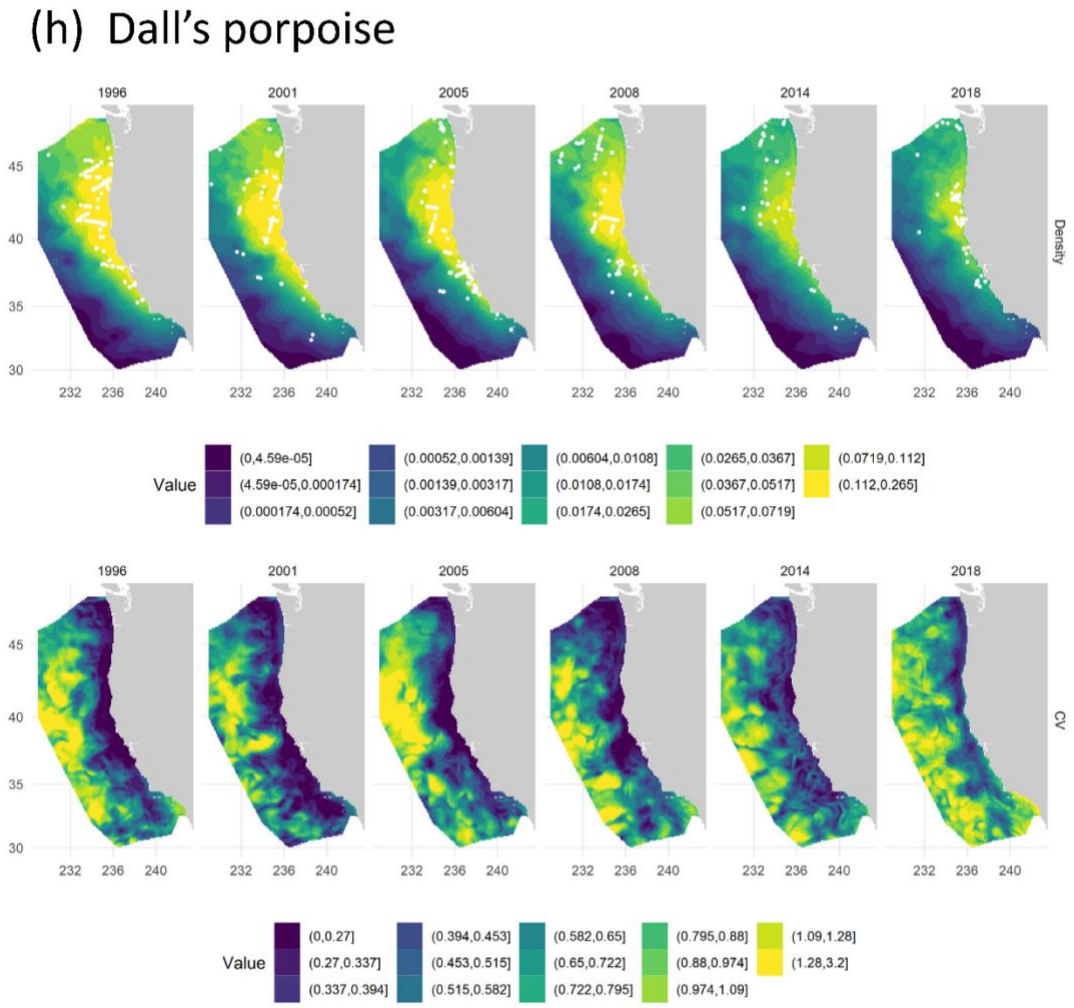

Figure 3h. Predicted annual (1996-2018) mean density (animals km^{-2}) and associated coefficients of variation (CV) from the 1991–2018 habitat-based density models for Dall's porpoise. Panels show the yearly average density based on predicted daily Dall's porpoise densities covering the 1996-2018 survey periods (summer/fall). Predictions are shown for the study area (1,141,800 km^2). White dots in the average plots show actual sighting locations from the respective SWFSC summer/fall ship surveys.

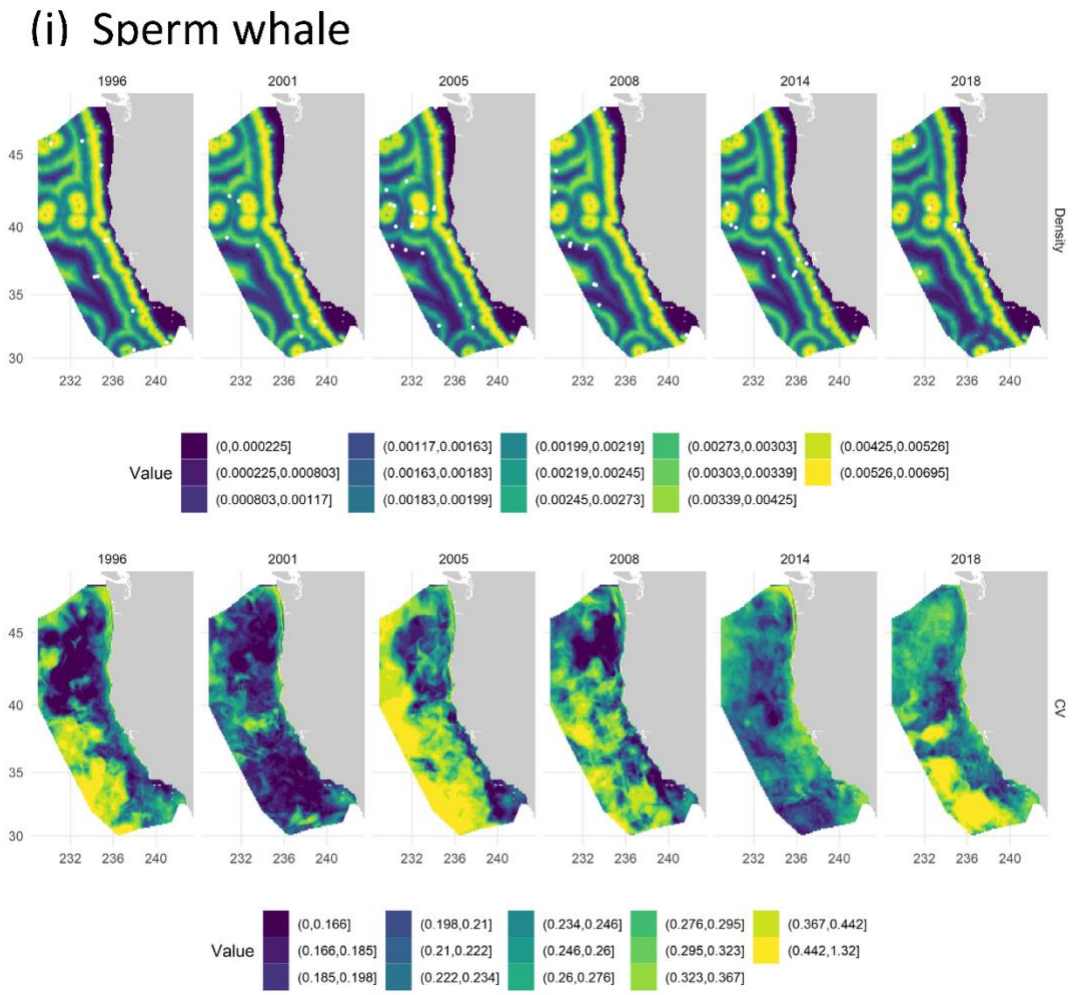

Figure 3i. Predicted annual (1996-2018) mean density (animals km^{-2}) and associated coefficients of variation (CV) from the 1991–2018 habitat-based density models for sperm whale. Panels show the yearly average density based on predicted daily sperm whale densities covering the 1996-2018 survey periods (summer/fall). Predictions are shown for the study area (1,141,800 km^2). White dots in the average plots show actual sighting locations from the respective SWFSC summer/fall ship surveys.

(j) Minke whale

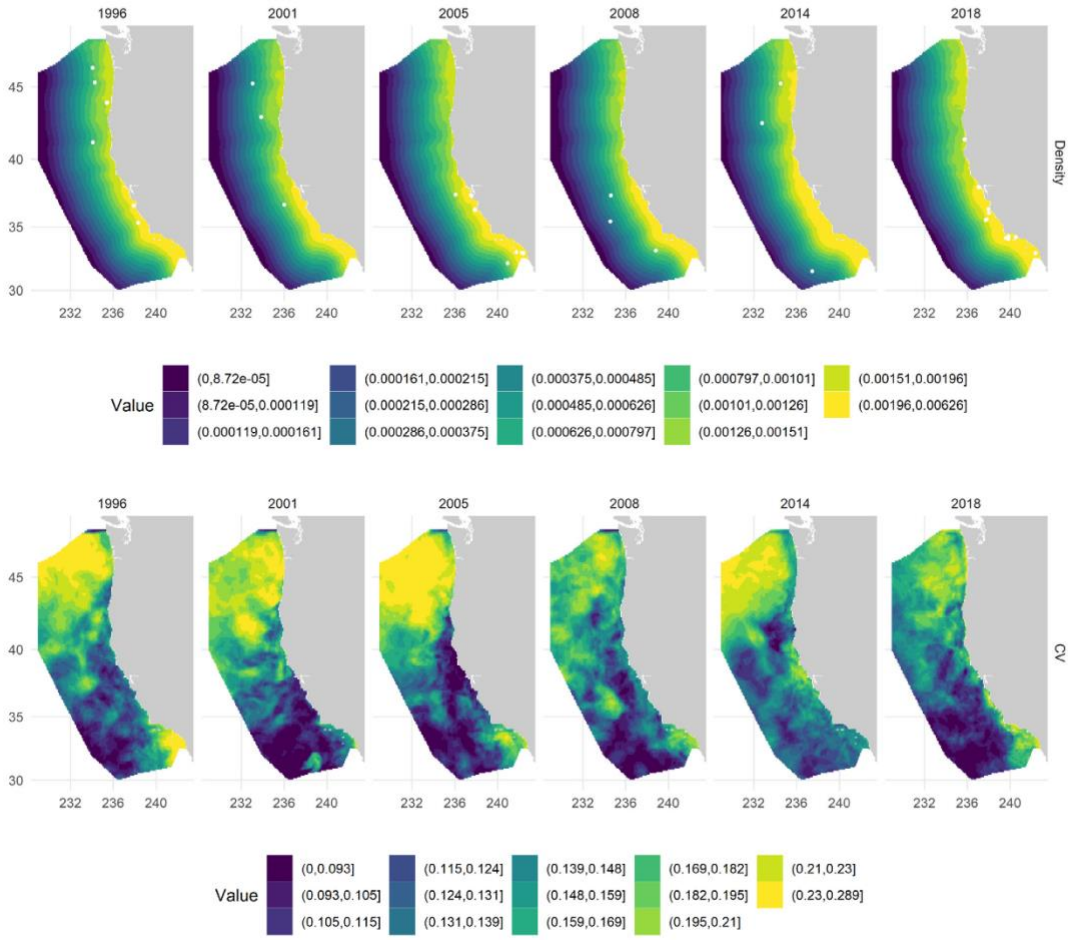

Figure 3j. Predicted annual (1996-2018) mean density (animals km^{-2}) and associated coefficients of variation (CV) from the 1991–2018 habitat-based density models for minke whale. Panels show the yearly average density based on predicted daily minke whale densities covering the 1996-2018 survey periods (summer/fall). Predictions are shown for the study area (1,141,800 km^2). White dots in the average plots show actual sighting locations from the respective SWFSC summer/fall ship surveys.

(k) Blue whale

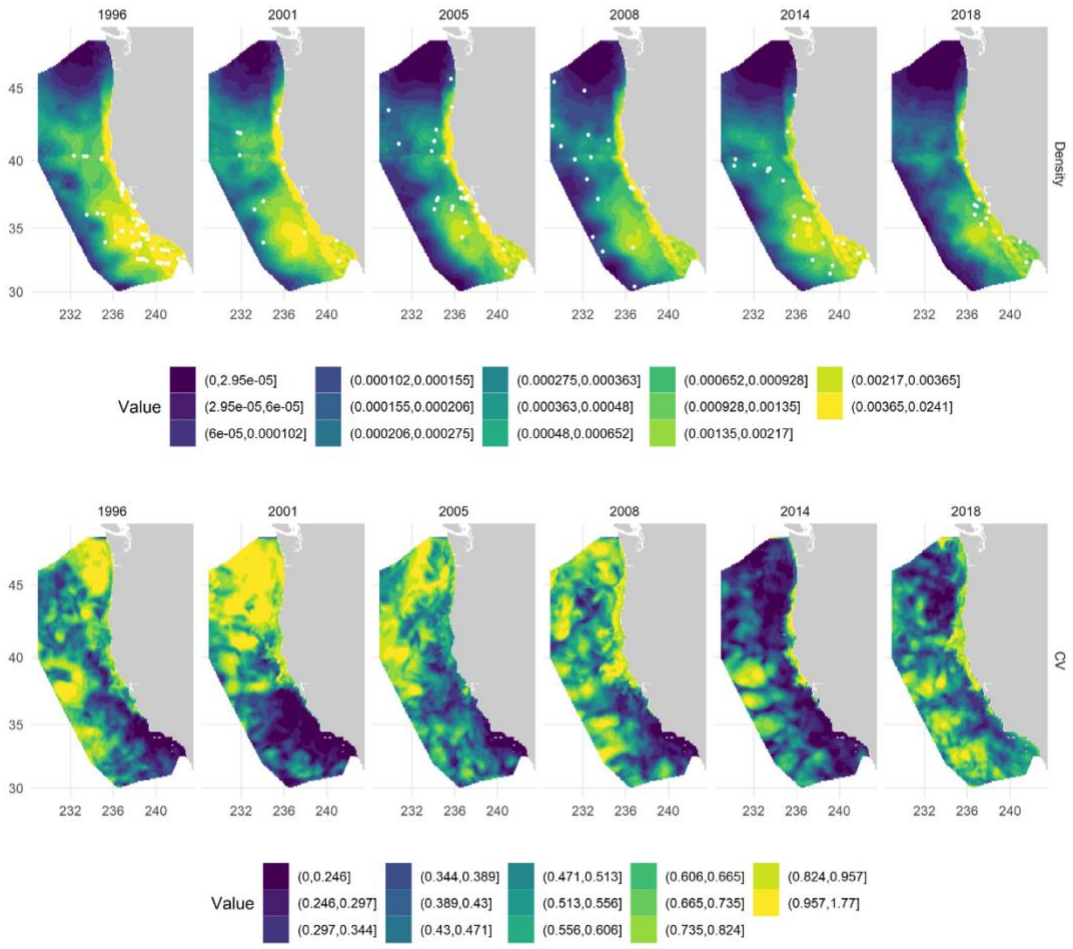

Figure 3k. Predicted annual (1996-2018) mean density (animals km^{-2}) and associated coefficients of variation (CV) from the 1991–2018 habitat-based density models for blue whale. Panels show the yearly average density based on predicted blue whale densities covering the 1996-2018 survey periods (summer/fall). Predictions are shown for the study area (1,141,800 km^2). White dots in the average plots show actual sighting locations from the respective SWFSC summer/fall ship surveys.

(l) Fin whale

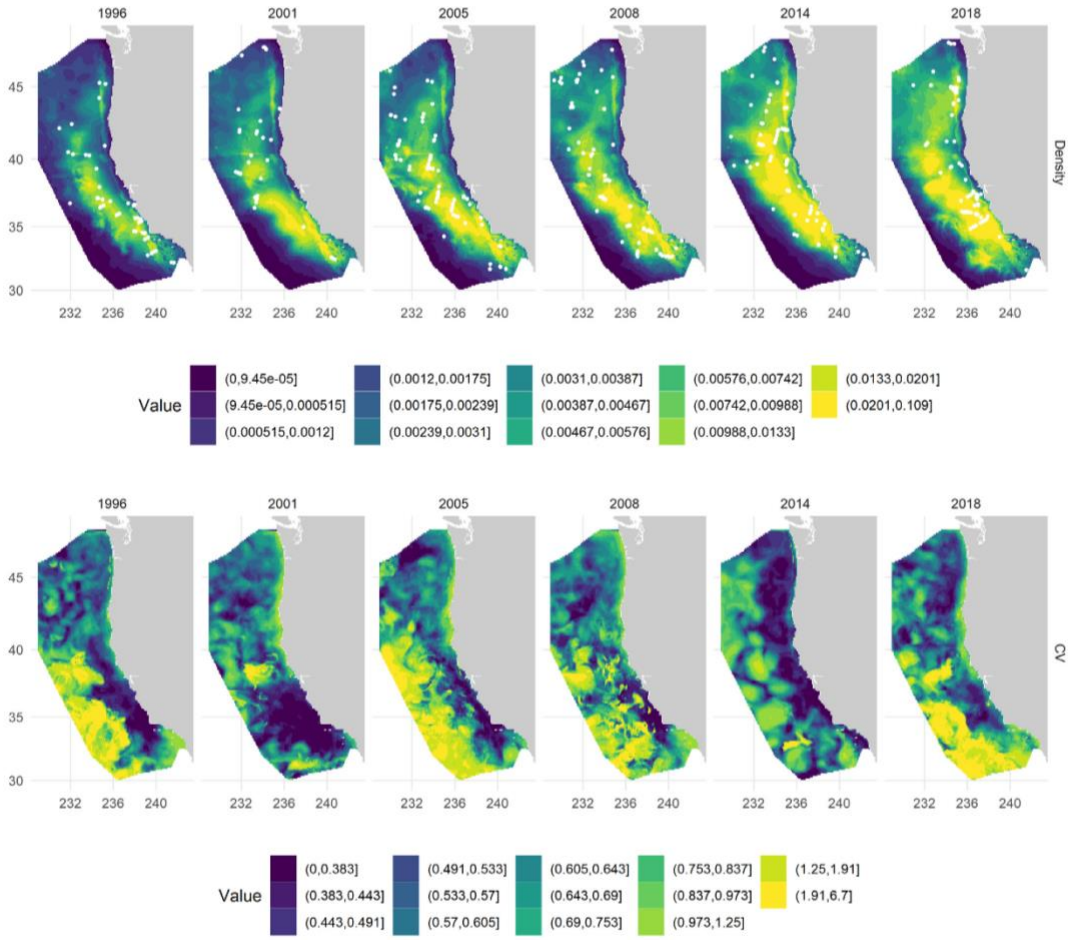

Figure 3l. Predicted annual (1996-2018) mean density (animals km^{-2}) and associated coefficients of variation (CV) from the 1991–2018 habitat-based density models for fin whale. Panels show the yearly average density based on predicted fin whale densities covering the 1996-2018 survey periods (summer/fall). Predictions are shown for the study area (1,141,800 km^2). White dots in the average plots show actual sighting locations from the respective SWFSC summer/fall ship surveys.

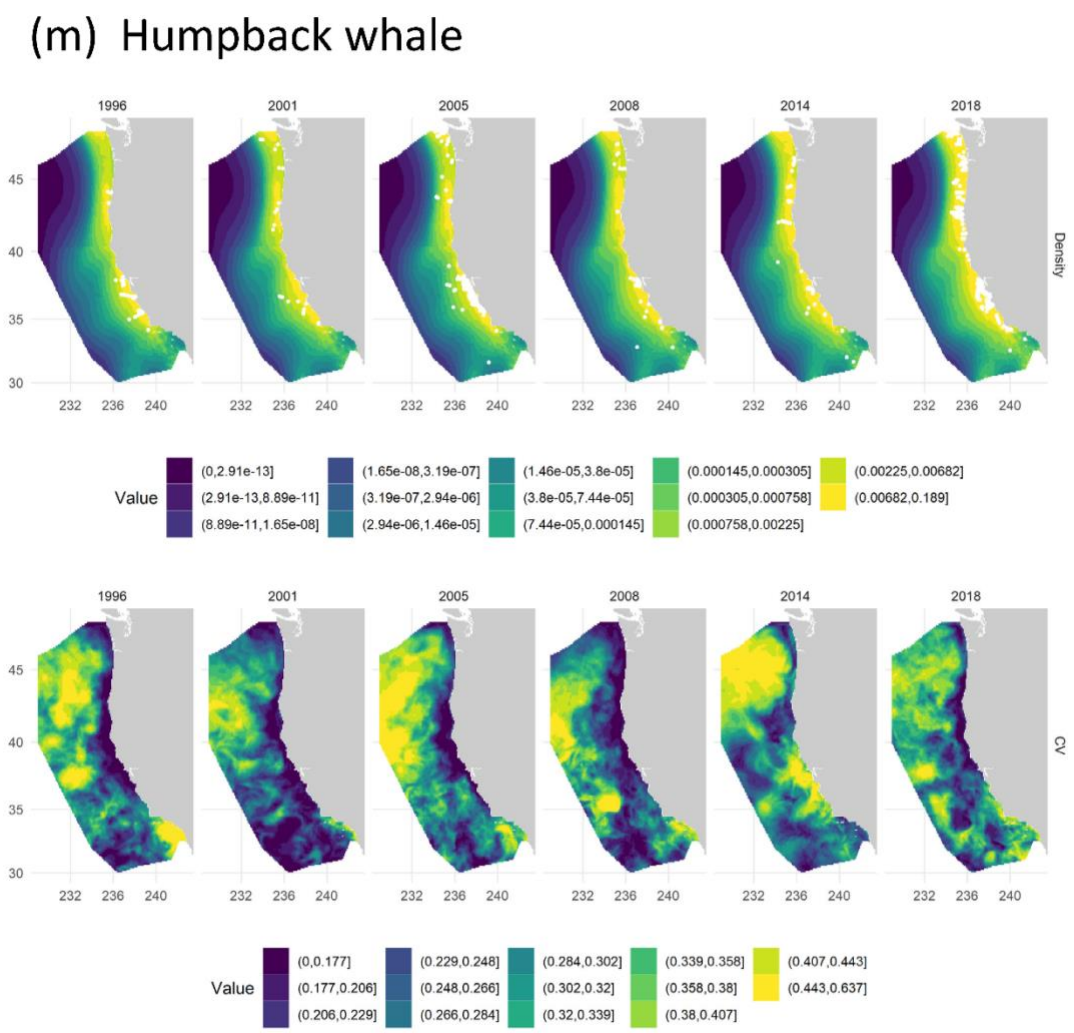

Figure 3m. Predicted annual (1996-2018) mean density (animals km^{-2}) and associated coefficients of variation (CV) from the 1991–2018 habitat-based density models for humpback whale. Panels show the yearly average density based on predicted humpback whale densities covering the 1996-2018 survey periods (summer/fall). Predictions are shown for the study area (1,141,800 km^2). White dots in the average plots show actual sighting locations from the respective SWFSC summer/fall ship surveys.

(n) Baird's beaked whale

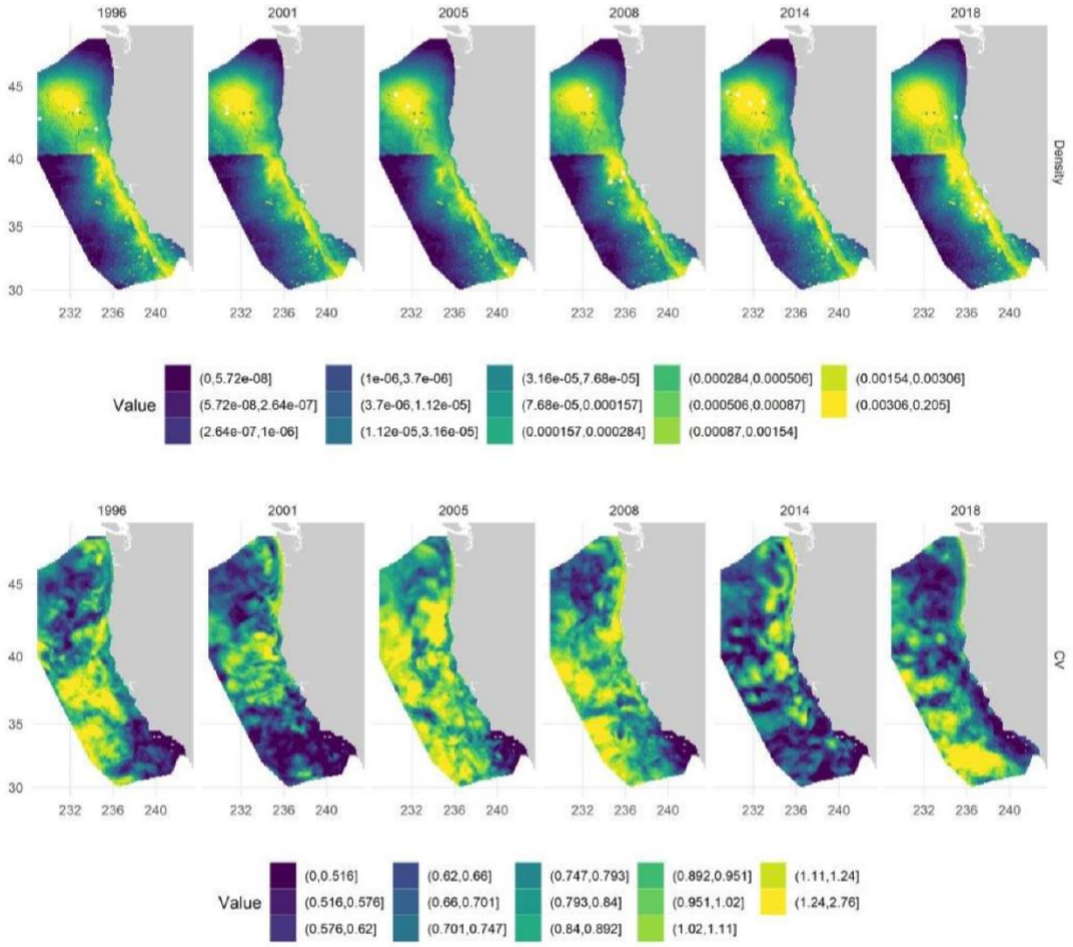

Figure 3n. Predicted annual (1996-2018) mean density (animals km^{-2}) and associated coefficients of variation (CV) from the 1991–2018 habitat-based density models for Baird's beaked whale. Panels show the yearly average density based on predicted Baird's beaked whale densities covering the 1996-2018 survey periods (summer/fall). Predictions are shown for the study area (1,141,800 km^2). White dots in the average plots show actual sighting locations from the respective SWFSC summer/fall ship surveys.

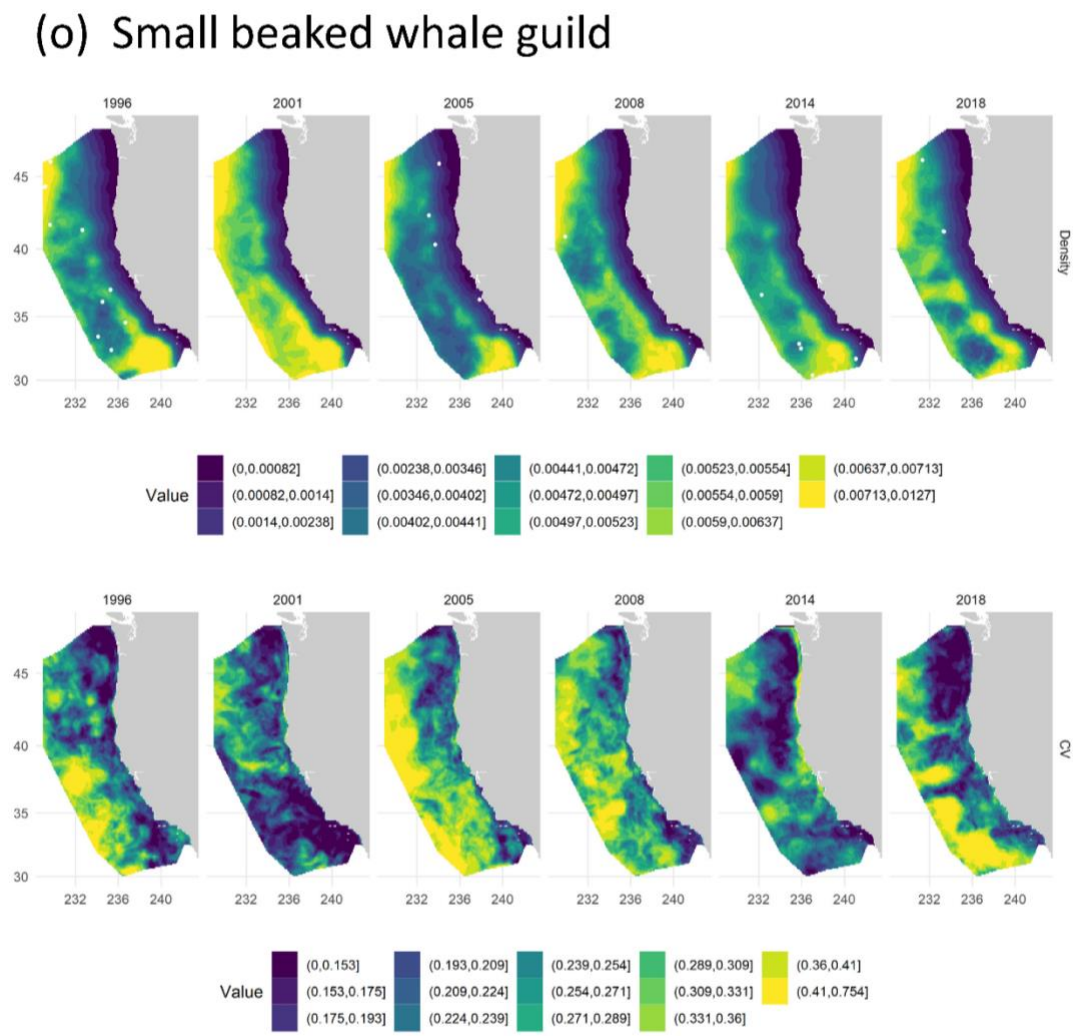

Figure 3o. Predicted annual (1996-2018) mean density (animals km^{-2}) and associated coefficients of variation (CV) from the 1991–2018 habitat-based density models for the small beaked whale guild (Mesoplodonts and Cuvier's beaked whale). Panels show the yearly average density based on predicted small beaked whale guild densities covering the 1996-2018 survey periods (summer/fall). Predictions are shown for the study area (1,141,800 km^2). White dots in the average plots show actual sighting locations from the respective SWFSC summer/fall ship surveys.

Appendix A: SDM functional plots

Final SDM response curves for (1) long-beaked common dolphin, (2) short-beaked common dolphin, (3) Risso's dolphin, (4), Pacific white-sided dolphin, (5) northern right whale dolphin, (6) striped dolphin, (7) common bottlenose dolphin, (8) sperm whale, (9) minke whale, (10) blue whale, (11) fin whale, (12) humpback whale, (13) Baird's beaked whale, and (14) the small beaked whale guild (*Mesoplondon* spp. and Cuvier's beaked whale). The suite of environmental and geographic covariates included: SST = sea surface temperature, sdSST = standard deviation of SST, MLD = mixed layer depth, SSH = sea surface height, sdSSH = standard deviation of SSH, depth = bathymetric depth, dShelf = distance to the 200m isobath, d2000 = distance to the 2,000m isobath, mlat = latitude, mlon = longitude, and yearCoVar = year. Models were constructed with both linear terms and smoothing splines. Degrees of freedom for single variables are shown in the parentheses on the y-axis. Variables for the interaction terms are shown on the x- and y-axes. For single variables the y-axes represent the term's (linear or spline) function. Zero on the y-axes corresponds to no effect of the predictor variable on the estimated response variable. Scaling of y-axis varies among predictor variables to emphasize model fit. The shading reflects 2x standard error bands (i.e., 95% confidence interval); tick marks ('rug plot') above the X axis show data values. For the interaction terms, yellow indicates higher prediction densities and red lower predicted densities.

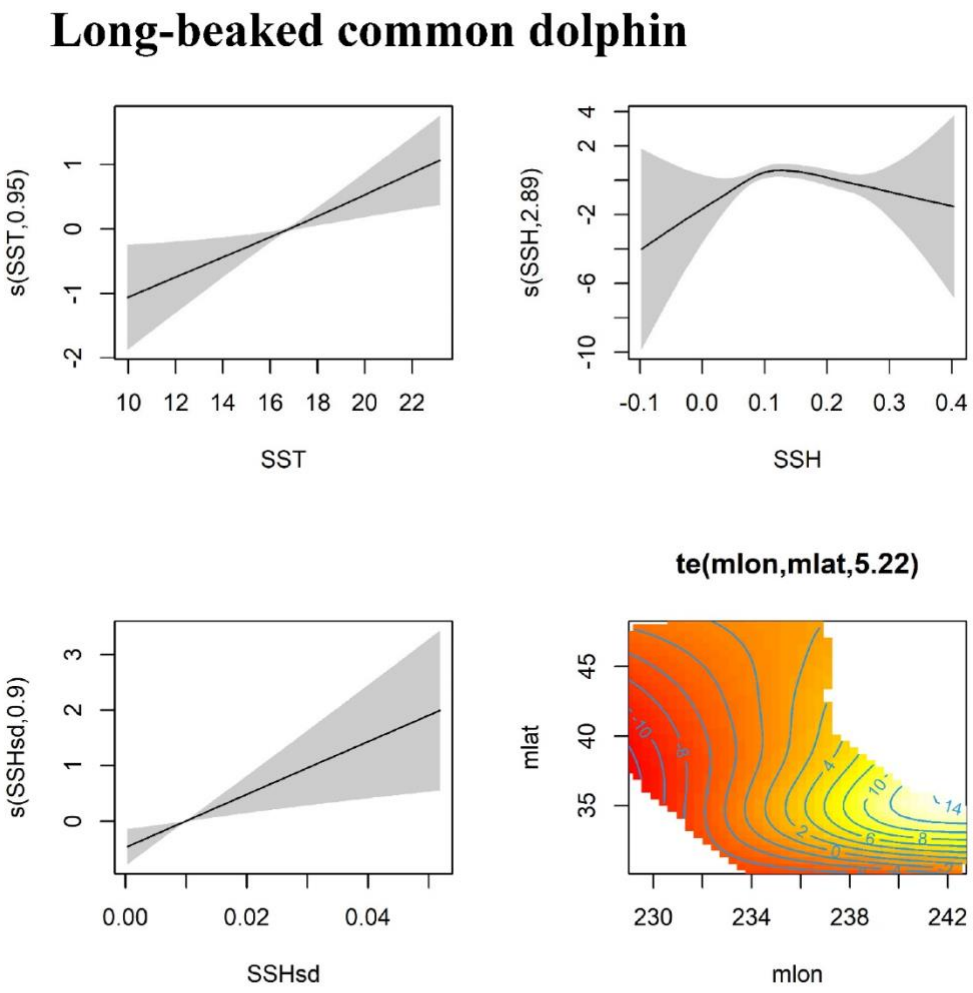

Figure A 1. Functional plot for long-beaked common dolphin (*Delphinus delphis bairdii*) encounter rate model.

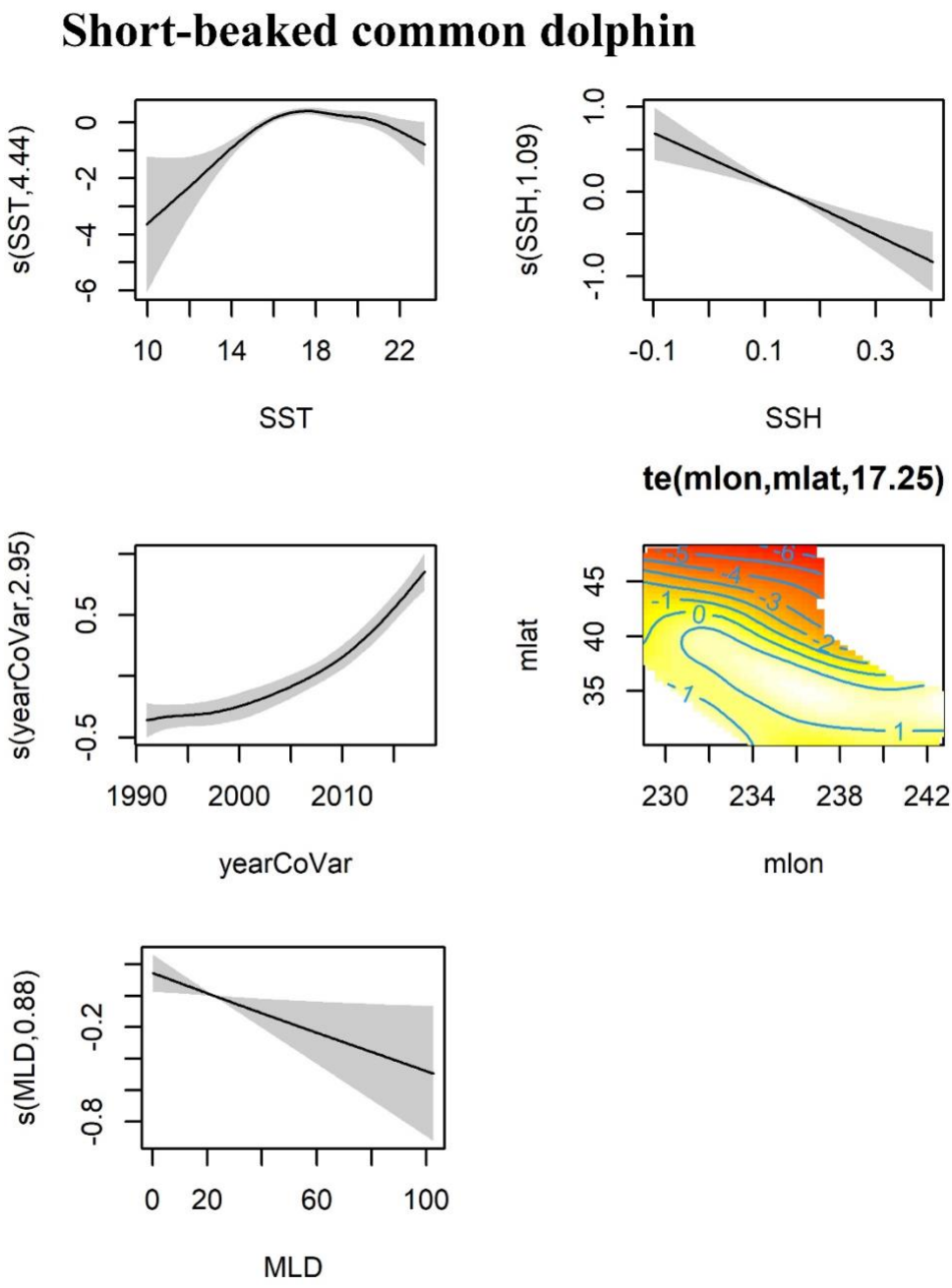

Figure A 2. Functional plot for short-beaked common dolphin (*Delphinus delphis delphis*) encounter rate model.

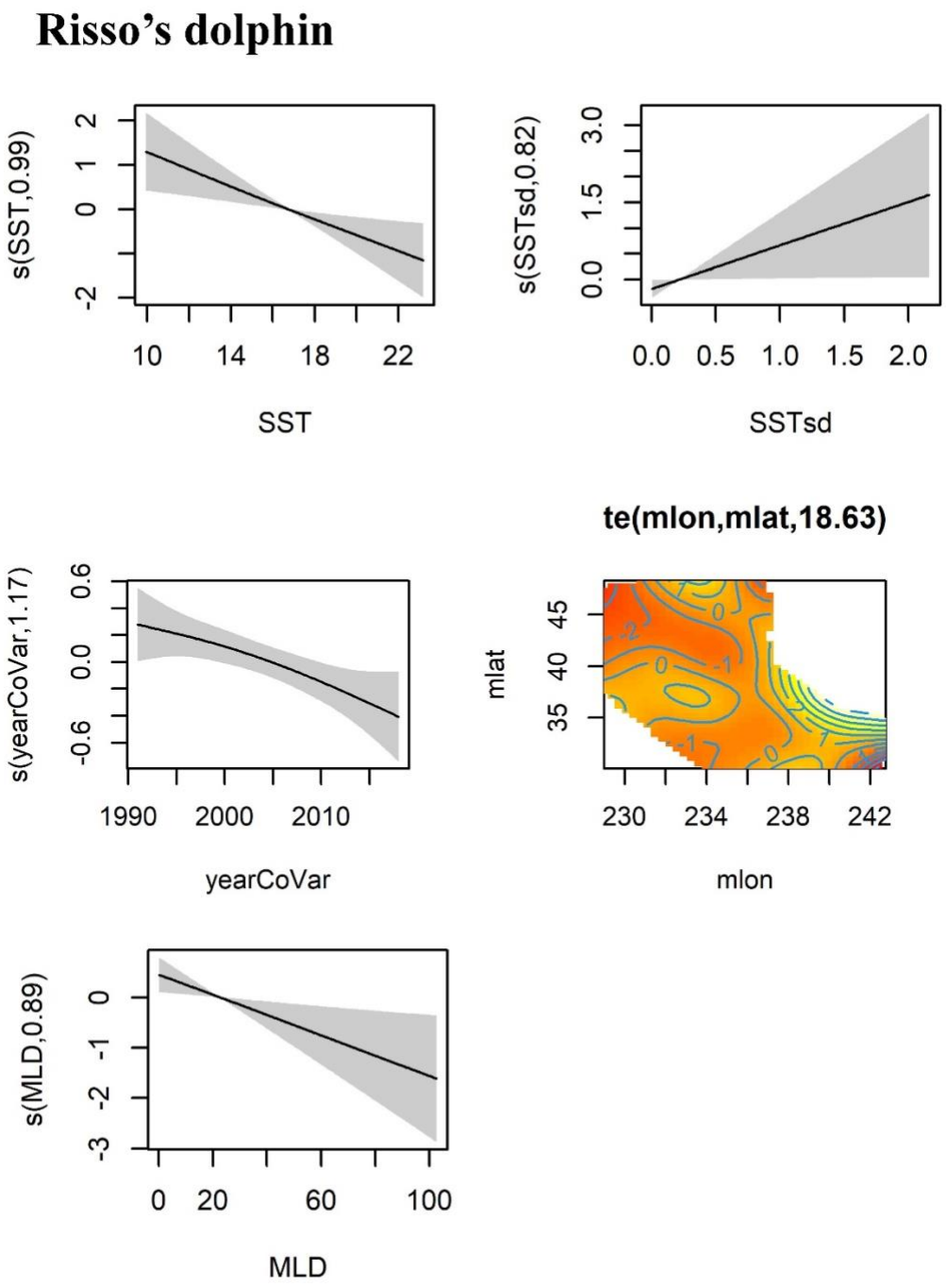

Figure A 3. Functional plot for Risso's dolphin (*Grampus griseus*) model.

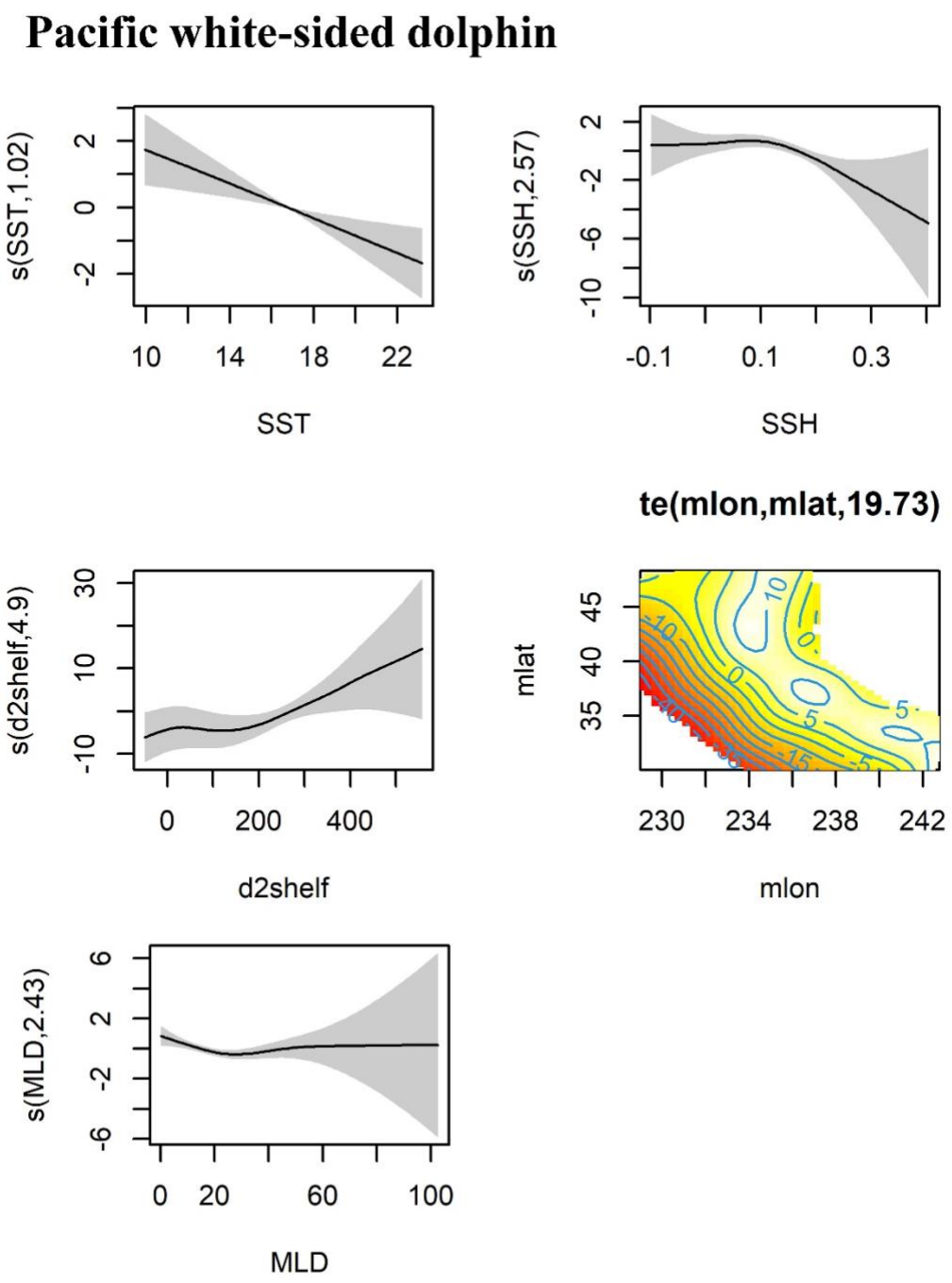

Figure A 4. Functional plot for Pacific white-sided dolphin (*Lagenorhynchus obliquidens*) model.

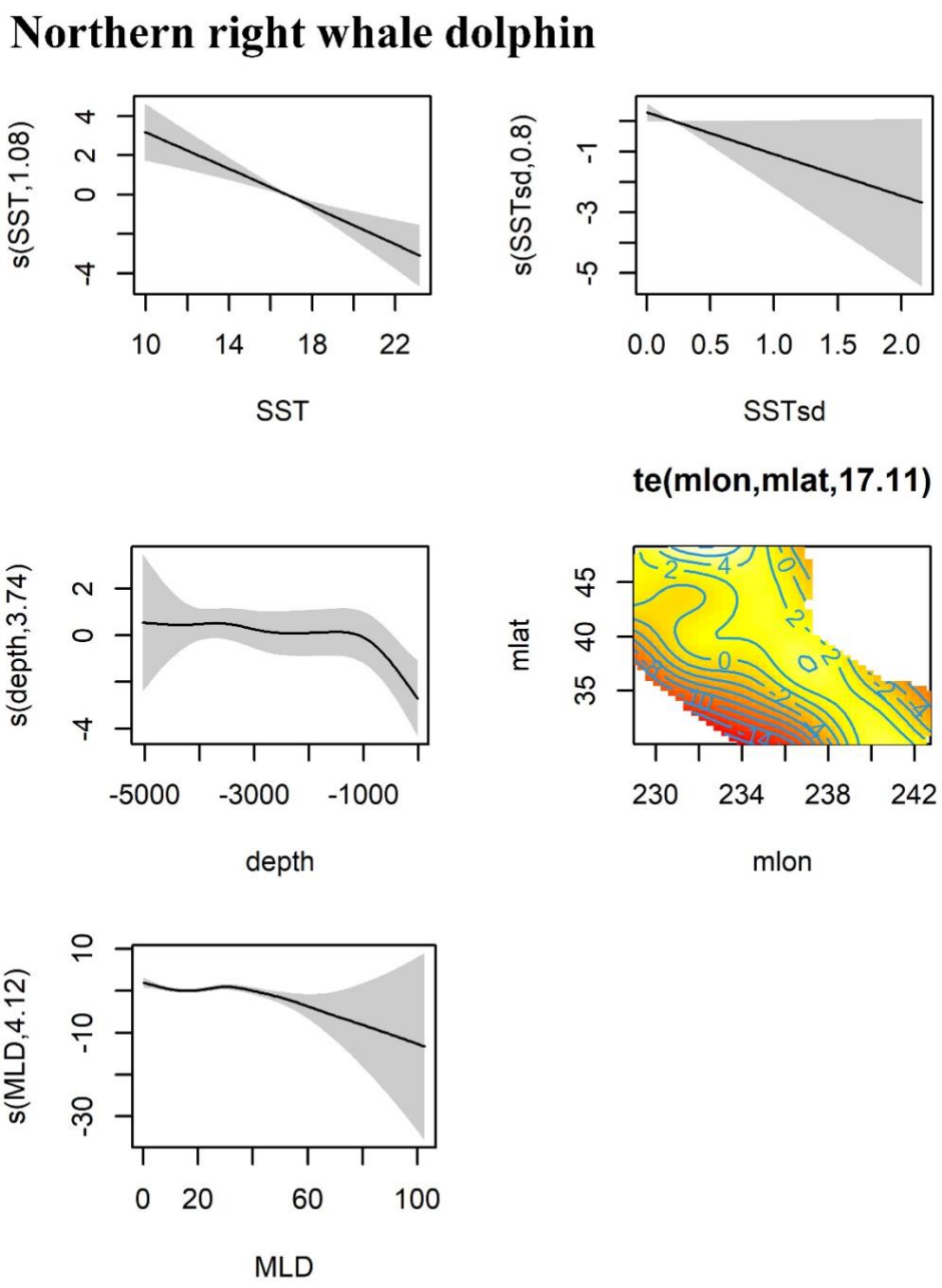

Figure A 5. Functional plot for northern right whale dolphin (*Lissodelphis borealis*) model.

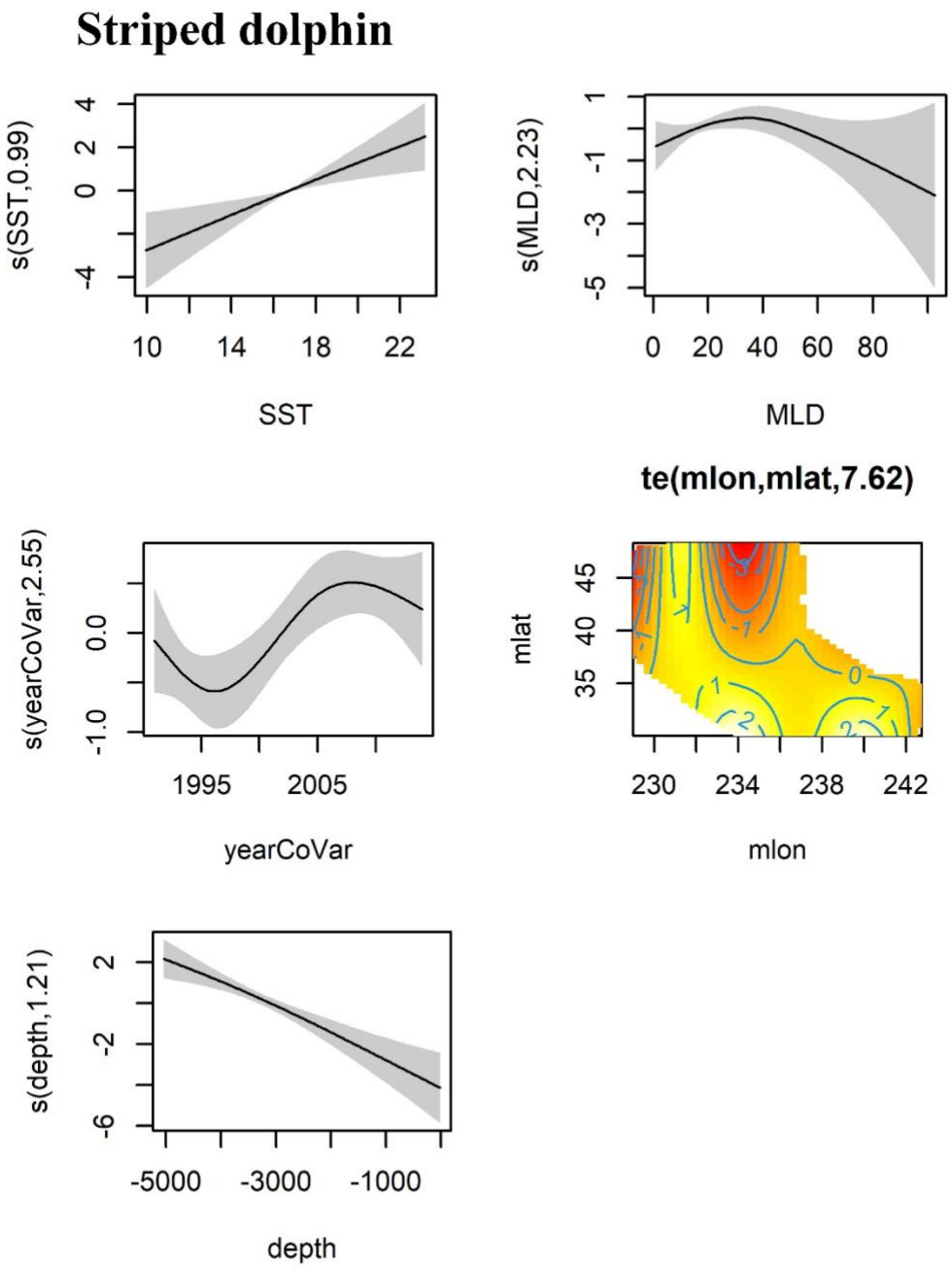

Figure A 6. Functional plot for striped dolphin (*Stenella coeruleoalba*) model.

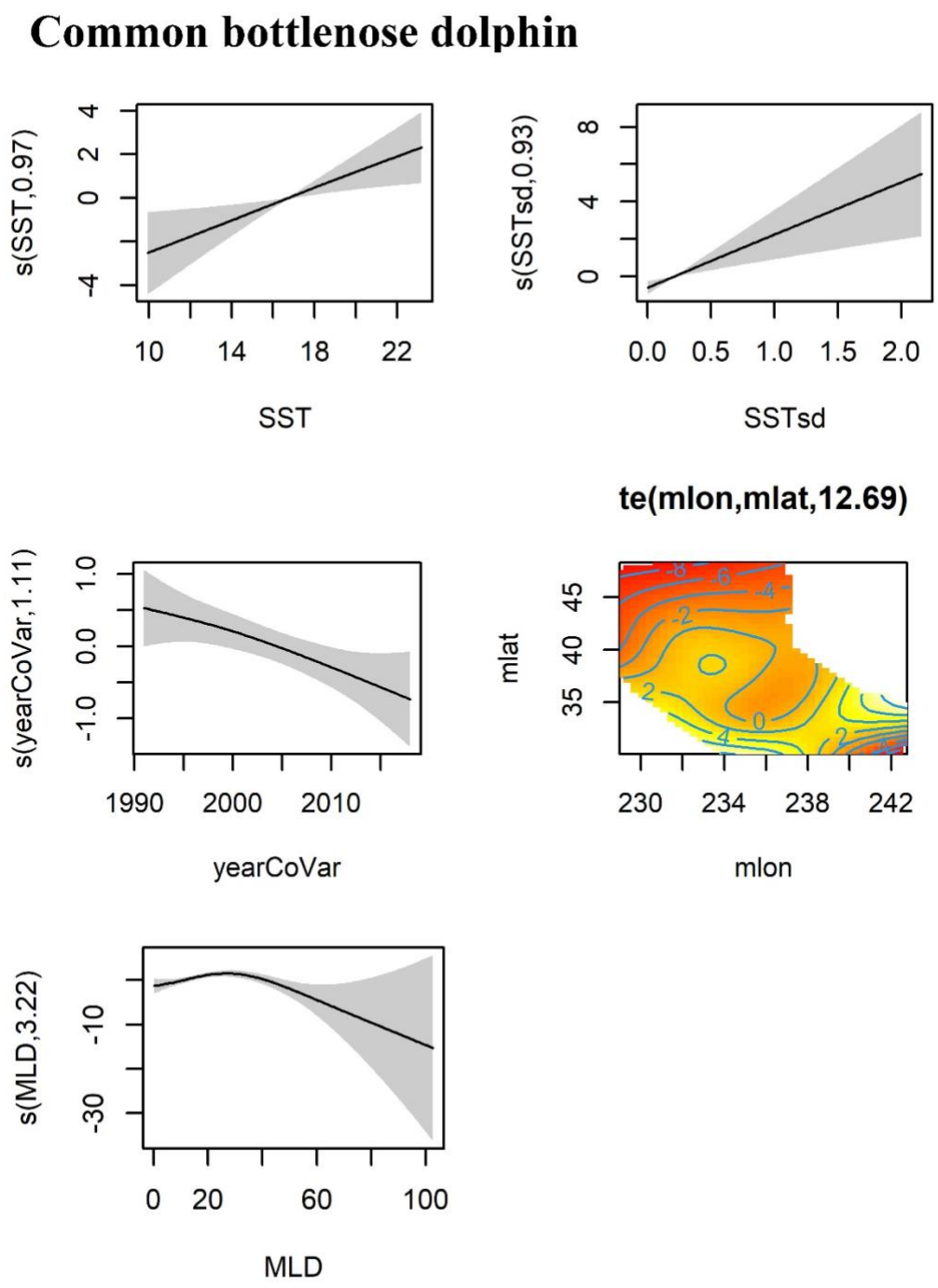

Figure A 7. Functional plot for common bottlenose dolphin (*Tursiops truncatus*) model.

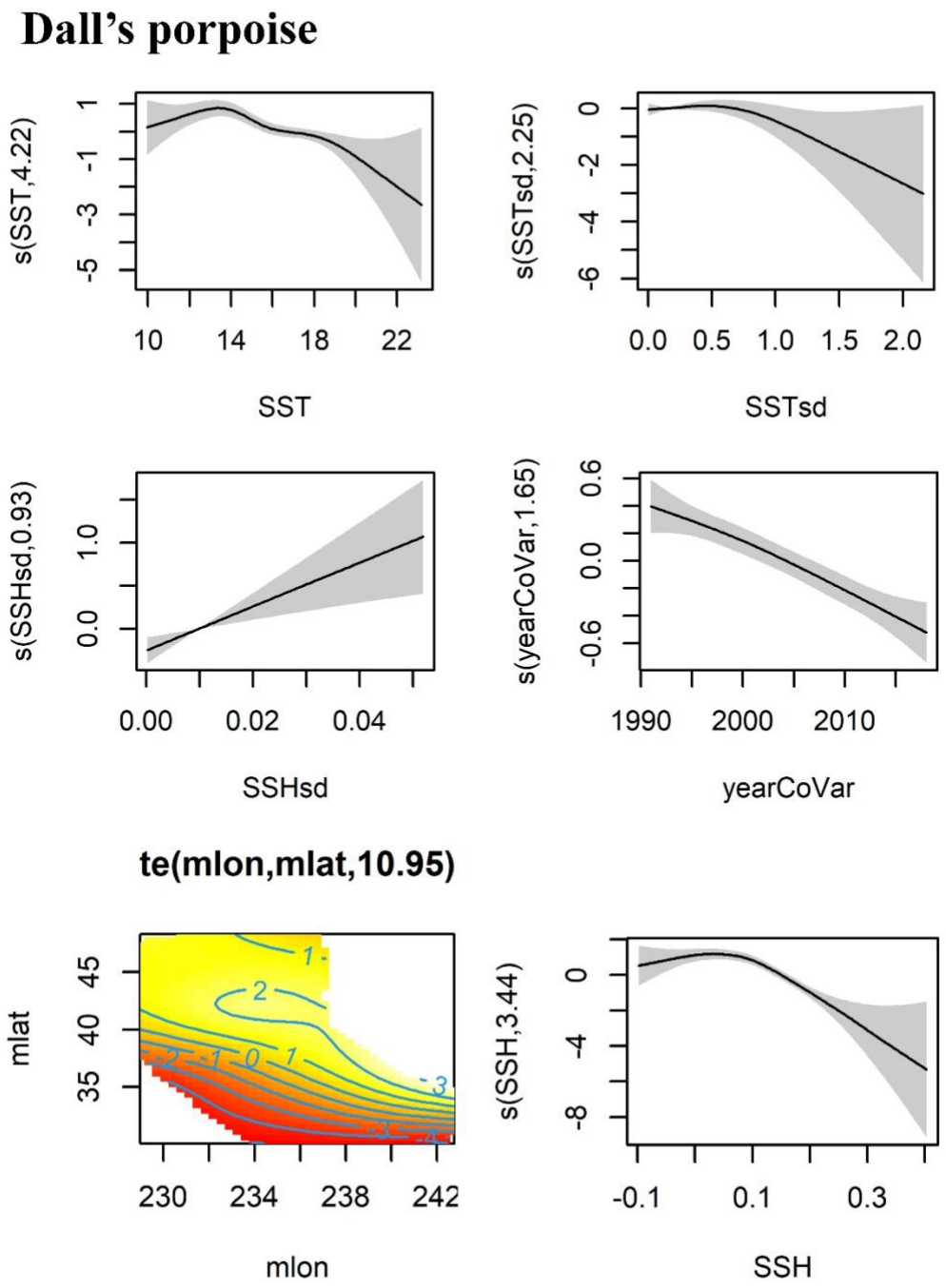

Figure A 8. Functional plot for Dall's porpoise (*Phocoenoides dalli*) model.

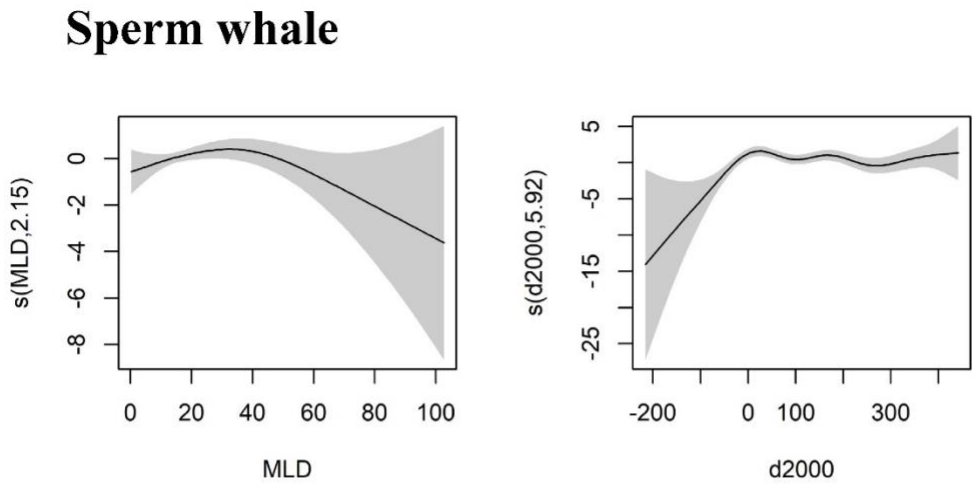

Figure A 9. Functional plot for sperm whale (*Physeter macrocephalus*) model.

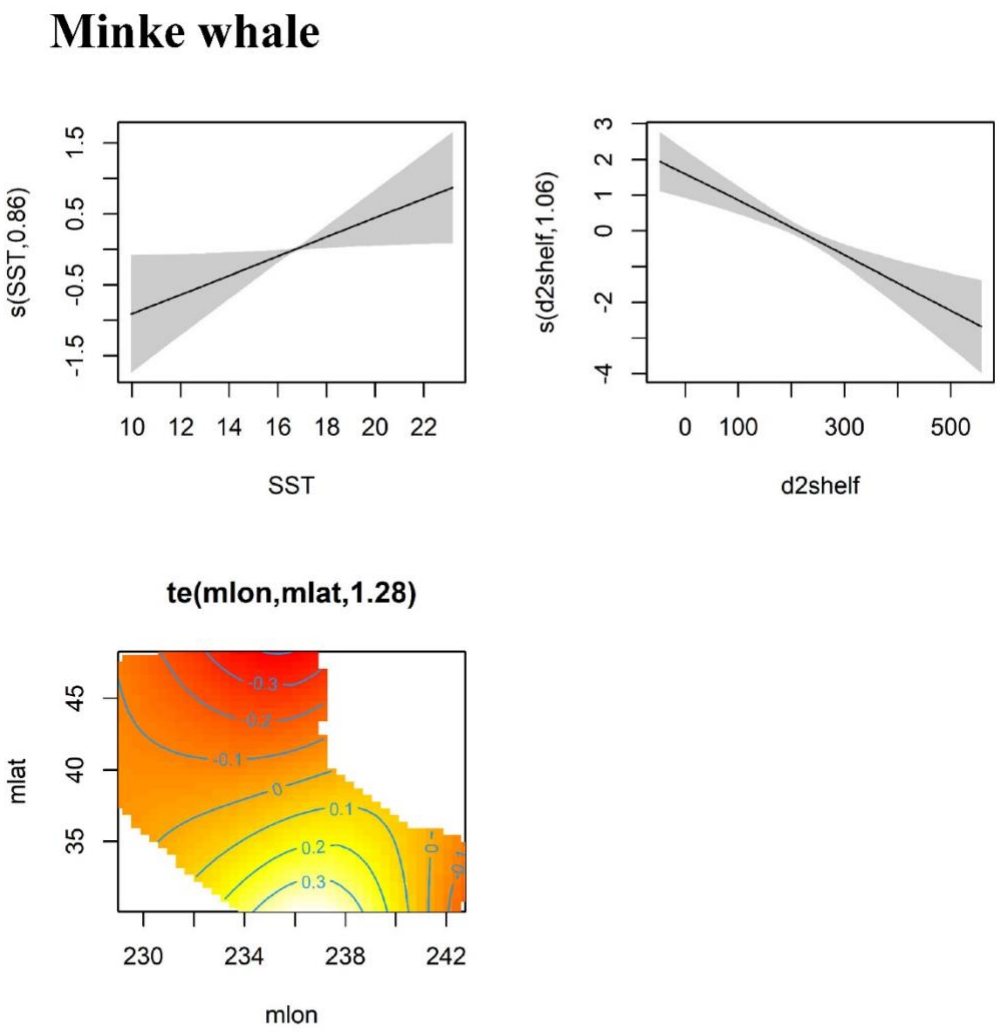

Figure A 10. Functional plot for minke whale (*Balaenoptera acutorostrata*) model.

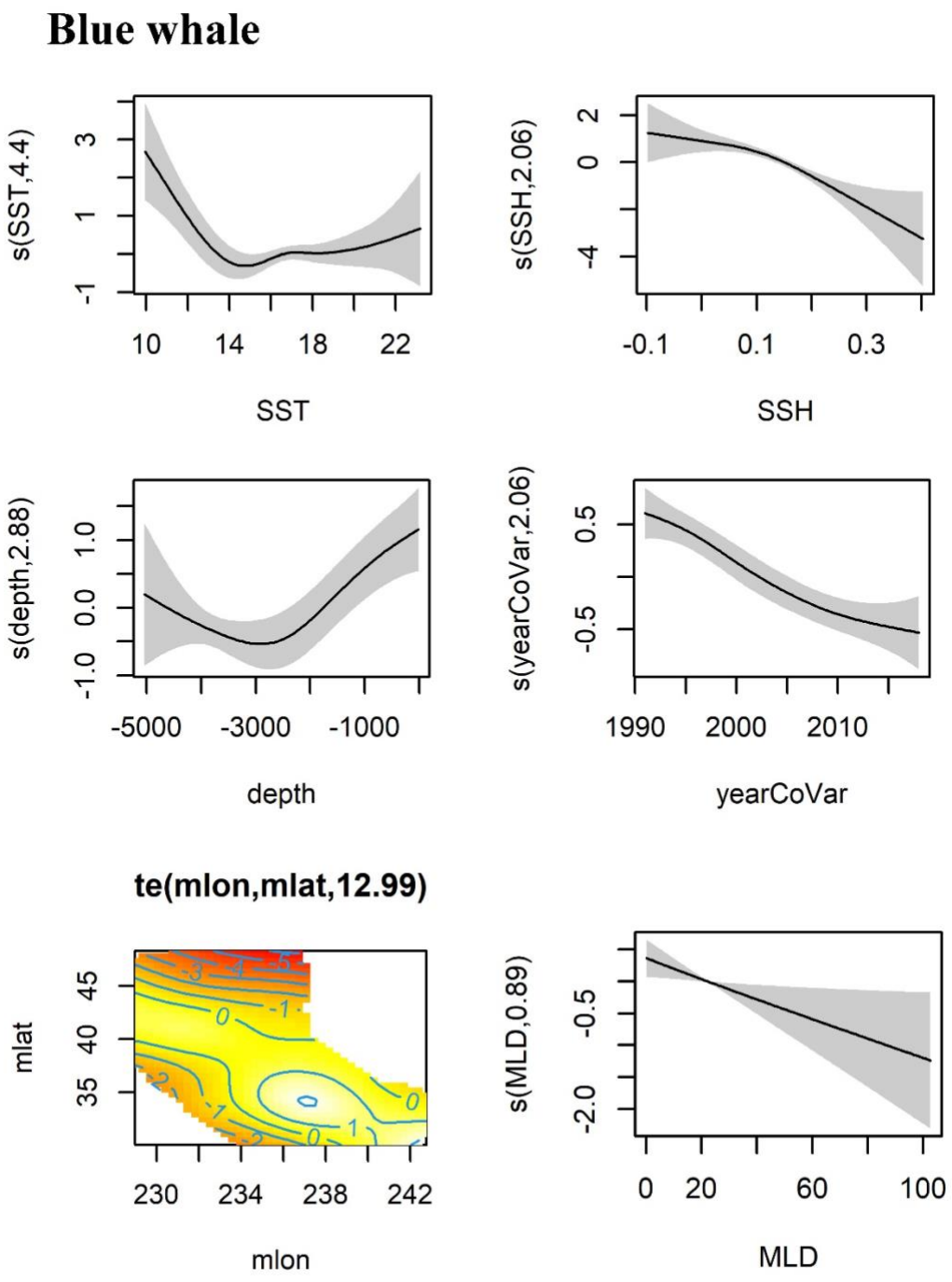

Figure A 11. Functional plot for blue whale (*Balaenoptera musculus*) model.

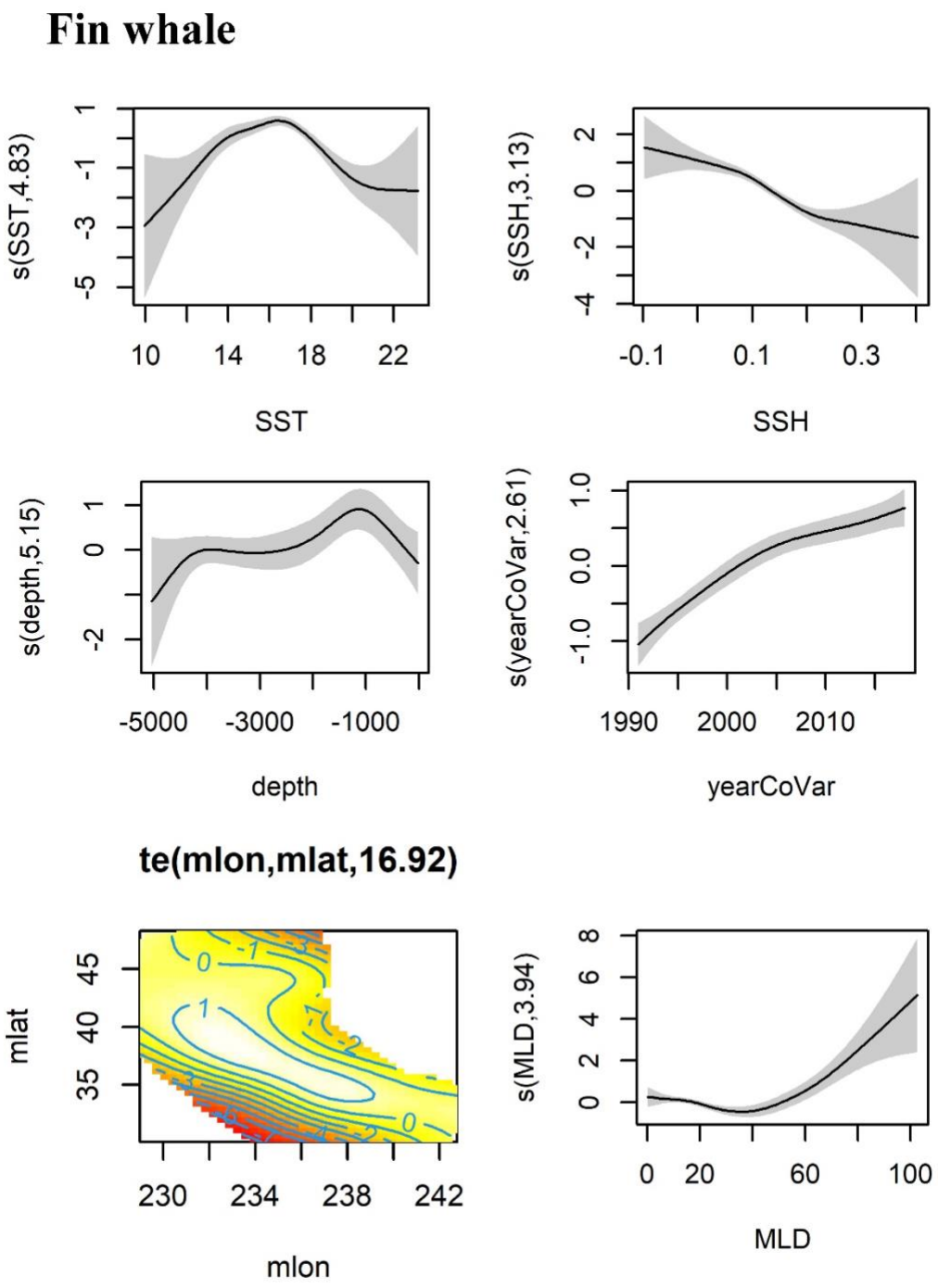

Figure A 12. Functional plot for fin whale (*Balaenoptera physalus*) model.

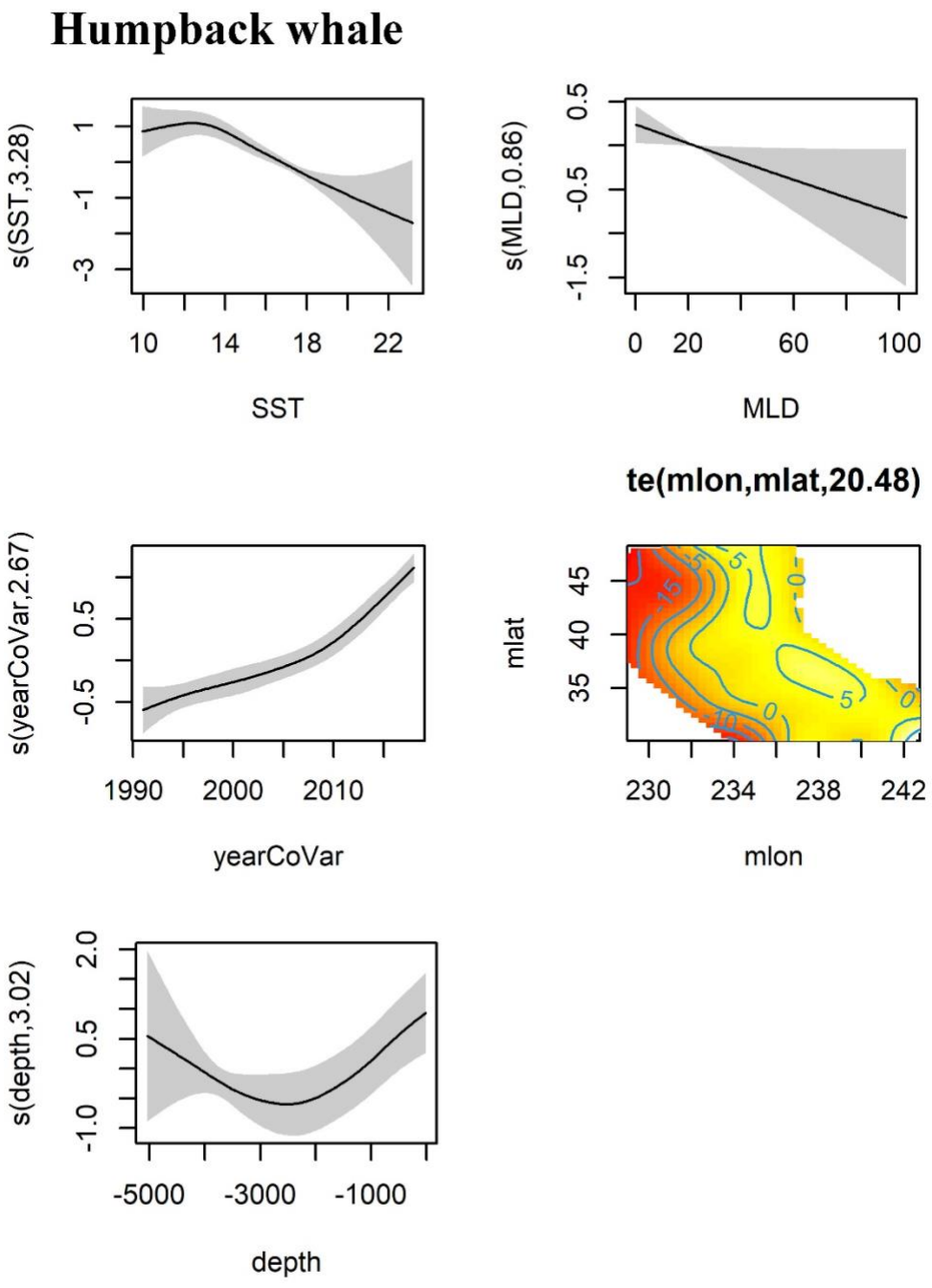

Figure A 13. Functional plot for fin whale (*Megaptera novaeangliae*) model.

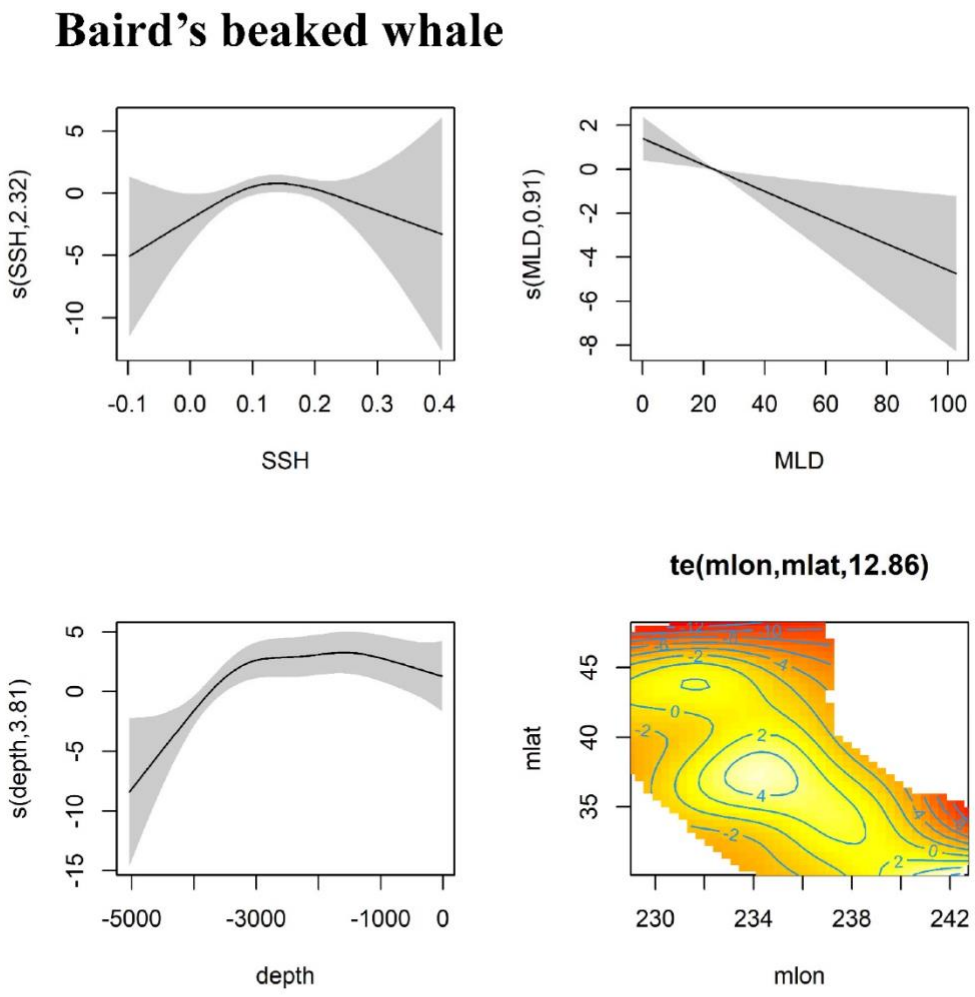

Figure A 14. Functional plot for Baird's beaked whale (*Berardius bairdii*) model.

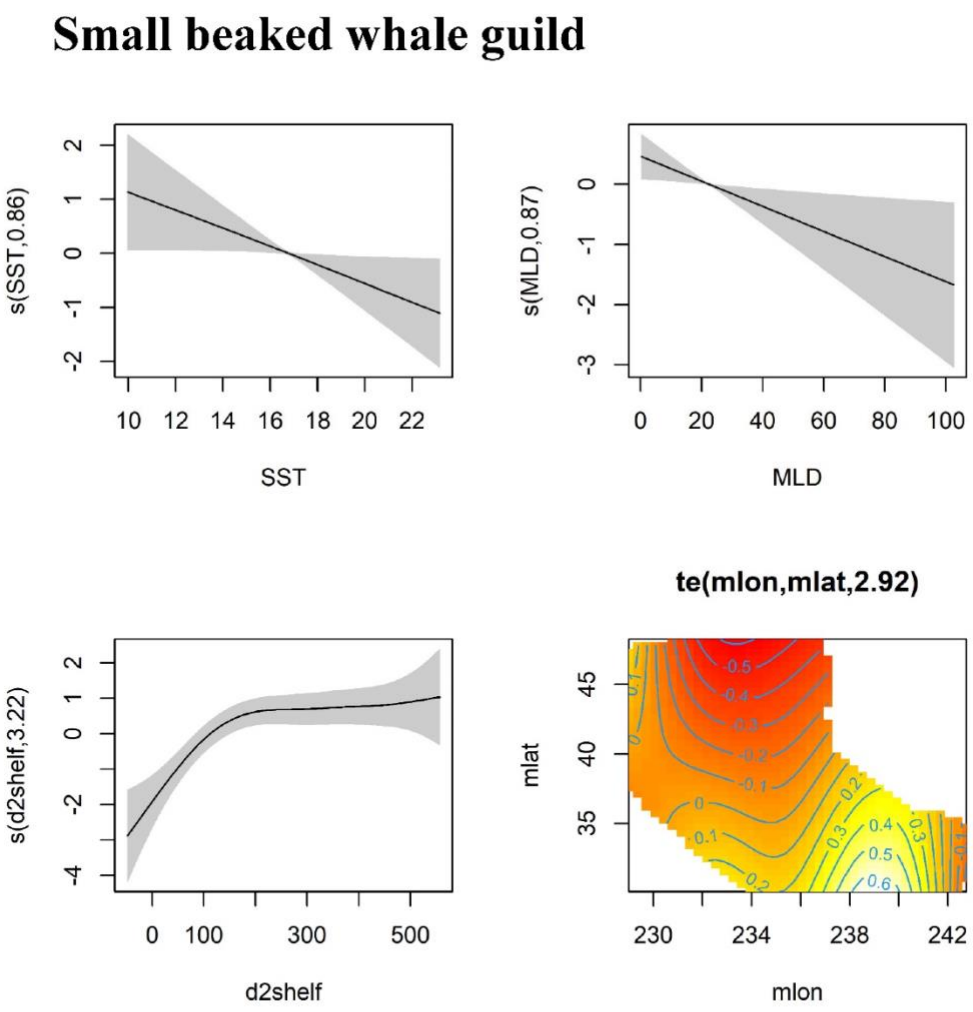

Figure A 15. Functional plot for the small beaked whale guild (*Mesoplondon spp. & Ziphius cavirostris*) model.